

# Membrane Roof for a Tennis Court

## Master-Thesis

A thesis submitted in partial fulfillment  
of the requirements for the degree of

## Master Membrane Structures

submitted to

Anhalt University of Applied Sciences

Faculty of Architecture,  
Facility Management and Geo Information

by

João Jorge Fernandes Abrantes

13 May 1980, Porto, Portugal

Matriculation number: 4053867

Submission: 24th July 2014

First Tutor: Prof. Dr.-Ing. Robert Off

Second Tutor: M.Eng. Atisit Sabmeethavorn

I hereby declare that the work presented in this Master Thesis, entitled

**Membrane Roof for Tennis Court**

is entirely my own and that I did not use any sources or auxiliary means other than those referenced.

Porto, Portugal. June 2014

## **Acknowledgment**

I am thankful to God for the many blessings that I have in my life.

All my gratitude to my parents, brother and girlfriend for the support during the Master Course.

To Mr. Rudolf Bergermann, founding partner of Schlaich Bergermann und Partner, who taught me almost everything about Structural Engineering.

To the tutors of this Master Thesis, for having accepted to guide me.

Table of Contents

1. Introduction..... 7

2. Design Process..... 13

    2.1 Architecture..... 13

    2.2 Formfinding..... 15

3. Materials..... 19

4. Structural Analysis..... 21

    4.1 Software ..... 21

    4.2 Structural System ..... 22

    4.3 Materials and Sections ..... 25

    4.4 Loads Assumptions..... 31

        4.4.1 Dead Load..... 31

        4.4.2 Prestress ..... 31

        4.4.3 Live Load..... 31

        4.4.4 Temperature..... 31

        4.4.5 Wind Load..... 32

        4.4.6 Snow Load ..... 35

        4.4.7 Imperfections (EN 1993-1-1:2005(D) Cl. 5.3.2) ..... 35

    4.5 Load Cases ..... 37

    4.6 Load Combination ..... 48

5. Dimensioning and Detailed Design ..... 50

    5.1 Steel Structure – Upper Compression Ring..... 50

    5.2 Steel Structure – Lower Compression Ring..... 58

    5.3 Steel Structure – Diagonals ..... 66

    5.4 Steel Structure – Columns..... 67

    5.6 Cable Structure – Radial Cables..... 68

    5.7 Cable Structure – Tension Ring ..... 72

    5.8 Cable Structure – Front Edge Cables..... 74

    5.9 Cable Structure – Back Edge Cables ..... 76

    5.10 Membrane Dimensioning..... 78

    5.11 Service – Displacements..... 80

    5.12 Ponding..... 81

    5.13 Detail – Column Foot..... 82

5.14 Detail – Membrane with flexible Edge ..... 84

6. Membrane Patterning ..... 86

7. Cost Estimation..... 89

8. Time Schedule ..... 91

9. Future Perspectives - PVDF-Foil as Structural Element..... 93

10. Bibliography..... 100



# 1 Introduction



## 1. Introduction

Tennis is a popular sport which can be played by any social class. It is an Olympic sport and the game reaches fans all over the world. There is a professional competition, which is played in different countries around the world, called ATP-Tour. The four major events of this Tour are the Australian Open, the French Open also known as Roland Garros, Wimbledon in the UK and the US Open. These events are usually covered by the media worldwide.

With the increase in the last years of the media coverage and the increase of the number of tennis fans, weather conditions have turned out to be a key factor for the success of the events. TV coverage cannot depend on weather conditions. Most of the events are played without a roof cover, which sometimes does not help the media work, the comfort of the spectators and the success of the tennis events.

In the last years, with the increase of tennis fans and the demands of media coverage, there has been taken into consideration the design of new roofs for tennis courts. The climate change and unpredictability of the weather conditions during the tennis events have also contributed to the design of new tennis court roofs.

Membrane roof structures are therefore a solution to be taken into account for the design of new tennis stadium roofs because they are light weight, translucent, economic, architecturally pleasant, UV and weather resistant.

Light weight is a decisive criteria, because the new roofs can be constructed on existing buildings which are not prepared to carry extra heavy loads. In the case that they are constructed without touching the existing buildings, being light weight is also an advantage for long spans.

Translucency benefits the court atmosphere and the players' performance, reducing the use of artificial lights.

Depending on the structural system and span, membrane structures can be economical and cost competitive compared to other materials.

The design of new roofs for tennis courts give also the opportunity to the design of new retractable roofs. These retractable roofs can be open during good weather and rapidly closed during bad weather.

"The famed Rod Laver Arena was the first ever sports stadium with a retractable roof when it was opened on 11th January, 1988." (Source: <http://www.tennisearth.com>) It is place of the Australian Open.



Figure 1 – Rod Laver Arena Retractable Roof in Australia (Source: [www.tennisticketnews.com](http://www.tennisticketnews.com))

The completed roof of the Rod Laver Arena has two rolling sections, each supported by steel trusses. The roof opens or closes with a speed of 1.3 meters per minute (Source: <http://www.rodlaverarena.com.au/>), taking 20 minutes complete the movement. The retractable has proved along the years to be a great help to the players when the temperatures drop or dramatically rise.

The Hisense Arena is located also in Melbourne, with a maximum capacity of 11000 people and the arena construction was completed in 2000. Is one of the few tennis arenas with a retractable roof.

A new design for the Margaret Court in the Melbourne Park has been proposed in 2012, namely a new retractable roof for the 7,500-seat Arena, which should be ready in 2015.



Figure 2 – Margaret Court Arena Redevelopment (Source: [www.austadiums.com](http://www.austadiums.com))

Gerry Weber Stadium is an indoor sports arena, located in Halle, in Germany. It is one of the first membrane retractable roof of a sports venue ever build. The outer roof is made of a pvc coated polyester fabric and the inner roof made of ETFE Cushions. The inner roof is made of two rolling sections that drive under the outer roof. The capacity of the arena is 12,300 people and it was opened in 1992. The tennis event Gerry Weber open is played in this stadium.



Figure 3 - Gerry Weber Stadium with ETFE Retractable Roof (Source: [www.skyscrapercity.com](http://www.skyscrapercity.com))



The Rothenbaum retractable membrane roof was constructed in 1999 in Germany and the membrane opens from a single point to the edges, covering the tennis court. The process of opening and closing takes about five minutes. The same system is used for the retractable roof of the football stadium roof in Warsaw and can only be done at temperatures above five degrees, with a low wind speed and not during rain. This aspect is the main disadvantage of this kind of retractable systems, because during the process of opening or closing, the movable membrane is not under tension. It can act as a sail during the process of opening or closing, introducing very high forces in the existing structure due to wind loads, for which the structure is usually not dimensioned for.



Figure 4 – Rothenbaum Tennis Court – Retractable Roof (Source: [www.hamburg-web.de](http://www.hamburg-web.de))

The steel roof of the Qi Zhong Stadium is composed by eight sliding petal-shaped pieces that close in eight minutes. The capacity of the stadium is 15,000 people. The stadium was constructed to host the ATP World Tour Finals between 2005 and 2008.

The stadium can host other international sport events such as basketball, volleyball, ping pong, or gymnastics. [Source: Wikipedia]



Figure 5 – Qi Zhong Stadium – Retractable Roof (Source: [www.tennisearth.com](http://www.tennisearth.com))

The “Magic Box” or “La Caja Mágica” in Madrid, also known as the Manzanares Park Tennis Center, is a sports center located at the Park Manzanares, used for the Madrid Masters tournament of the ATP Tour. It was opened in 2009. There is a series of retractable roofs at this sport center, but none of them has a membrane roof.



Figure 6 – Magic Box Stadium in Madrid – Retractable Roof (Source: [www.nytimes.com](http://www.nytimes.com))



The membrane roof of the center court in Wimbledon has been designed to “maintain pre-existing levels of light and air to the court when the roof is open, and when closed, an air flow system removes condensation from within the bowl to provide good court surface conditions conducive to the playing of tennis”. (Source: <http://www.wimbledon.com/>)

The retractable roof is made of two parts and it folds like a “concertina”. The roof closes in eight to ten minutes when bad weather occurs. It was built in 2009 and the structural translucent fabric covers 5,200 square meters.



Figure 7 – Centre Court Wimbledon – Retractable Roof (Source: [www.nytimes.com](http://www.nytimes.com))

There are plans to build new retractable roofs for the tennis court number one in Wimbledon, for the Center Tennis Court in Roland Garros and US Open. Thus, there is the possibility and the opportunity of building lightweight membrane structures with structural fabric.

The present work focus on the use of pvc coated polyester fabric for a roof cover of a tennis court. The retractable inner ETFE roof mechanical system will be not presented in this work, neither the textile façade of the proposed stadium will be considered.

The present Master-Thesis pretends to show that the use of the structural system “spoked wheel roof”, well known and constructed in many football stadium roofs, can also be applied to tennis courts and as an almost rectangular shape. It will be treated in this work as “Modified Spoked Wheel System”.

A “new” material, PVDF Foil, will be presented as potential structural material and analysed as an alternative to ETFE.



## 2 Design Process



## 2. Design Process

### 2.1 Architecture

The structural system “Modified Spoked Wheel System” determines into a certain degree the aesthetical appearance of the stadium roof. The valley and ridge cables together with the membrane geometry give the rhythm of the structure. The v-shaped columns are bonded together with the geometry of the valley and ridge cables and membrane.

The Ete – Cushions “fly” above the tennis ground giving the idea of a sky with clouds, letting natural light come in into the stadium. The Ete Cushions give a sense of lightweight to the retractable roof. The pvc coated polyester fabric is a translucent material, allowing the spectators to have a natural light environment.

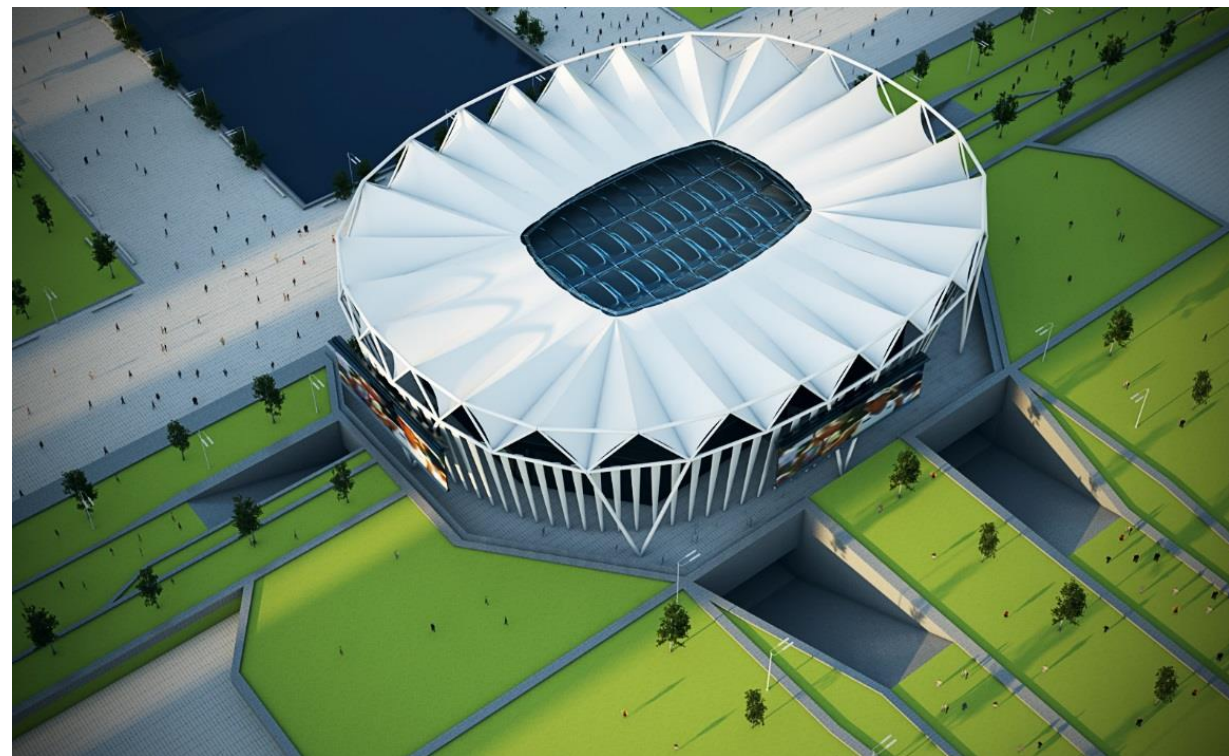


Figure 8 – Aerial View of Proposed Solution (Rendering: Miguel Cristina/João Abrantes)

The ETFE cushions inner roof are hanging on the outer membrane roof. The inner roof is made of two parts which slide under the outer roof. The outer membrane roof is a “modified spoked wheel system”, where the steel compression ring is parallel at only certain parts to the tension cable ring.



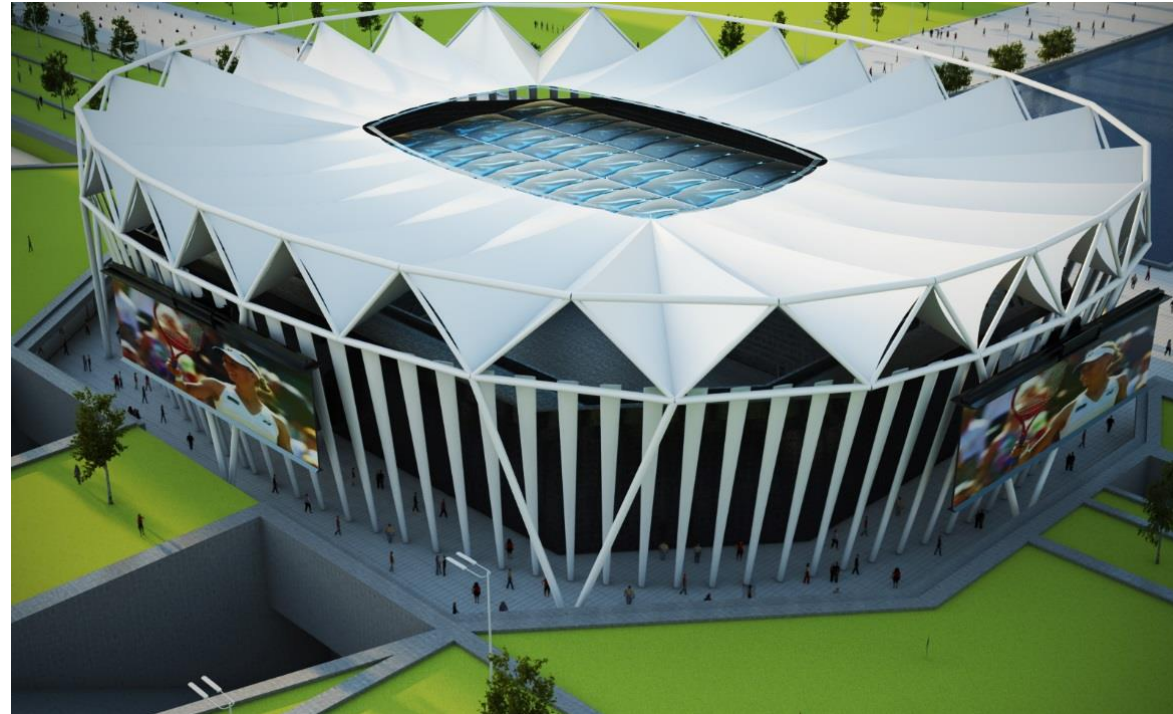


Figure 9 – Side View of Proposed Solution (Rendering: Miguel Cristina/João Abrantes)



Figure 10 – Front View of Proposed Solution (Rendering: Miguel Cristina /João Abrantes)

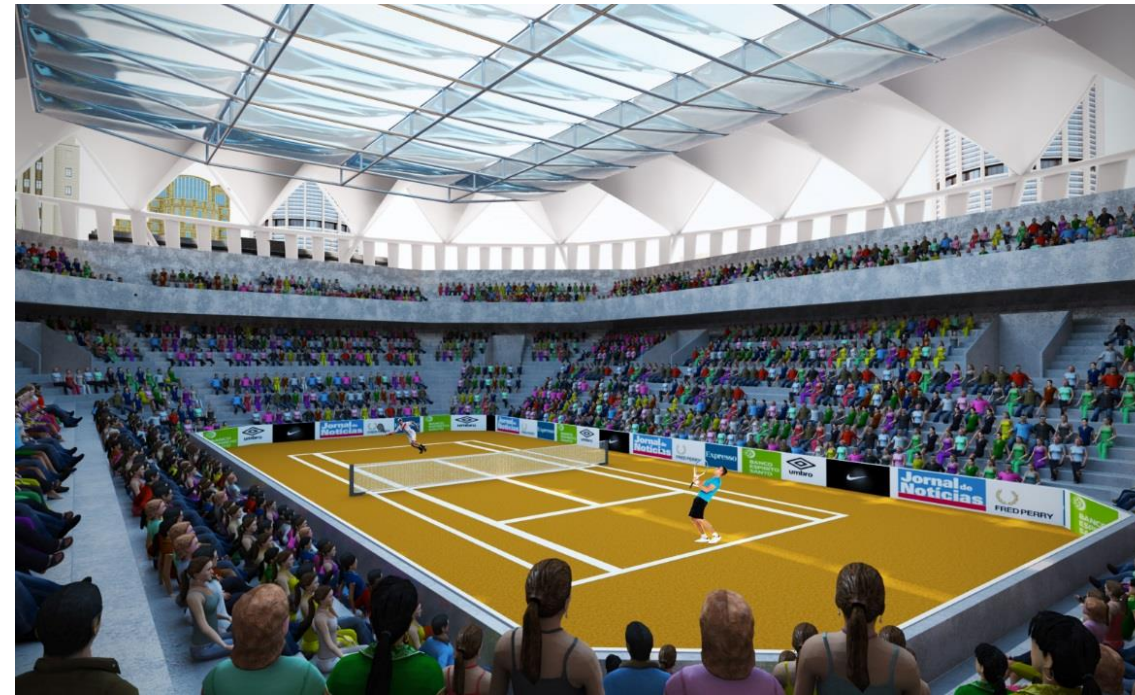


Figure 11 – Inner View of Proposed Solution (Rendering: Miguel Cristina/João Abrantes)

## 2.2 Formfinding

Through the Formfinding process an equilibrium of the geometry and structural elements is determined. Formfinding can be used for membrane structures, cables and also for steel structures. At an initial stage, the structure presents a deflection under dead load and under a predetermined prestress condition. After the reshape of the structural elements such as membrane, cables and steel, the deformation of the structural elements tend to decrease. An iterative process of finding a new form is then made and the structure deformation tend to zero, being usually a convergent solution. The initial prestress state of the membrane and cables determines the end geometry of the structural elements.

There are several methods to do the Formfinding process of a structure. The most common ones is the force-density method.

1) The force density method can be described as:

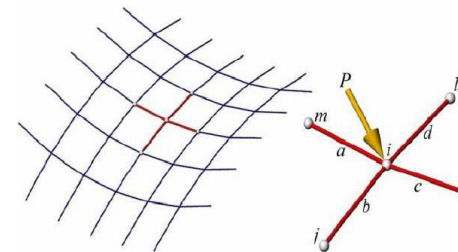


Figure 12 - Force Density - Point i Analysis (Source: Google images)

Non – linear Equations:

$$\begin{aligned}
 x: \frac{x_m - x_i}{l_a} s_a + \frac{x_j - x_i}{l_b} s_b + \frac{x_k - x_i}{l_c} s_c + \frac{x_l - x_i}{l_d} s_d - p_x &= 0 \\
 y: \frac{y_m - y_i}{l_a} s_a + \frac{y_j - y_i}{l_b} s_b + \frac{y_k - y_i}{l_c} s_c + \frac{y_l - y_i}{l_d} s_d - p_y &= 0 \\
 z: \frac{z_m - z_i}{l_a} s_a + \frac{z_j - z_i}{l_b} s_b + \frac{z_k - z_i}{l_c} s_c + \frac{z_l - z_i}{l_d} s_d - p_z &= 0
 \end{aligned}$$

Force Density:  $q = \frac{s}{l}$

Linear Equations by defining the force density q:

$$\begin{aligned}
 x: (x_m - x_i)q_a + (x_j - x_i)q_b + (x_k - x_i)q_c + (x_l - x_i)q_d - p_x &= 0 \\
 y: (y_m - y_i)q_a + (y_j - y_i)q_b + (y_k - y_i)q_c + (y_l - y_i)q_d - p_y &= 0 \\
 z: (z_m - z_i)q_a + (z_j - z_i)q_b + (z_k - z_i)q_c + (z_l - z_i)q_d - p_z &= 0
 \end{aligned}$$

- 2) For the Membrane Formfinding, the stiffness of the membrane was reduced to a value near zero, so that the induced prestress together with the dead load defines the shape of the membrane. Once the geometry is updated, the stiffness can be set to “normal” stiffness of the fabric.
- 3) The stiffness of the steel cables were also set to a value near zero during the Formfinding process, being just adjusted the prestress level.
- 4) The initial geometry of the steel compression rings, given by the architecture, was changed in order to reduce the bending moments and reduce material. By reducing the bending moments, the cross section can be also reduced and the solution is more economical.

The initial bending moments Mz of the steel compression rings present a value of 1083 kNm. After an iterative process of form finding, the bending moments of the steel compression rings are 179 kNm. The reduction is dramatic showing that a Formfinding process leads also to economic solutions.



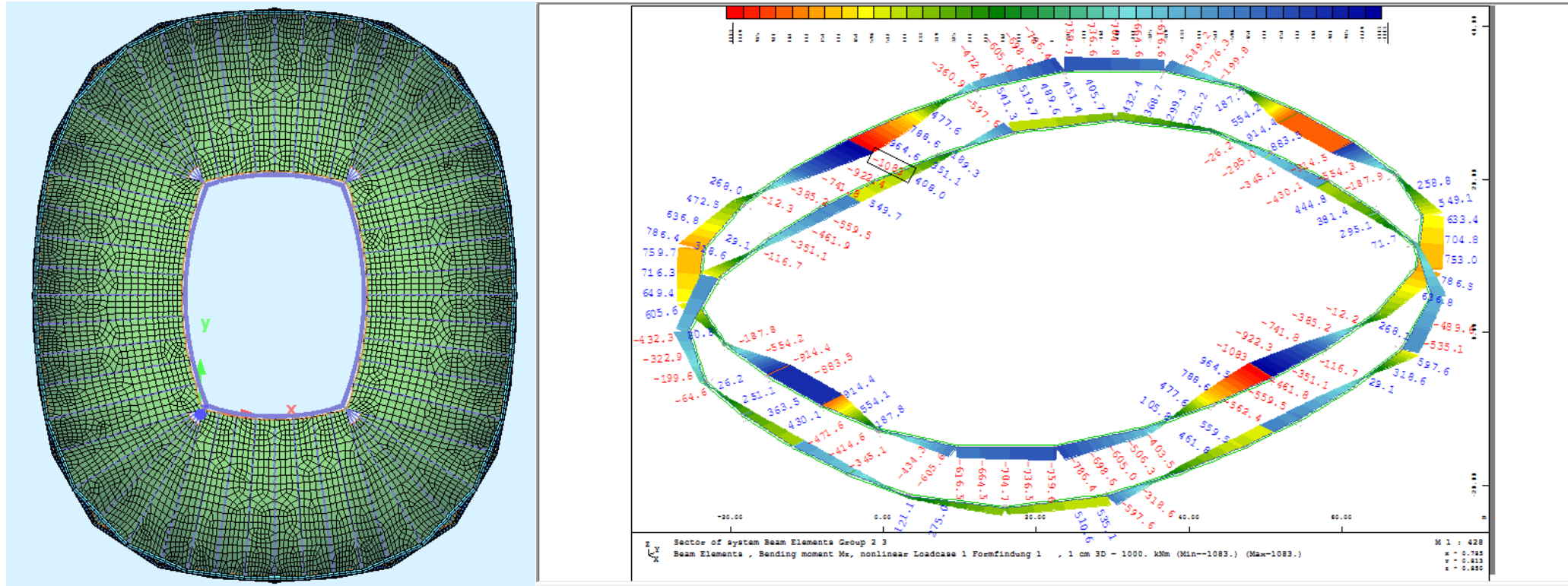


Figure 13 – Initial Geometry, before Formfinding  $M_{z,max} = 1083 \text{ kNm}$

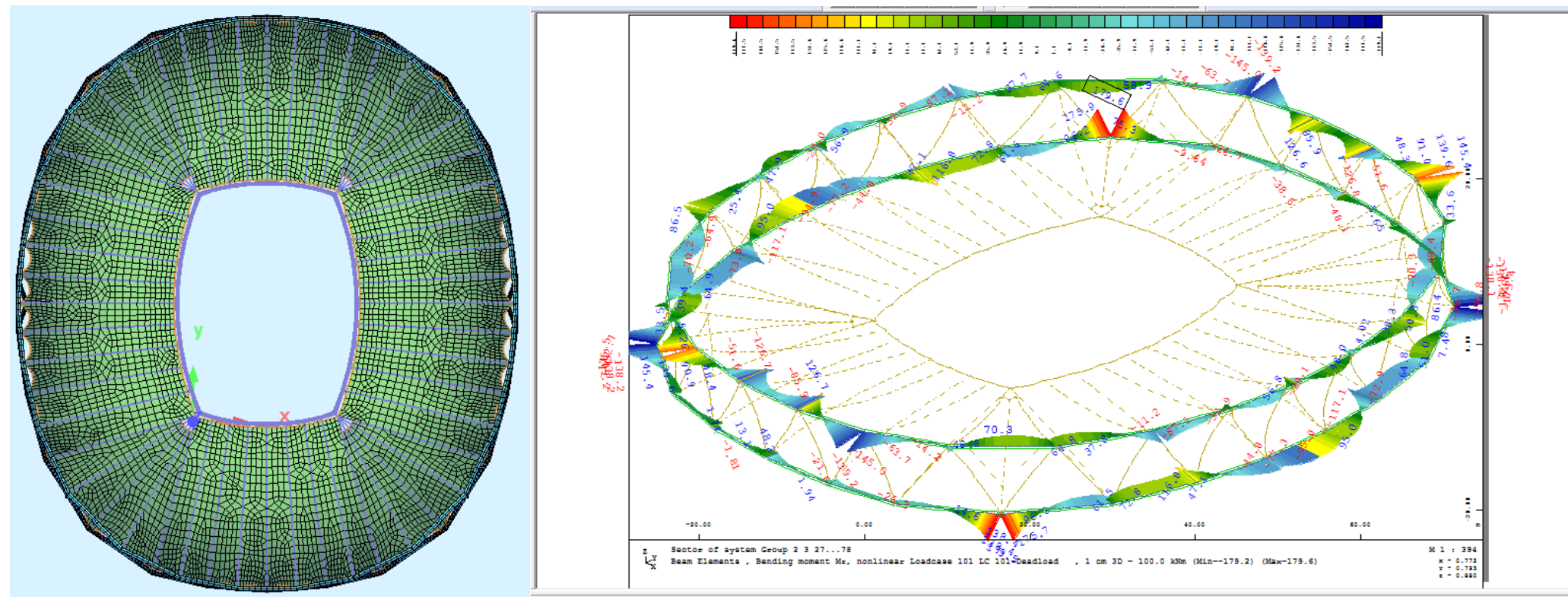


Figure 14 – Corrected Geometry, after Formfinding  $M_{z,max} = 179 \text{ kNm}$





### 3 Materials



### 3. Materials

#### 3.1 Membrane Roof PVC coated Polyester Fabric

These were the values adopted for the structural analysis:

Material	Type	Tensile Strength $Z_r, k$		Tensile Stiffness $EA$		Shear Stiffness $GA$	Self Weight $g$
		Warp	Fill	Warp	Fill		
Ferrari 1202		N/5 cm	N/5 cm	MN	MN	MN	kN/m <sup>2</sup>
PVC/PES	III	5600	5600	1.0	0.7	0.07	0.010

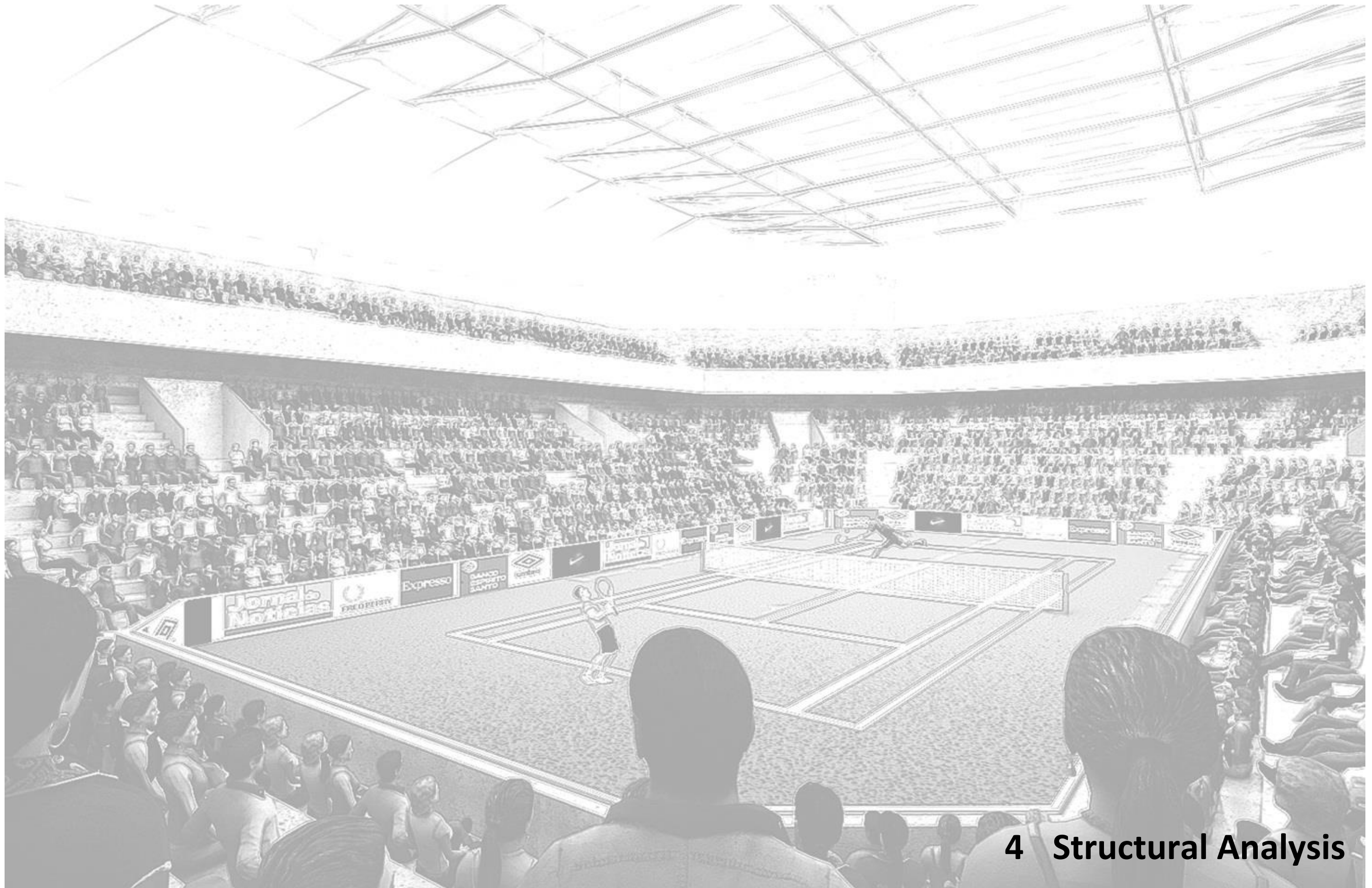
For a construction design, material tests should be carried to define in a more accurate way the material characteristics.

#### 3.2 ETFE Cushions

These were the values adopted for the structural analysis:

ETFE Film - material data (T=23 Degrees , monoaxial Test)							
Material	Thickness	Tensile Strength $F_u, k$	Yield Strength $f_y, k$	Tensile Modulus $E$	Shear Modulus $G$	Poisson's Ratio	Density
		N/mm <sup>2</sup>	N/mm <sup>2</sup>	N/mm <sup>2</sup>	N/mm <sup>2</sup>	-	g/cm <sup>3</sup>
ETFE	250 $\mu$ m	48	21	900	310	0,45	1,75

For a construction design, material tests should be carried to define in a more accurate way the material characteristics.



## 4 Structural Analysis

## 4. Structural Analysis

### 4.1 Software

The software used for the structural analysis is called SOFiSTiK. This finite element program is based on a modular basis where all modules interchange data and save their results in a common database in a binary format. The results in this database can be accessed either by graphical interactive modules or by modules that run in batch mode and have ASCII input.

The following modules are used:

- **AQUA** calculates the properties of cross sections of any shape and made of any material. The cross section properties for a static analysis are determined, as well as characteristic magnitudes for the calculation of normal and shear stresses.
- **ASE** calculates the static and dynamic effects of general loading on any type of structure. To start the calculations the user divides the structure to be analyzed into an assembly of individual elements interconnected at nodes (Finite Element Method). Possible types of elements are: haunched beams, springs, cables, truss elements, plane triangular or quadrilateral shell elements and three-dimensional continuum elements.

The program handles structures with rigid or elastic types of support. An elastic support can be applied to an area, a line or at nodal points. Rigid elements or skew supports can be taken into account.

ASE calculates the effects of nodal, line and block loads. The loads can be defined independently from the selected element mesh. The generation of loads from stresses of a primary loadcase allows the consideration of construction stages, redistribution and creep effects.

Nonlinear calculations enables the user to take the failure of particular elements into account, such as: cables in compression, uplifting of supported plates, yielding, and friction or crack effects for spring and foundation elements.

Nonlinear materials are available for three-dimensional and shell elements.

Geometrical nonlinear computations allow the investigation of 2nd and 3rd order theory effects by cable, beam and shell structures. In case of beam structures, the program can calculate warping torsion with up to 7 degrees of freedom per node.

The analysis of folded structures or shells with finite elements requires considerable experience. The user of ASE should therefore gather experience from simple examples before tackling more complicated structures. A check of the results through approximate engineering calculations is imperative.

The structural analysis of the membrane roof is based on a geometrically non-linear calculation.

The software ixForten 4000 is used for patterning and wind local analysis.

## 4.2 Structural System

Groups								
Grp	Number	type	min-no	max-no	Title			
2	292	BEAM	1	292	Compression	Ring	Upper	
3	300	BEAM	1001	1300	Compression	Ring	Lower	
4	544	BEAM	2001	2544	Compression	Ring	Diagonals	
7	565	CABL	3001	3565	Ring	Cables		
10	145	CABL	4001	4145	Connection			
11	168	BEAM	5001	5168	V-Columns			
13	176	CABL	6001	6176	Edge	Cables	Front	
14	520	CABL	7001	7520	Edge	Cables	Back	
17	176	BEAM	8001	8176	V-Columns			
27	146	QUAD	9001	9146	Memb	1		
28	146	QUAD	10001	10146	Memb	2		
29	128	QUAD	11001	11128	Memb	3		
30	130	QUAD	12001	12130	Memb	4		
31	141	QUAD	13001	13141	Memb	5		
32	156	QUAD	14001	14156	Memb	6		
33	104	QUAD	15001	15104	Memb	7		
34	102	QUAD	16001	16102	Memb	8		
35	92	QUAD	17001	17092	Memb	9		
36	107	QUAD	18001	18107	Memb	10		
37	115	QUAD	19001	19115	Memb	11		
38	142	QUAD	20001	20142	Memb	12		
39	118	QUAD	21001	21118	Memb	13		
40	144	QUAD	22001	22144	Memb	14		
41	144	QUAD	23001	23144	Memb	15		
42	134	QUAD	24001	24134	Memb	16		
43	138	QUAD	25001	25138	Memb	17		
44	123	QUAD	26001	26123	Memb	18		
45	107	QUAD	27001	27107	Memb	19		
46	92	QUAD	28001	28092	Memb	20		
47	102	QUAD	29001	29102	Memb	21		
48	92	QUAD	30001	30092	Memb	22		
49	151	QUAD	31001	31151	Memb	23		
50	141	QUAD	32001	32141	Memb	24		
51	154	QUAD	33001	33154	Memb	25		
52	136	QUAD	34001	34136	Memb	26		

53	142	QUAD	35001	35142	Memb	27		
54	146	QUAD	36001	36146	Memb	28		
55	136	QUAD	37001	37136	Memb	29		
56	154	QUAD	38001	38154	Memb	30		
57	141	QUAD	39001	39141	Memb	31		
58	153	QUAD	40001	40153	Memb	32		
59	92	QUAD	41001	41092	Memb	33		
60	102	QUAD	42001	42102	Memb	34		
61	92	QUAD	43001	43092	Memb	35		
62	107	QUAD	44001	44107	Memb	36		
63	123	QUAD	45001	45123	Memb	37		
64	138	QUAD	46001	46138	Memb	38		
65	134	QUAD	47001	47134	Memb	39		
66	144	QUAD	48001	48144	Memb	40		
67	144	QUAD	49001	49144	Memb	41		
68	134	QUAD	50001	50134	Memb	42		
69	138	QUAD	51001	51138	Memb	43		
70	123	QUAD	52001	52123	Memb	44		
71	107	QUAD	53001	53107	Memb	45		
72	94	QUAD	54001	54094	Memb	46		
73	102	QUAD	55001	55102	Memb	47		
74	108	QUAD	56001	56108	Memb	48		
75	151	QUAD	57001	57151	Memb	49		
76	141	QUAD	58001	58141	Memb	50		
77	154	QUAD	59001	59154	Memb	51		
78	136	QUAD	60001	60136	Memb	52		
79	24	CABL	61001	61024	Upper	Radial	C	1
80	24	CABL	62001	62024	Upper	Radial	C	2
81	22	CABL	63001	63022	Upper	Radial	C	3
82	21	CABL	64001	64021	Upper	Radial	C	4
83	21	CABL	65001	65021	Upper	Radial	C	5
84	22	CABL	66001	66022	Upper	Radial	C	6
85	22	CABL	67001	67022	Upper	Radial	C	7
86	22	CABL	68001	68022	Upper	Radial	C	8
87	22	CABL	69001	69022	Upper	Radial	C	9
88	21	CABL	70001	70021	Upper	Radial	C	10
89	21	CABL	71001	71021	Upper	Radial	C	11
90	22	CABL	72001	72022	Upper	Radial	C	12
91	24	CABL	73001	73024	Upper	Radial	C	13
92	24	CABL	74001	74024	Upper	Radial	C	14
93	24	CABL	75001	75024	Upper	Radial	C	15
94	22	CABL	76001	76022	Upper	Radial	C	16

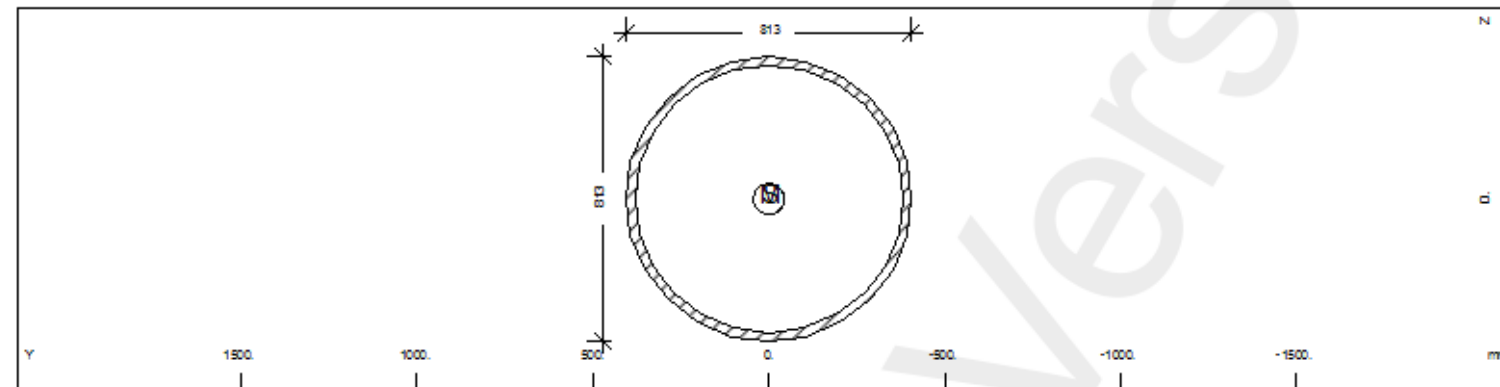


95	21	CABL	77001	77021	Upper	Radial	C	17
96	21	CABL	78001	78021	Upper	Radial	C	18
97	22	CABL	79001	79022	Upper	Radial	C	19
98	22	CABL	80001	80022	Upper	Radial	C	20
99	22	CABL	81001	81022	Upper	Radial	C	21
100	22	CABL	82001	82022	Upper	Radial	C	22
101	21	CABL	83001	83021	Upper	Radial	C	23
102	21	CABL	84001	84021	Upper	Radial	C	24
103	22	CABL	85001	85022	Upper	Radial	C	25
104	24	CABL	86001	86024	Upper	Radial	C	26
105	22	CABL	87001	87022	Lower	Radial	C	1
106	22	CABL	88001	88022	Lower	Radial	C	2
107	22	CABL	89001	89022	Lower	Radial	C	3
108	21	CABL	90001	90021	Lower	Radial	C	4
109	22	CABL	91001	91022	Lower	Radial	C	5
110	20	CABL	92001	92020	Lower	Radial	C	6
111	20	CABL	93001	93020	Lower	Radial	C	7
112	20	CABL	94001	94020	Lower	Radial	C	8
113	22	CABL	95001	95022	Lower	Radial	C	9
114	21	CABL	96001	96021	Lower	Radial	C	10
115	22	CABL	97001	97022	Lower	Radial	C	11
116	22	CABL	98001	98022	Lower	Radial	C	12
117	22	CABL	99001	99022	Lower	Radial	C	13
118	22	CABL	100001	100022	Lower	Radial	C	14
119	22	CABL	101001	101022	Lower	Radial	C	15
120	22	CABL	102001	102022	Lower	Radial	C	16
121	21	CABL	103001	103021	Lower	Radial	C	17
122	22	CABL	104001	104022	Lower	Radial	C	18
123	20	CABL	105001	105020	Lower	Radial	C	19
124	20	CABL	106001	106020	Lower	Radial	C	20
125	20	CABL	107001	107020	Lower	Radial	C	21
126	22	CABL	108001	108022	Lower	Radial	C	22
127	21	CABL	109001	109021	Lower	Radial	C	23
128	22	CABL	110001	110022	Lower	Radial	C	24
129	22	CABL	111001	111022	Lower	Radial	C	25
130	22	CABL	112001	112022	Lower	Radial	C	26

4.3 Materials and Sections

Upper Compression Ring:

Cross section No. 1 - D 813 / 25 mm



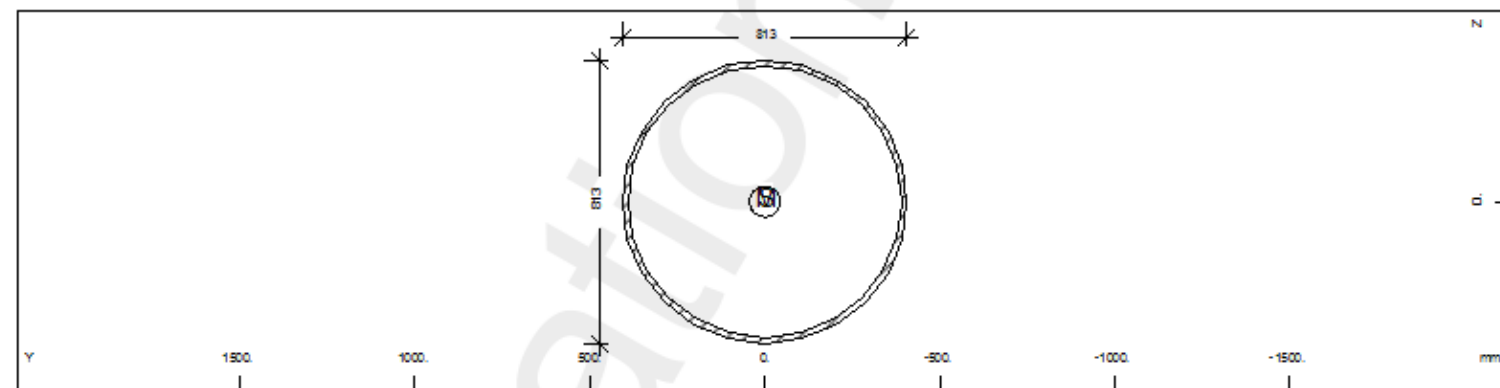
Cross section No. 1 - D 813 / 25 mm

Static properties of cross section

No.	Mat	A[m2]	Ay/Az/Ayz [m2]	Iy/Iz/Iyz [m4]	ys/zs [mm]	y/z-sc [mm]	modules [N/mm2]	gam [kN/m]
1	=	D 813 / 25 mm						
	NoR	It[m4]						
	1	6.1889E-02	3.172E-02	4.809E-03	0.0	0.0	210000	4.86
		9.617E-03	3.172E-02	4.809E-03	0.0	0.0	80769	

Lower Compression Ring:

Cross section No. 2 - D 813 / 16 mm



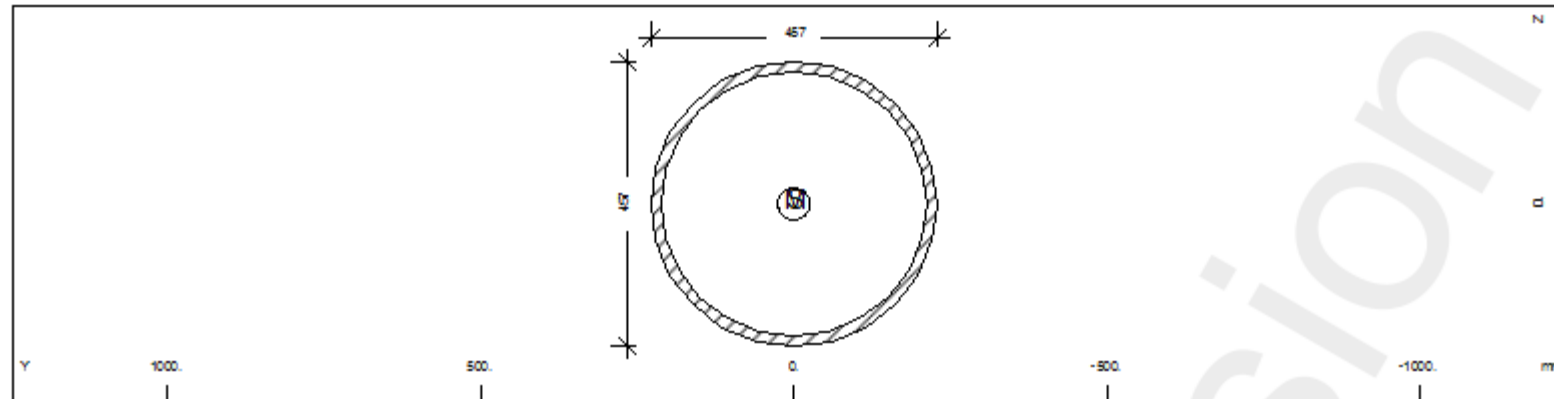
Cross section No. 2 - D 813 / 16 mm

Static properties of cross section

No.	Mat	A[m2]	Ay/Az/Ayz [m2]	Iy/Iz/Iyz [m4]	ys/zs [mm]	y/z-sc [mm]	modules [N/mm2]	gam [kN/m]
2	=	D 813 / 16 mm						
	NoR	It[m4]						
	1	4.0062E-02	2.035E-02	3.182E-03	0.0	0.0	210000	3.14
		6.364E-03	2.035E-02	3.182E-03	0.0	0.0	80769	

Diagonals:

Cross section No. 3 - D 457 / 16 mm



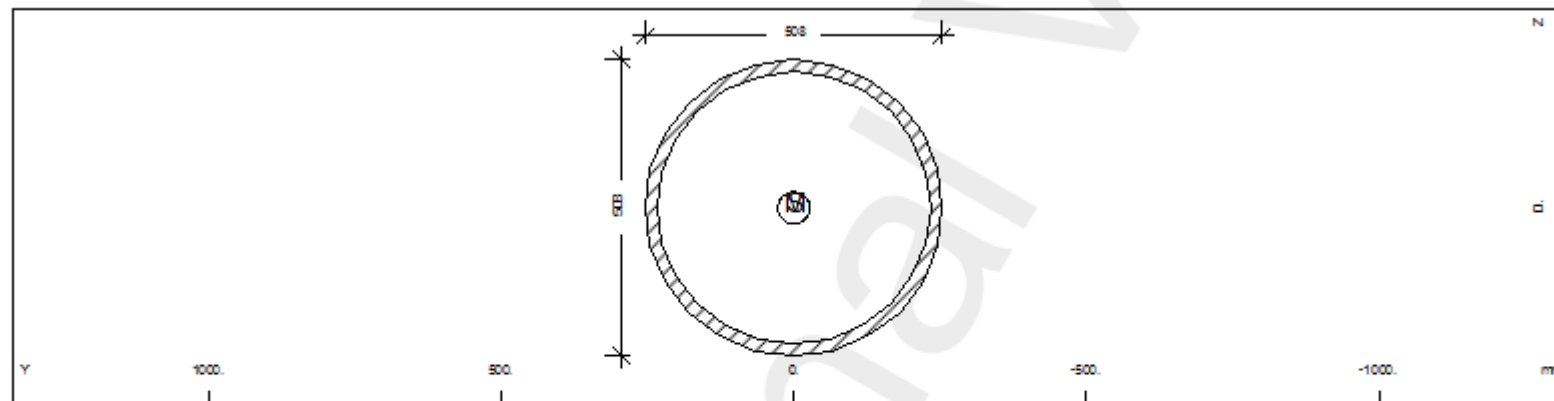
Cross section No. 3 - D 457 / 16 mm

Static properties of cross section

No.	Mat	A[m2]	Ay/Az/Ayz	Iy/Iz/Iyz	ys/zs	y/z-sc	modules	gam
	NoR	It[m4]	[m2]	[m4]	[mm]	[mm]	[N/mm2]	[kN/m]
3	=	D 457 / 16 mm						
	1	2.2167E-02	1.140E-02	5.396E-04	0.0	0.0	210000	1.74
		1.079E-03	1.140E-02	5.396E-04	0.0	0.0	80769	

V - Columns:

Cross section No. 4 - D 508 / 20 mm



Cross section No. 4 - D 508 / 20 mm

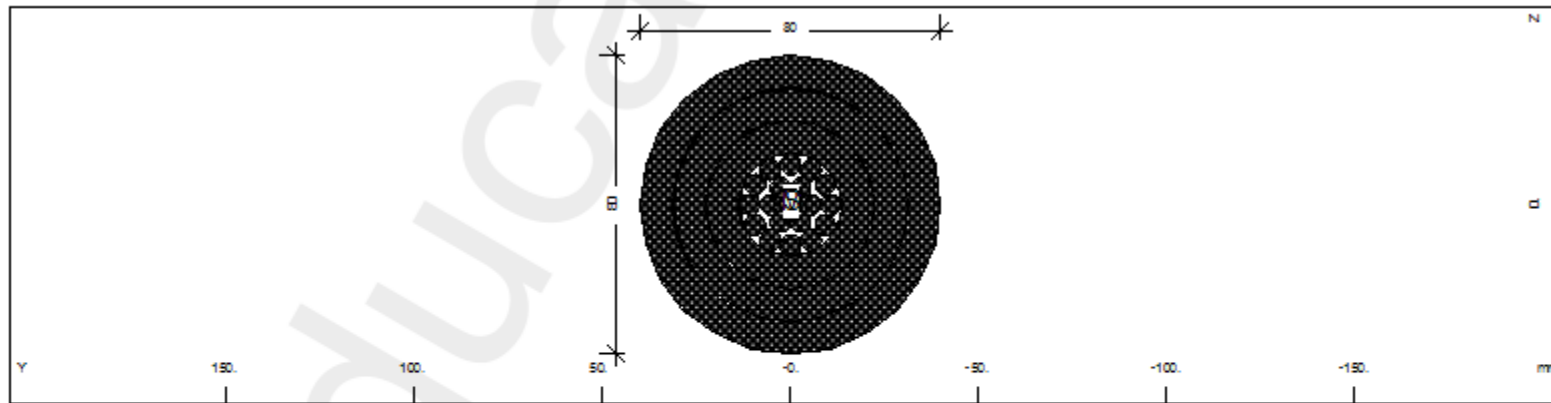
Static properties of cross section

No.	Mat	A[m2]	Ay/Az/Ayz	Iy/Iz/Iyz	ys/zs	y/z-sc	modules	gam
	NoR	It[m4]	[m2]	[m4]	[mm]	[mm]	[N/mm2]	[kN/m]
4	=	D 508 / 20 mm						
	1	3.0662E-02	1.582E-02	9.143E-04	0.0	0.0	210000	2.41
		1.829E-03	1.582E-02	9.143E-04	0.0	0.0	80769	



Upper Radial Cables:

Cross section No. 5 - Cable 80 PV-640 - SEL



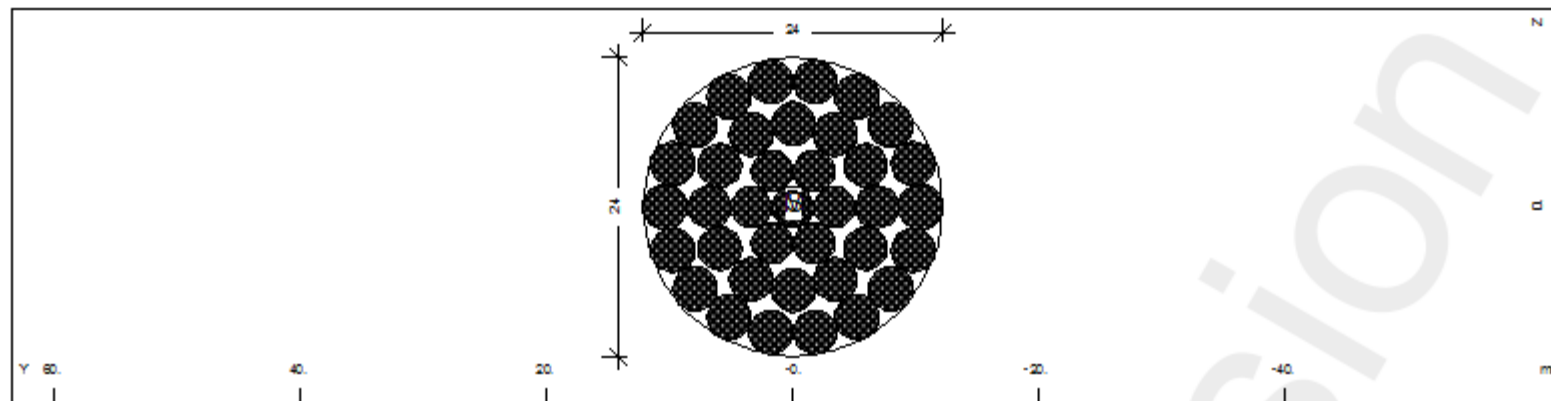
Cross section No. 5 - Cable 80 PV-640 - SEL

Static properties of cross section

No.	Mat	A[m2]	Ay/Az/Ayz	Iy/Iz/Iyz	ys/zs	y/z-sc	modules	gam
	NoR	It[m4]	[m2]	[m4]	[mm]	[mm]	[N/mm2]	[kN/m]
5	=	Cable 80	PV-640 - SEL					
(CABL)	3	4.4198E-03		1.768E-06	0.0	0.0	160000	0.36
		0.000E+00		1.768E-06	0.0	0.0	61538	

Front and Back Edge Cables:

Cross section No. 6 - Cable 24.4 PG-55



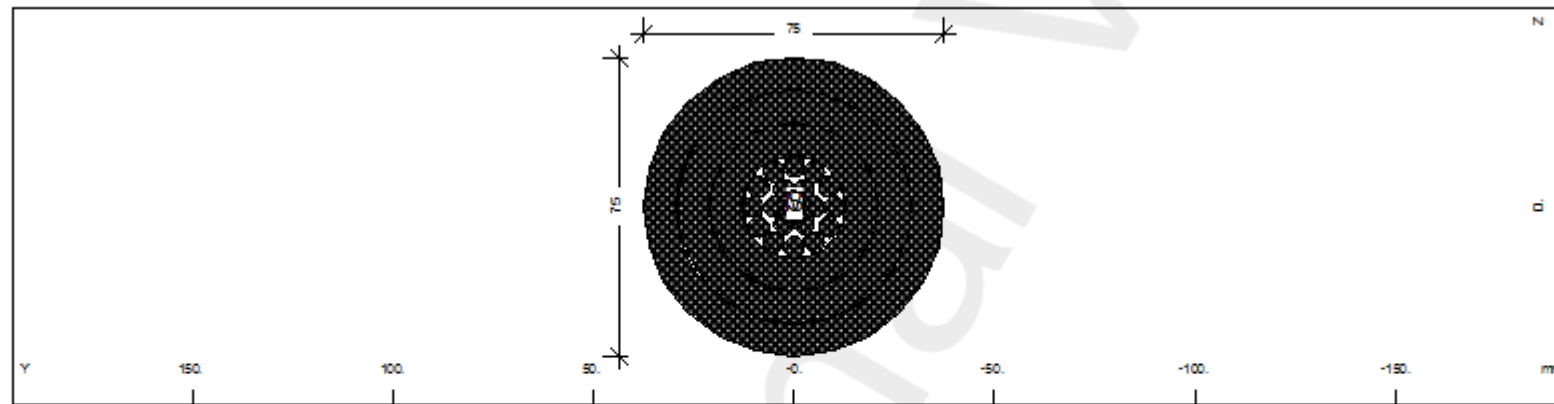
Cross section No. 6 - Cable 24.4 PG-55

Static properties of cross section

No.	Mat	A[m2]	Ay/Az/Ayz	Iy/Iz/Iyz	ys/zs	y/z-sc	modules	gam
	NoR	It[m4]	[m2]	[m4]	[mm]	[mm]	[N/mm2]	[kN/m]
6	=	Cable 24.4	PG-55					
(CABL)	2	3.4700E-04		1.291E-08	0.0	0.0	160000	0.03
		0.000E+00		1.291E-08	0.0	0.0	61538	

Tension Ring Cables:

Cross section No. 7 - Cable 75 PV-560 - SEL



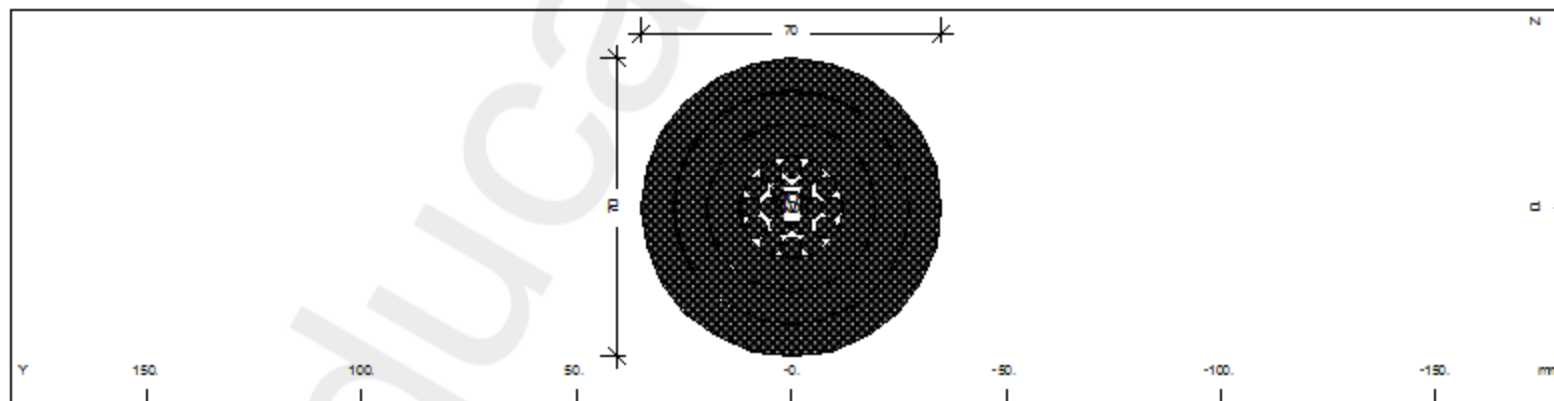
Cross section No. 7 - Cable 75 PV-560 - SEL

Static properties of cross section

No.	Mat	A[m2]	Ay/Az/Ayz	Iy/Iz/Iyz	ys/zs	y/z-sc	modules	gam
	NoR	It[m4]	[m2]	[m4]	[mm]	[mm]	[N/mm2]	[kN/m]
7	=	Cable 75	PV-560 - SEL					
(CABL)	3	3.8903E-03		1.368E-06	0.0	0.0	160000	0.32
		0.000E+00		1.368E-06	0.0	0.0	61538	

Lower Radial Cables:

Cross section No. 8 - Cable 70 PV-490 - SEL



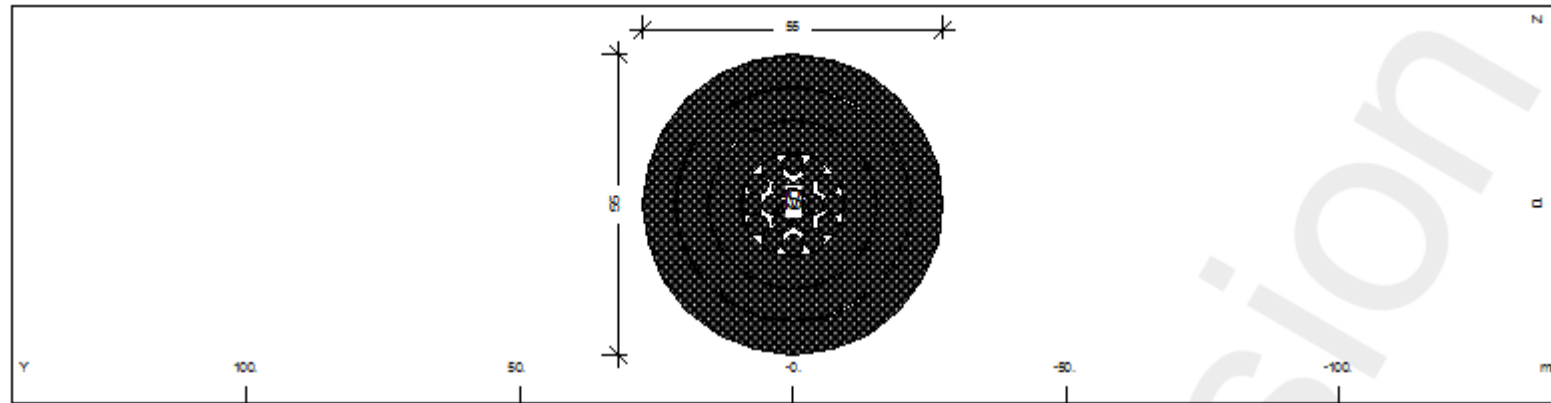
Cross section No. 8 - Cable 70 PV-490 - SEL

Static properties of cross section

No.	Mat	A[m2]	Ay/Az/Ayz	Iy/Iz/Iyz	ys/zs	y/z-sc	modules	gam
	NoR	It[m4]	[m2]	[m4]	[mm]	[mm]	[N/mm2]	[kN/m]
8	=	Cable 70	PV-490 - SEL					
(CABL)	3	3.3898E-03		1.038E-06	0.0	0.0	160000	0.28
		0.000E+00		1.038E-06	0.0	0.0	61538	

Upper and Lower Radial Cables:

Cross section No. 9 - Cable 55 PV-300 - SEL



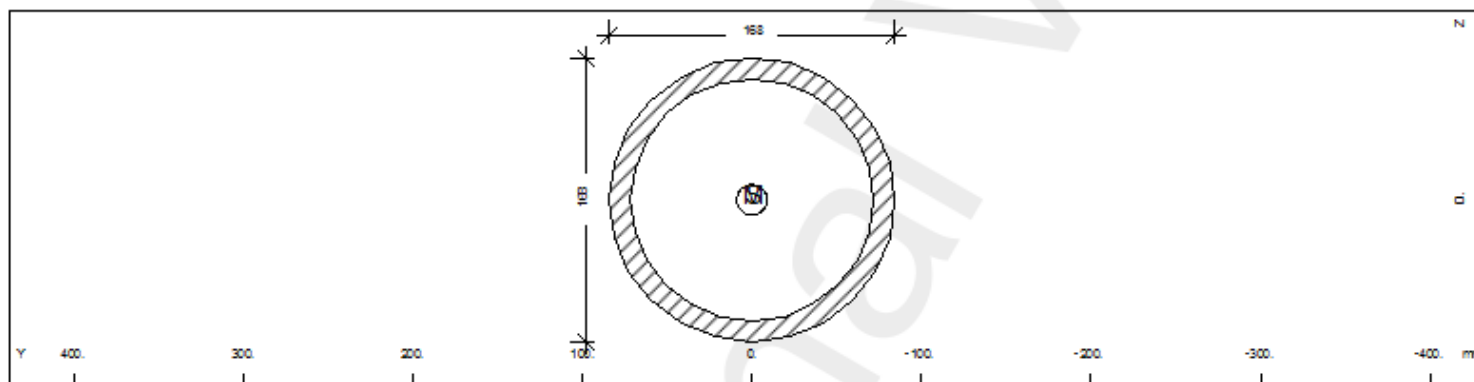
Cross section No. 9 - Cable 55 PV-300 - SEL

Static properties of cross section

No.	Mat	A[m2]	Ay/Az/Ayz	Iy/Iz/Iyz	ys/zs	y/z-sc	modules	gam
	NoR	It[m4]	[m2]	[m4]	[mm]	[mm]	[N/mm2]	[kN/m]
9	=	Cable 55 PV-300 - SEL						
(CABL)	3	2.0900E-03		3.951E-07	0.0	0.0	160000	0.17
		0.000E+00		3.951E-07	0.0	0.0	61538	

Helpers:

Cross section No. 10 - D 168.3 / 12.5 mm



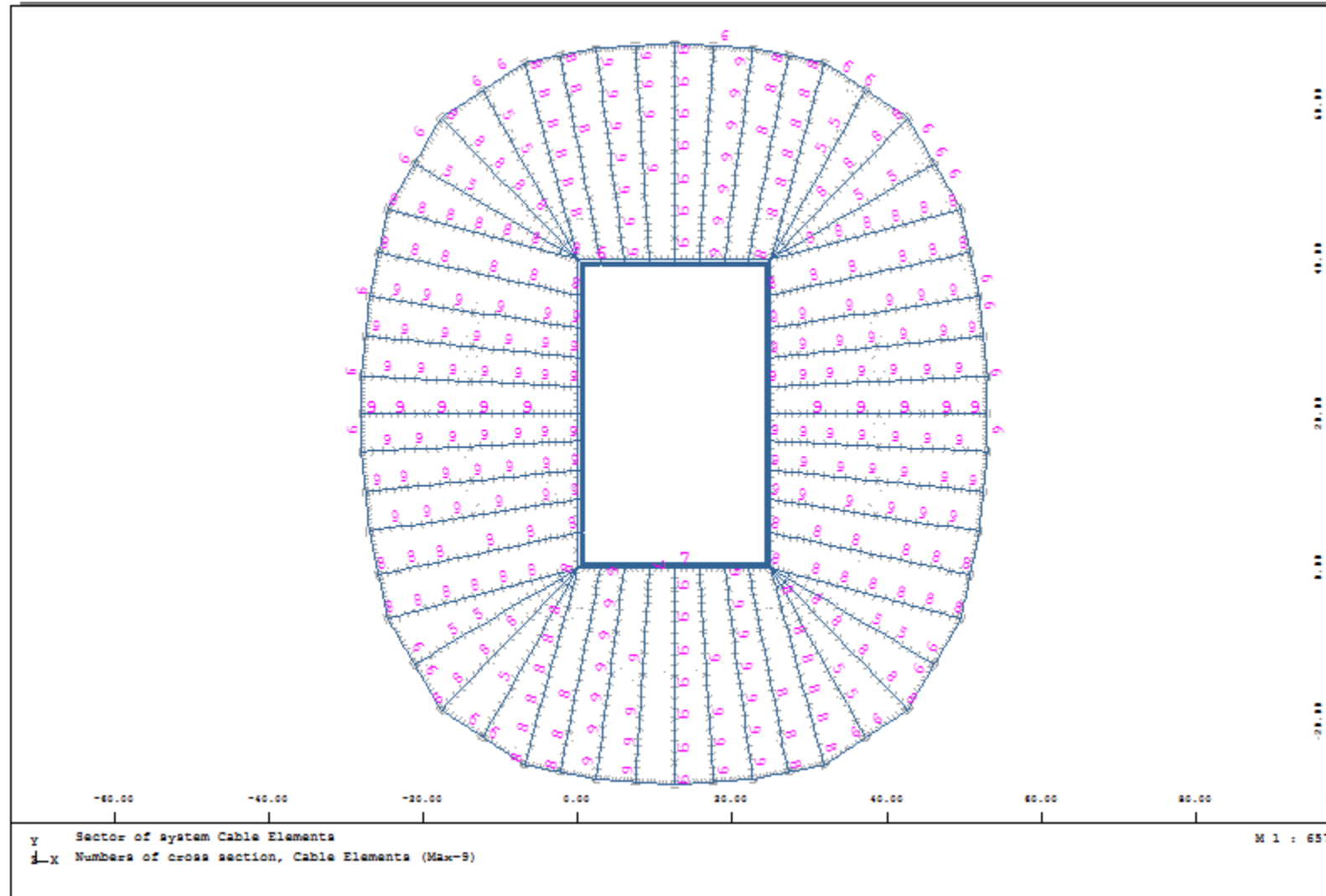
Cross section No. 10 - D 168.3 / 12.5 mm

Static properties of cross section

No.	Mat	A[m2]	Ay/Az/Ayz	Iy/Iz/Iyz	ys/zs	y/z-sc	modules	gam
	NoR	It[m4]	[m2]	[m4]	[mm]	[mm]	[N/mm2]	[kN/m]
10	=	D 168.3 / 12.5 mm						
	1	6.1183E-03	3.248E-03	1.868E-05	0.0	0.0	210000	0.48
		3.737E-05	3.248E-03	1.868E-05	0.0	0.0	80769	



Cable Arrangement and Cross Section numbers for Upper and Lower Radial Cables, including Front and Back Edge Cables:



#### 4.4 Loads Assumptions

##### 4.4.1 Dead Load

Respectively for reinforced concrete and steel, using the section values and a unit weight of 25.0 kN/m<sup>3</sup> and 78.5 kN/m<sup>3</sup>.

Extraordinary details of Structural Steelwork are considered with additional nodal loads (e.g. steel cast cable nodes). Further primary steel structure that is not modeled within the global model is considered as additional loads, linear or nodal onto the primary structure.

For Cables, using the section values and a unit weight of 83.0 kN/m<sup>3</sup> (includes corrosion protection)

##### 4.4.2 Prestress

Cable supported structures require a regular pre stressed initial stage. Therefore prestress is a regular part of all stages of investigations together with the dead load. All cables and membranes are regular pre stressed according to the results of the form finding process.

This needs to be considered for the determination of the cutting length of the cables and the fabrication geometry of the steel structure.

##### 4.4.3 Live Load

The roof is considered Category H with a load of 0.4 kN/m<sup>2</sup>, not accessible except for normal maintenance and repair. It is not to be superimposed with other extreme loads. Since the wind loads are much higher than the live load, the live load will not be taken into account in the structural analysis.

##### 4.4.4 Temperature

The city of Oeiras in Portugal is located in the Zone B according to the EN 1991 1-5.

T<sub>max</sub> (summer) : 40 Degrees

T<sub>min</sub> (winter) : 0 Degrees

T<sub>in</sub> (summer) : 25 Degrees

T<sub>in</sub> (winter) : 18 Degrees

Uniform Variation:

Summer:  $T = (40+2+25)/2 = 34.5$  Degrees

Winter:  $T = (0+18)/2 = 9$  Degrees

## 4.4.5 Wind Load

(1) The basic wind velocity shall be calculated:

$$V_b = C_{dir} \cdot C_{season} \cdot V_{b,0}$$

$$C_{dir} = 1.0$$

$$C_{season} = 1.0$$

According to the National Annex to the Eurocode:

$$v_{b,0} = 30 \text{ m/s (Zone B – Near the Coast)}$$

$$v_b = 1.0 \cdot 1.0 \cdot 30 = 30 \text{ m/s}$$

(2) Peak Velocity Pressure

$$q_b = 0.5 \cdot \rho \cdot v_b^2 = 0.56 \text{ kN/m}^2$$

$$Z = 27.32 \text{ m (Maximum Roof Height – On the Safe Side)}$$

Terrain Category – II

$$q_p = C_e(Z) \cdot q_b = 3.0 \cdot 0.56 = 1.7 \text{ kN/m}^2$$

(3) Wind Pressure

*a) Steel Structure Analysis – Global Analysis*

$$F_w = C_s \cdot C_d \cdot C_f \cdot q_p(z_e) \cdot A_{ref}$$

$$C_s = \frac{1+7 \times I_v(z_s) \times \sqrt{B^2}}{1+7 \times I_v(z_s)} = \frac{1+7 \times I_v(z_s) \times \sqrt{1^2}}{1+7 \times I_v(z_s)} = 0.81$$

$$B^2 = 1.0 \text{ (Conservative value)}$$

$$I_v(z) = \frac{k_1}{c_0(z) \times \ln(z/z_0)} = 0.167$$

$$c_0(20) = 1.0$$

$$k_1 = 1.0$$

$$z_0 = 0.05 \text{ m}$$



$z = 20$  m (Maximum column height)

$$c_d = \frac{1 + 2 \times k_p \times I_v(z_s) \times \sqrt{B^2 + R^2}}{1 + 7 \times I_v(z_s) \times \sqrt{B^2}} = 1.0$$

Force Coefficient  $c_f$  for a finite circular cylinder:

$$c_f = c_{f,0} \cdot \Psi_\lambda = 1.2$$

Steel Columns:

$$F_w = 0.81 \cdot 1.0 \cdot 1.2 \cdot 1.7 \cdot 0.45 = 0.75 \text{ kN/m}$$

Compression Ring:

Force Coefficient  $c_f$  for a Spatial Truss Structure:

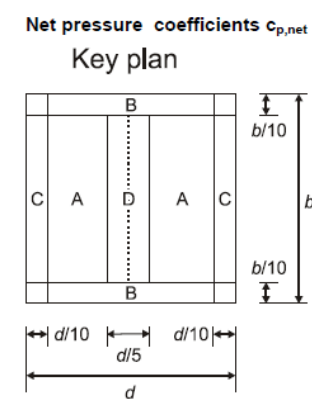
$$c_f = c_{f,0} \cdot \Psi_\lambda = 2.0$$

$$F_w = 0.81 \cdot 1.0 \cdot 2.0 \cdot 1.7 \cdot 1.0 = 2.75 \text{ kN/m}$$

b) PVC - Membrane Roof

$$W = q_p(z) \cdot c_p$$

It is considered a Multibay Canopy Roof. The Net Pressure Coefficients and overall Force Coefficient are according to the Eurocode EN 1991-1-4:2005, Table 7.7 for duo pitch canopies. A reduction factor of 0.8 was considered for the upward forces and pressures in order to consider the Multibay Effect.



Roof Angle	Blockage	Overall Force Coef. Cf	Pressure Coefficients Cp			
			Zone A	Zone B	Zone C	Zone D
55	Maximum All	1.90	1.80	1.90	1.60	1.70
	Minimum 1	-1.04	-1.12	-0.64	-0.72	-1.60
"+ Values indicate a net downward wind action"						
"- Values indicate a net upward wind action"						

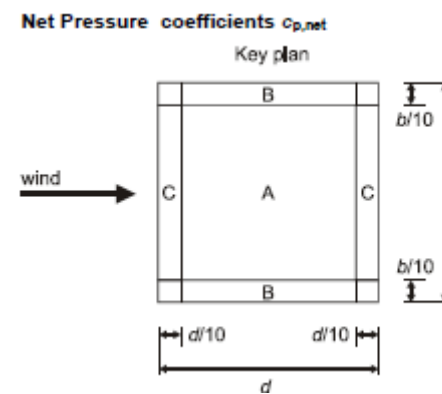
c) ETFE Cushion Roof

$$W = q_p(z) \cdot c_p$$

Z = 20.02 m (ETFE Roof Height)

Terrain Category – II

$$q_p = C_e(Z) \cdot q_b = 2.8 \cdot 0.56 = 1.6 \text{ kN/m}^2$$



Roof Angle	Blockage	Overall Force Coef. Cf	Pressure Coefficients Cp		
			Zone A	Zone B	Zone C
0	Maximum All	0.2	0.5	1.8	1.1
	Minimum 1	-1.3	-1.5	-1.8	-2.2
"+ Values indicate a net downward wind action"					
"- Values indicate a net upward wind action"					

4.4.6 Snow Load

$$S = \mu_i S_k C_e C_t$$

$$S_k = 0.1 \text{ kN/m}^2$$

$$C_e = 1.0$$

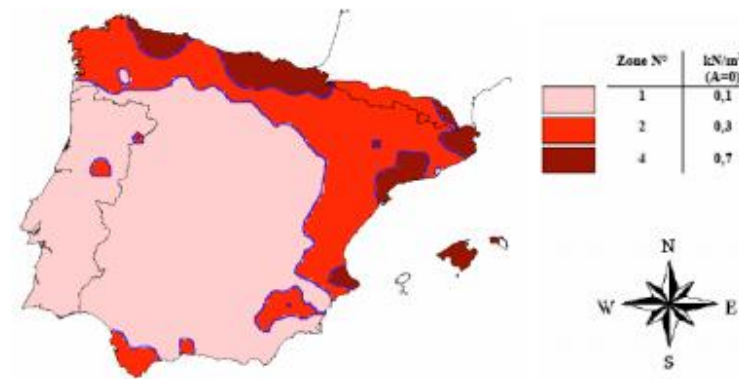
$$C_t = 1.0$$

$$\mu_1 = 0.13$$

$$\mu_2 = 1.60$$

$$S_1 = 0.13 * 0.1 * 1 * 1 = 0.013 \text{ kN/m}^2$$

$$S_2 = 1.60 * 0.1 * 1 * 1 = 0.160 \text{ kN/m}^2$$



Altitude	$\psi_0$	$\psi_1$	$\psi_2$
$h > 1000 \text{ m}$	0.70	0.50	0.20
$h < 1000 \text{ m}$	0.50	0.20	0.00

4.4.7 Imperfections (EN 1993-1-1:2005(D) Cl. 5.3.2)

a) Compression Ring

- Precurvature

Tab. 6.2 Hollow Section -> Buckling curve "a"

Tab. 5.1 Elastic design :  $e_{0,d}/L = 1/300$

Equivalent Horizontal Forces:

$$q_i = 8 N_{ed} e_{0,d} / L^2 = 8 \times 9693 \times 1/300 \times 1/10 = 25.85 \text{ kN/m}$$



$$H_i = 4 N_{ed} e_{0,d} / L = 4 \times 9693 \times 1/300 = 129 \text{ kN}$$

- Preinclination

Compression Ring horizontal inaccuracies (ovalization due to deviation angle in head plates)

Relevant buckling mode shapes for the Compression Ring are scaled to form a maximum imperfection of  $w_0$  which is applied onto the structural steelwork as a stress-free pre deflection.

$$s_k = 48 \text{ m}$$

Structural imperfections:

$$e_0 = L / 300 = 48 \text{ m} / 300 = 160 \text{ mm}$$

Structural part thereof  $e_0 = 50\%$  of  $e_{0,d} = 80 \text{ mm}$

For the stability analyses imperfections for the Compression Ring are considered as:

Using this strategy a maximum tolerance or geometrical imperfection of:

$$w_{geom,k} = 4 \cdot (L_{sys} \cdot \Delta\varphi \cdot 2) = 4 \times 13000 \times 0.5/1000 \times 2 = 52 \text{ mm}, \text{ may occur due to the manufacture of the CR elements } (\pm 0.5\text{mm} / 1000\text{mm} \text{ (2 machined surfaces per element)}).$$

$$w_0, geom. = 1.5 \times 52 = 78$$

$$w_0, struct = 80 \text{ mm}$$

Ersatz imperfections of  $w_{0,d} = w_0, geom + w_0, struct$

$$w_{0,d} = 158 \text{ mm}$$

## b) Diagonals

- Precurvature

Tab. 6.2 Hollow Section -> Buckling curve "a"

Tab. 5.1 Elastic design :  $e_{0,d}/L = 1/300$

Equivalent Horizontal Forces:

$$q_i = 8 N_{ed} e_{0,d} / L^2 = 8 \times 1916 \times 1/300 \times 1/10 = 5 \text{ kN/m}$$

$$H_i = 4 N_{ed} e_{0,d} / L = 4 \times 1916 \times 1/300 = 25 \text{ kN}$$

- Preinclination

$$\phi = \phi_0 \alpha_h \alpha_m$$

$$\phi = 1/200 \times 0.685 \times 0.7 = 0,0024$$

$$H_i = \phi \times N_{ed} = 0.0024 \times 1916 = 4.6 \text{ kN}$$

## c) Columns

- Precurvature
- Tab. 6.2 Hollow Section -> Buckling curve "a"
- Tab. 5.1 Elastic design :  $e_{0,d}/L = 1/300$
- 
- Equilivalent Horizontal Forces:
- $q_i = 8 N_{ed} e_{0,d} / L^2 = 8 \times 2934 \times 1/300 \times 1/20.5 = 3,82 \text{ kN/m}$
- $H_i = 4 N_{ed} e_{0,d} / L = 4 \times 2934 \times 1/300 = 39 \text{ kN}$

- Preinclination

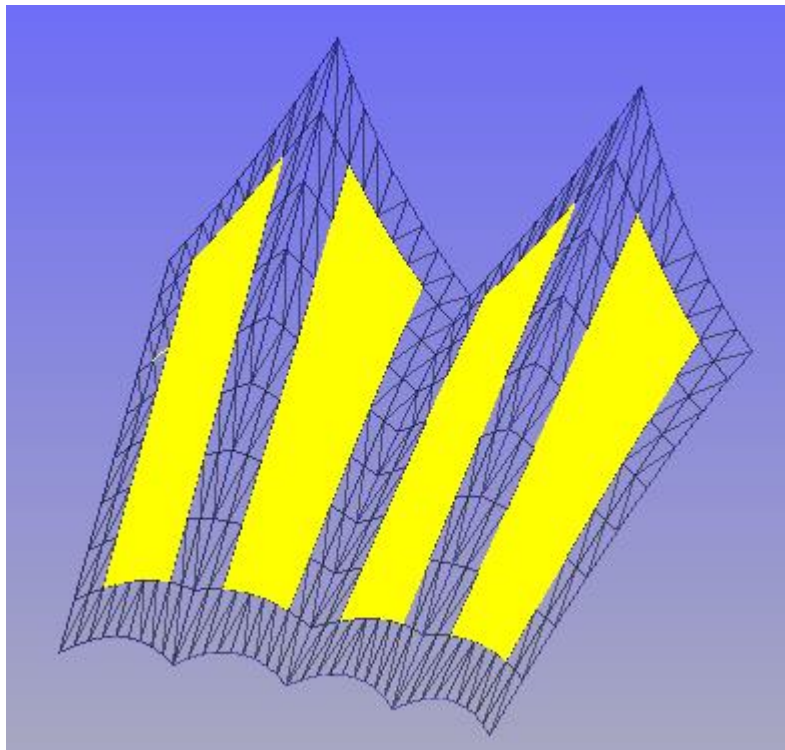
$$\phi = \phi_0 \alpha_h \alpha_m$$

$$\phi = 1/200 \times 0.667 \times 0.73 = 0,0024$$

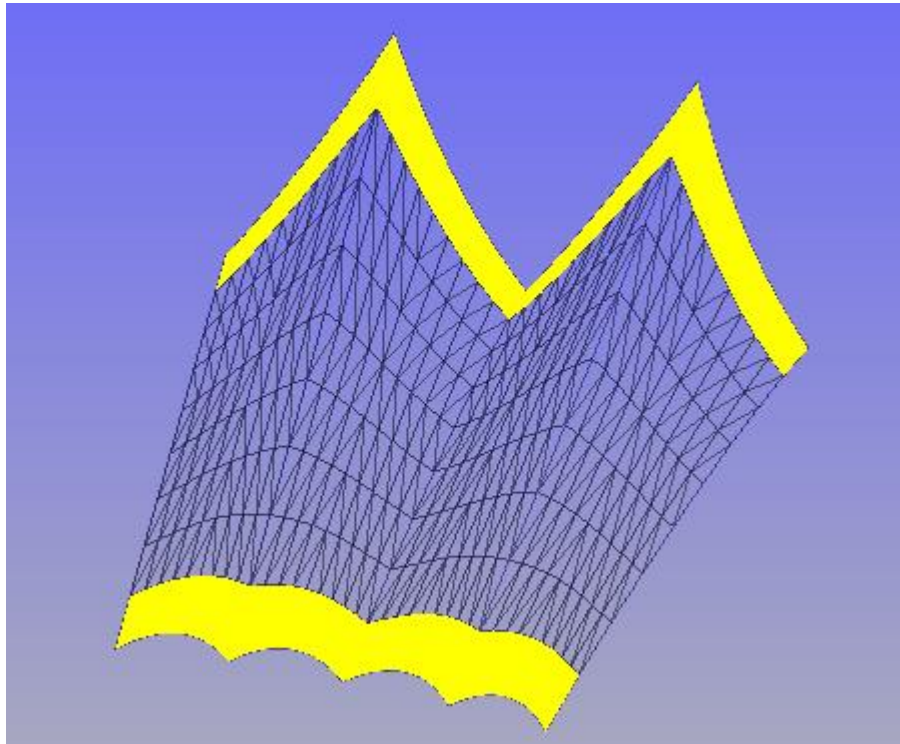
$$H_i = \phi \times N_{ed} = 0.0024 \times 2934 = 7.15 \text{ kN}$$

## 4.5 Load Cases

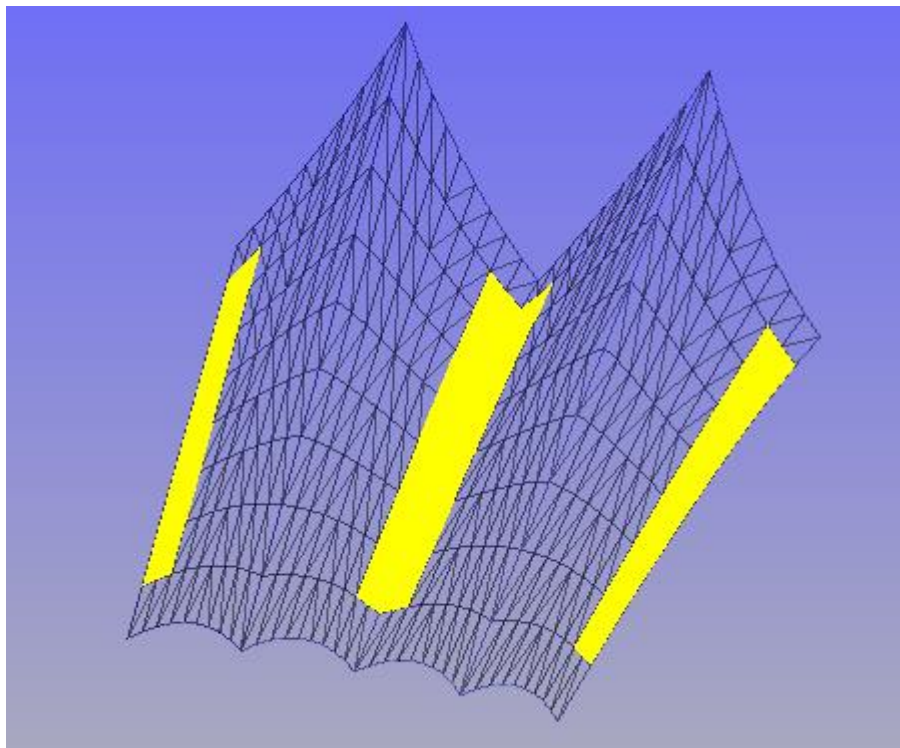
## Membrane Local Wind Analysis – Forten CP Value Zone A



Membrane Local Wind Analysis – Forten - CP Value Zone B

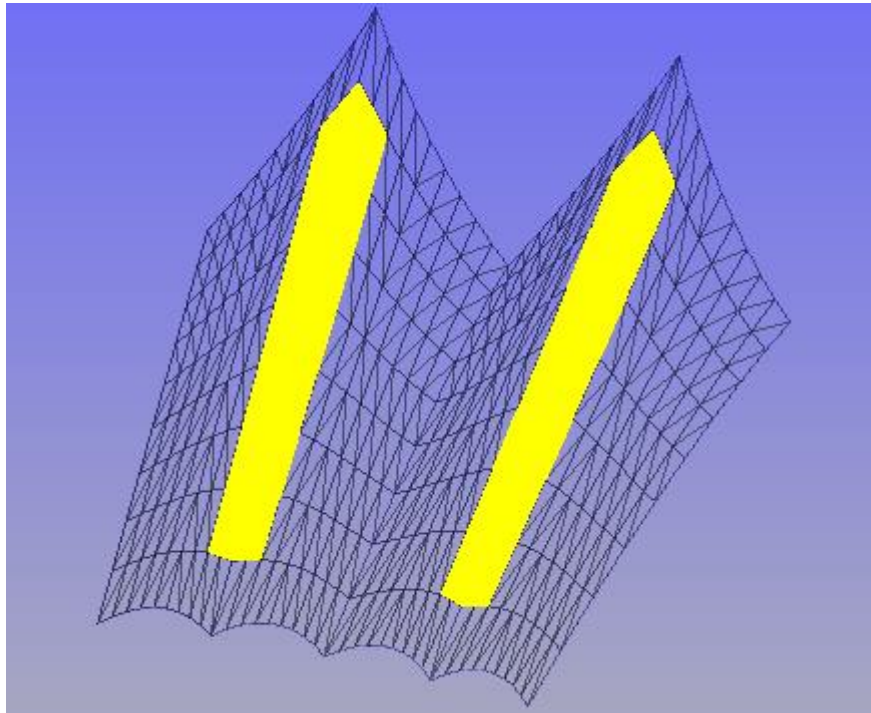


Membrane Local Wind Analysis – Forten - CP Value Zone C

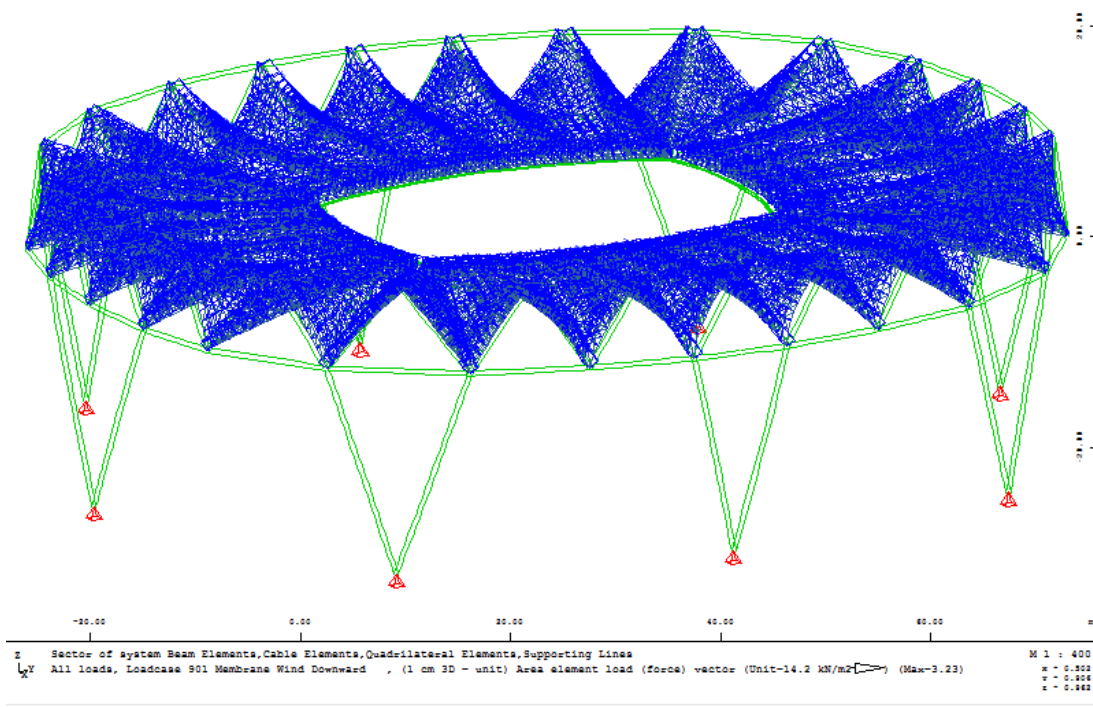




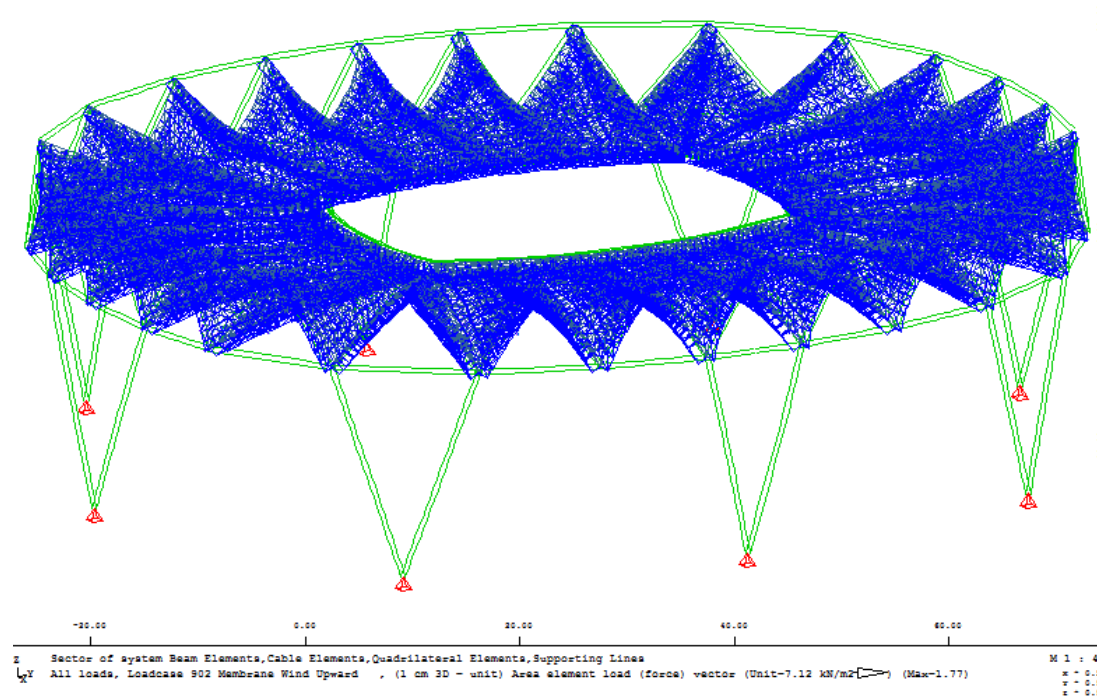
Membrane Local Wind Analysis – Forten - CP Value Zone D



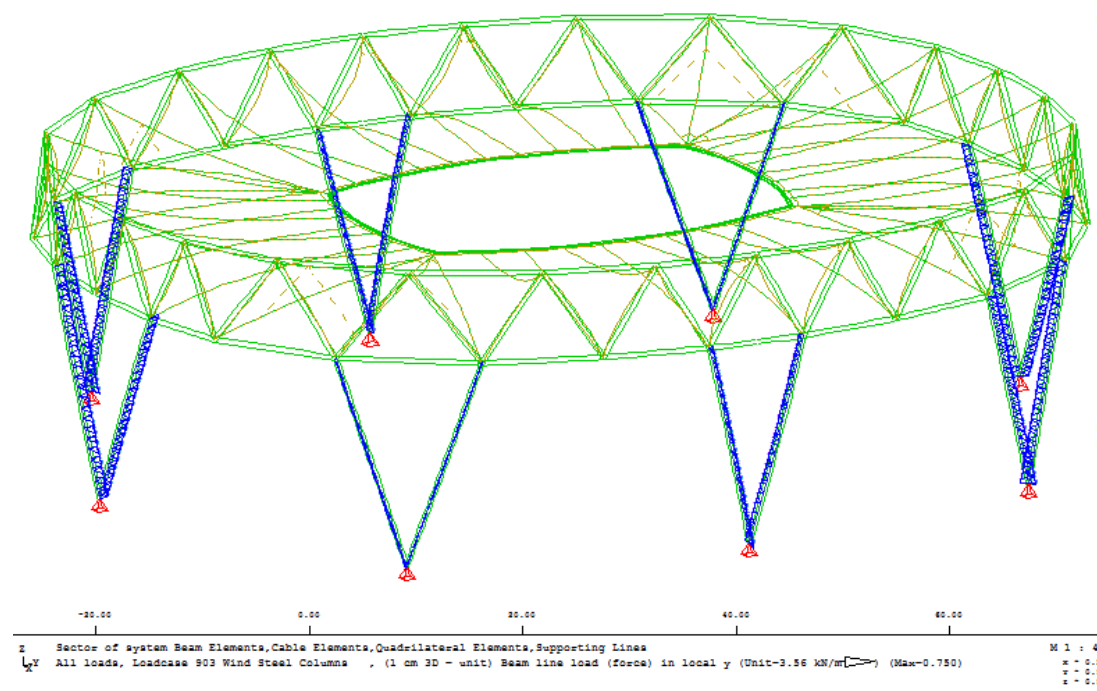
Load Case 901 - 'Membrane Wind Downward' – Global Analysis



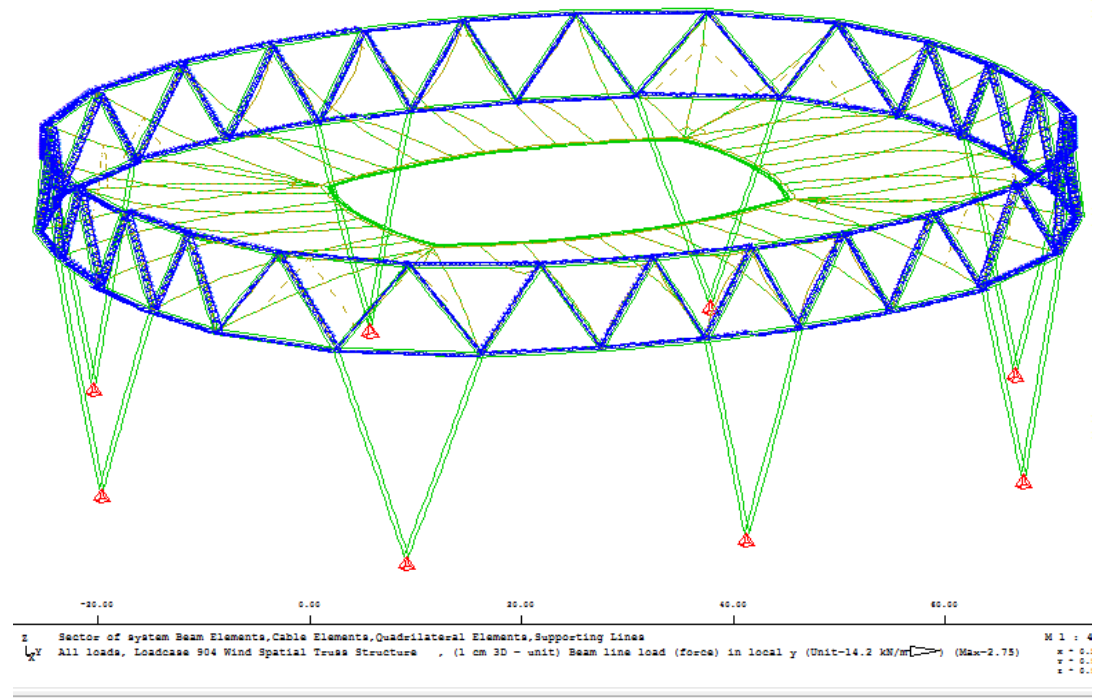
Load Case 902 - 'Membrane Wind Upward' – Global Analysis



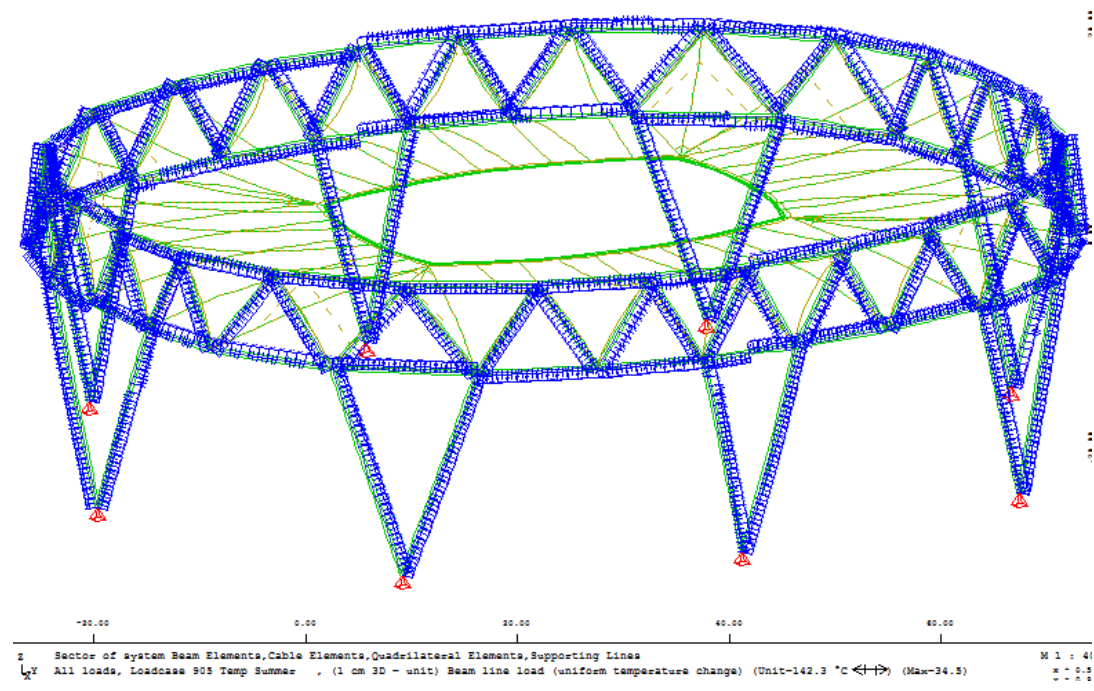
Load Case 903 - Wind Steel Columns – Global Analysis



Load Case 904 - Wind Spatial Truss Structure – Global Analysis

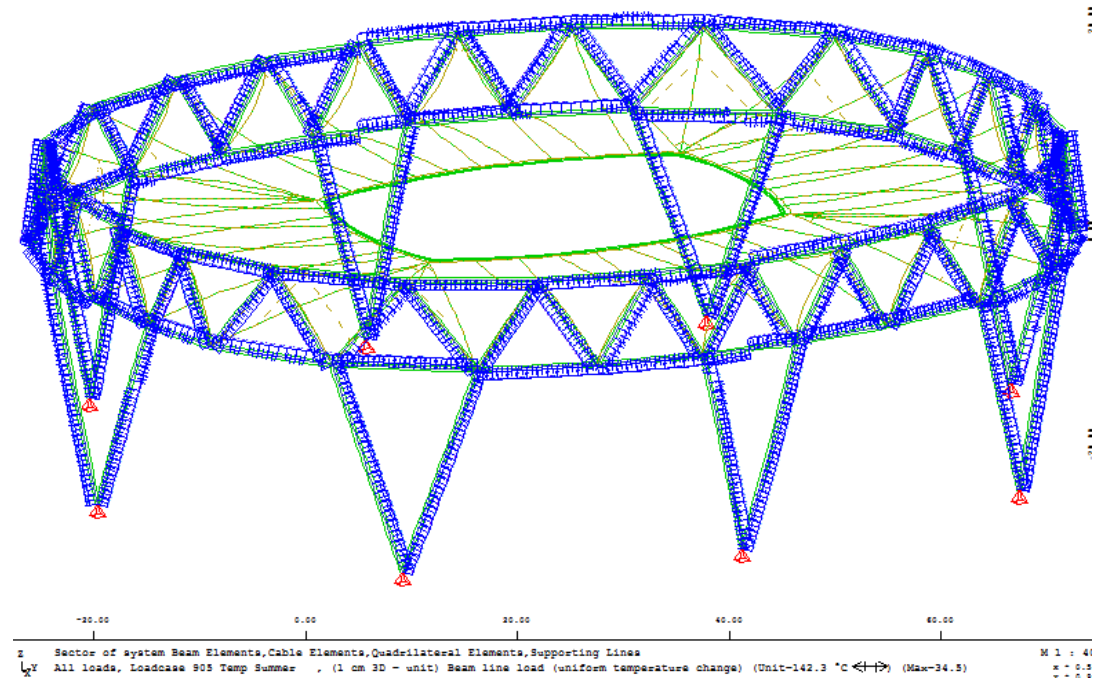


Load Case 905 - 'Temp Summer' – Global Analysis

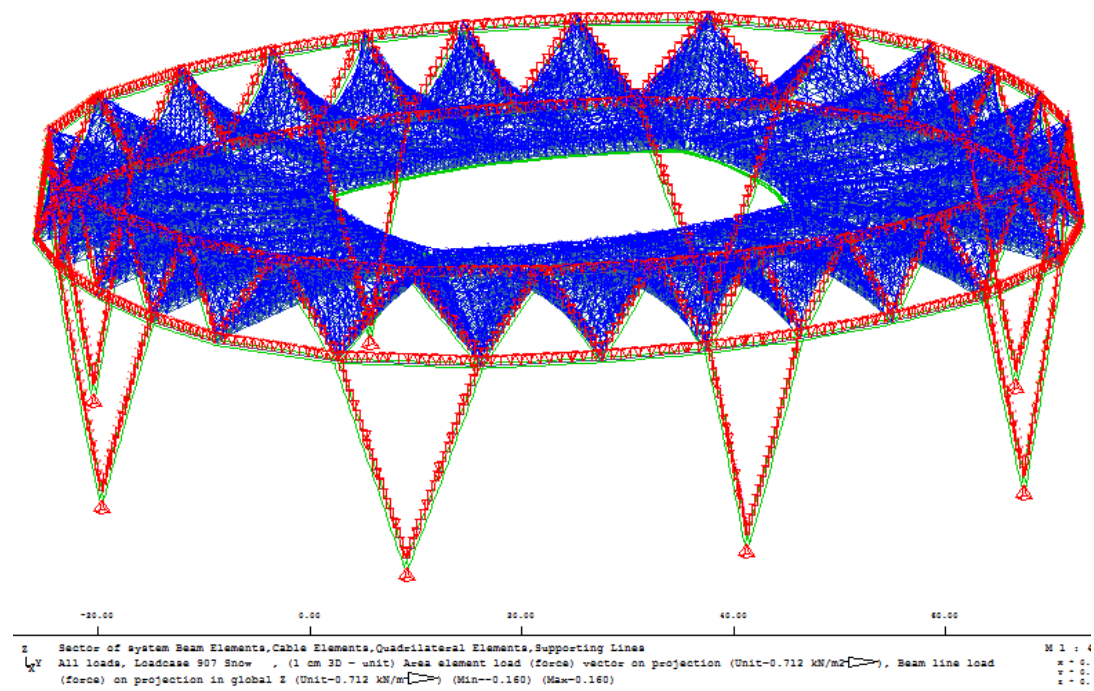




Load Case 906 - 'Temp Winter' – Global Analysis

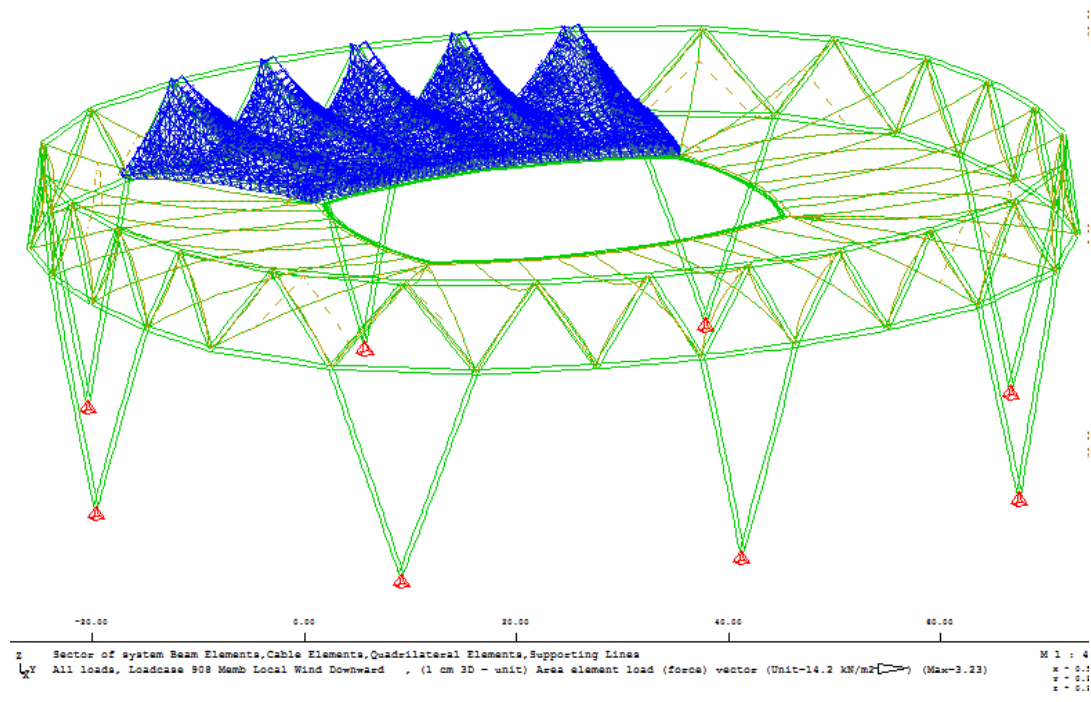


Load Case 907 – Snow – Global Analysis

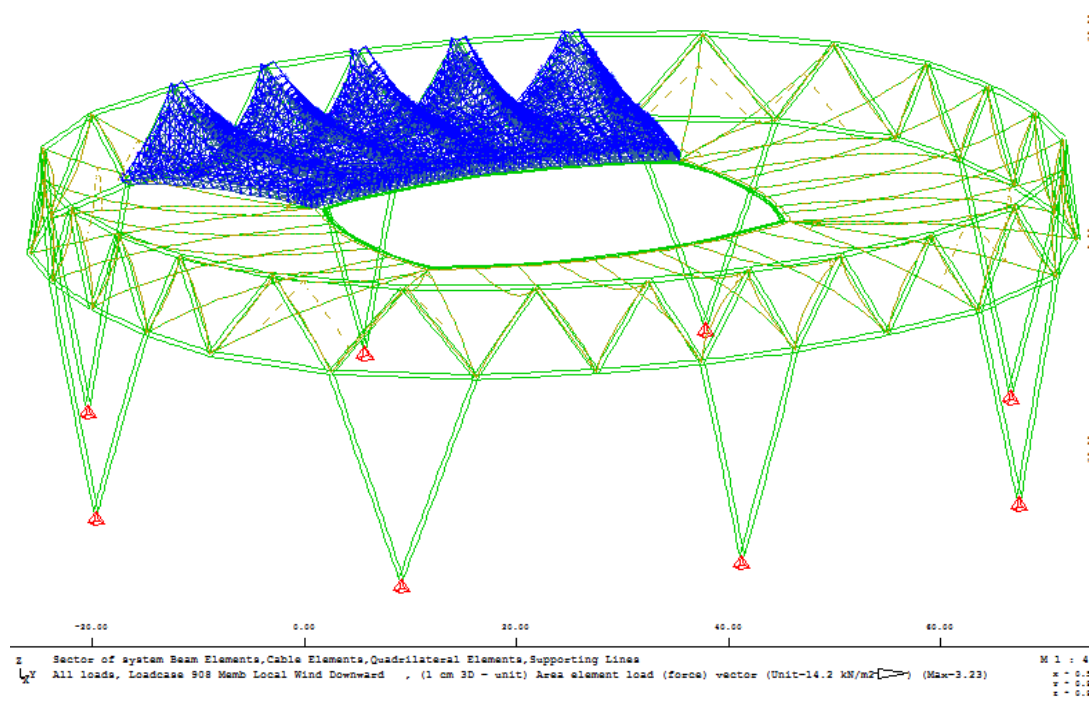




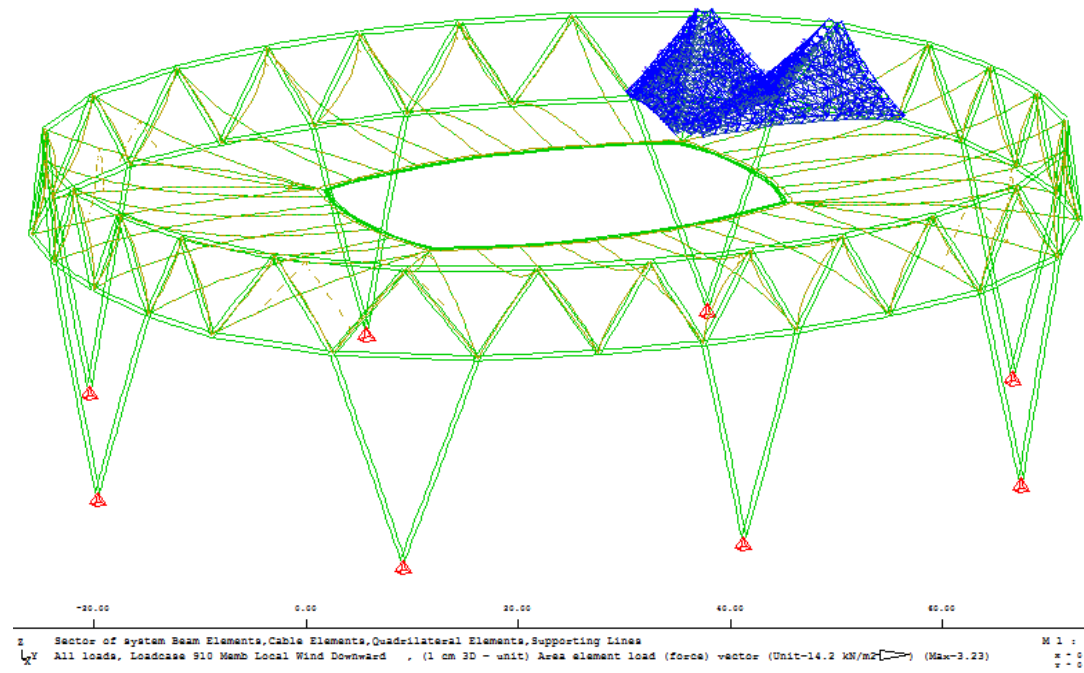
Load Case 908 – 'Memb Local Wind Downward'



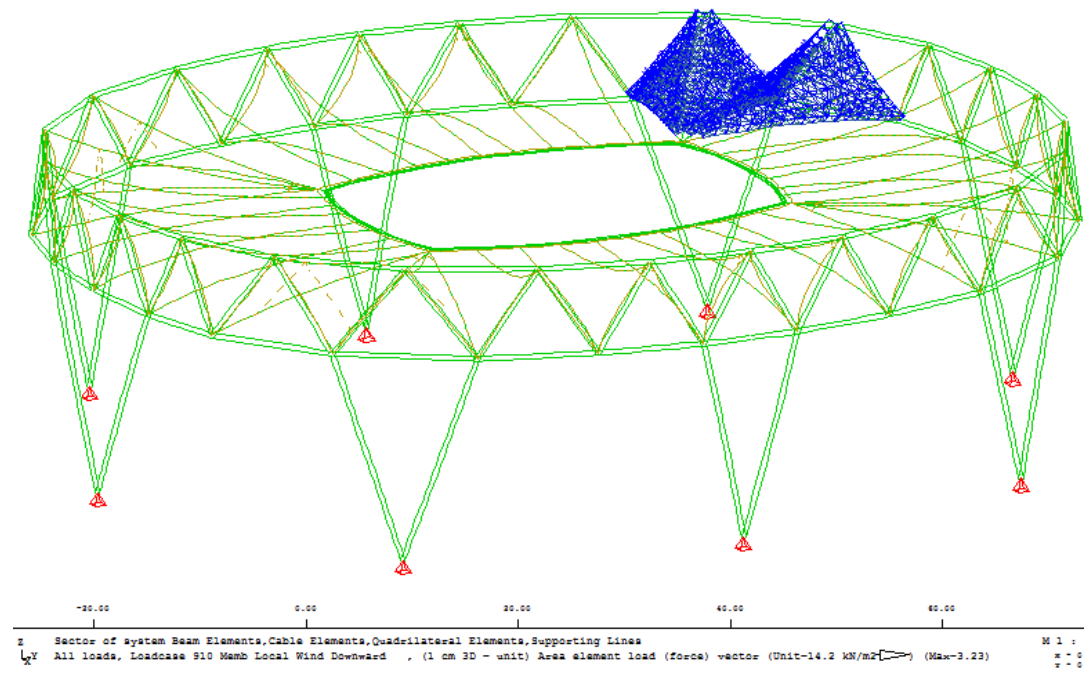
Load Case 909 – 'Memb Local Wind Upward'



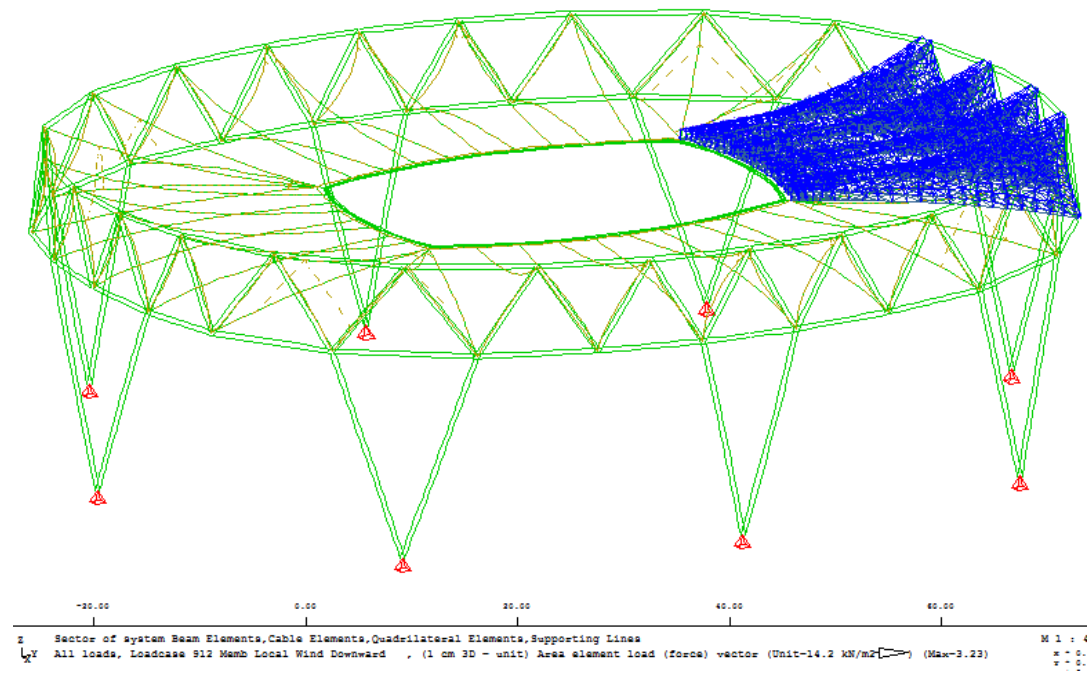
Load Case 910 – 'Memb Local Wind Downward'



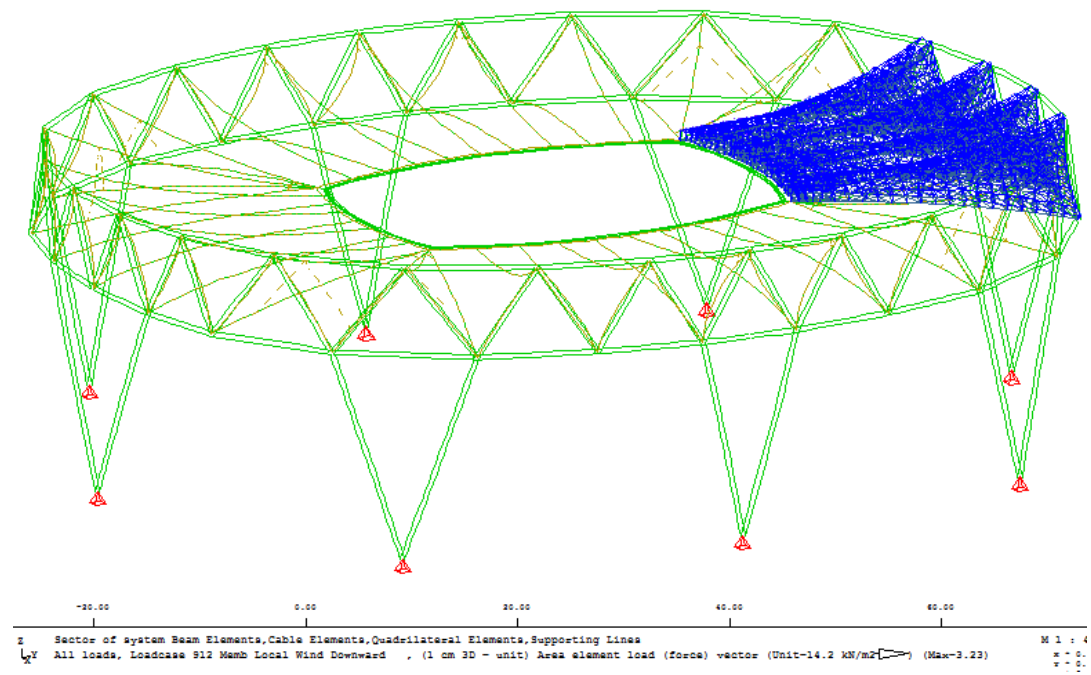
Load Case 911 – 'Memb Local Wind Upward'



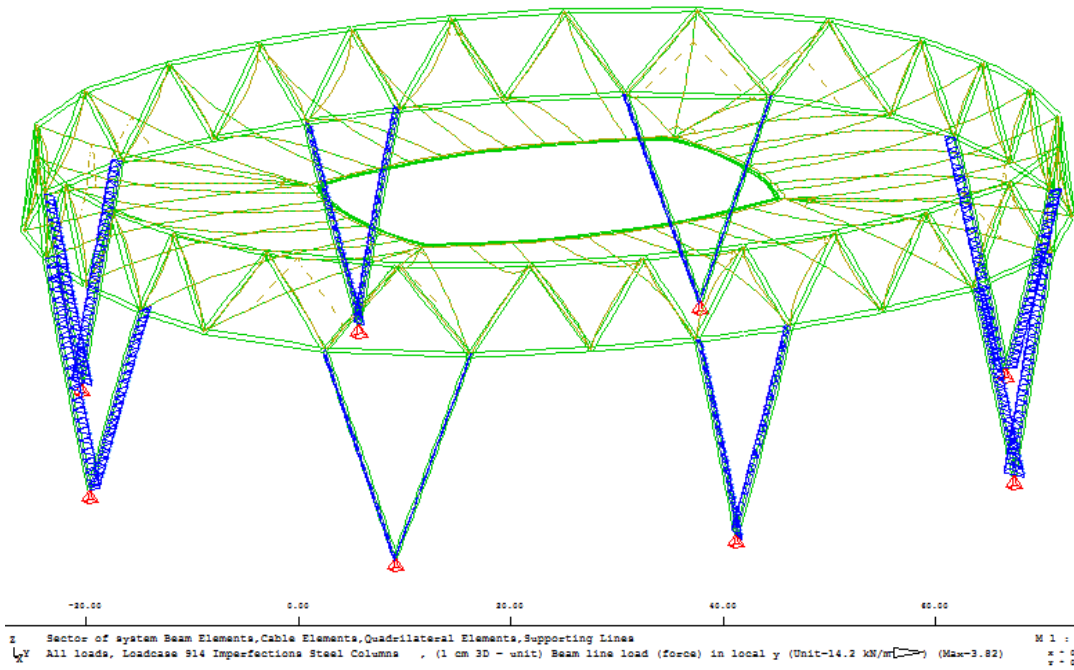
Load Case 912 – 'Memb Local Wind Downward'



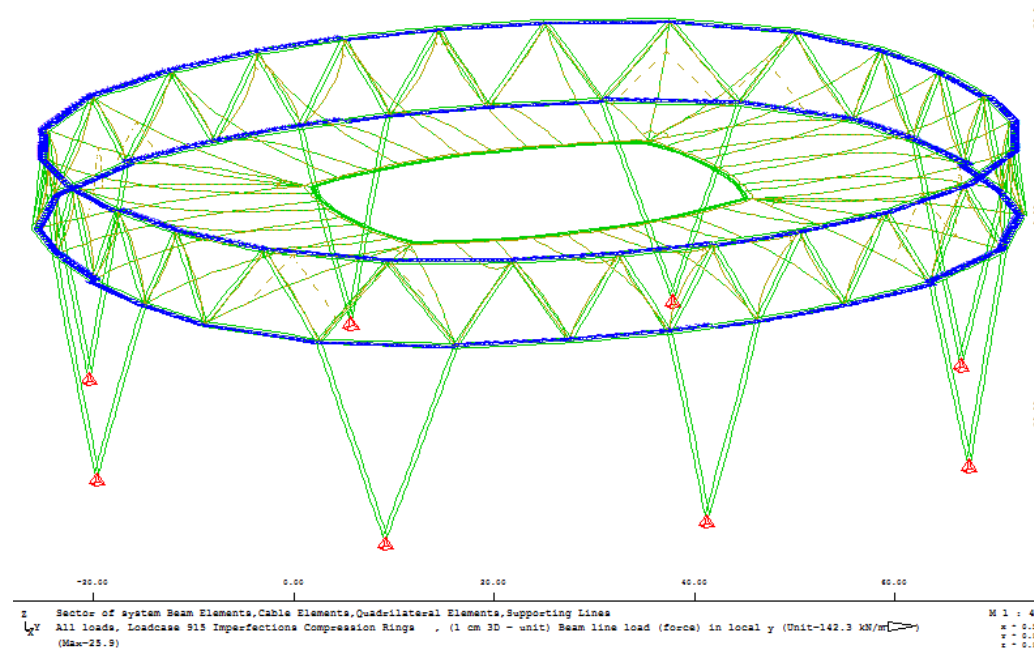
Load Case 913 – 'Memb Local Wind Upward'



Load Case 914 – 'Imperfections Steel Columns' - Global

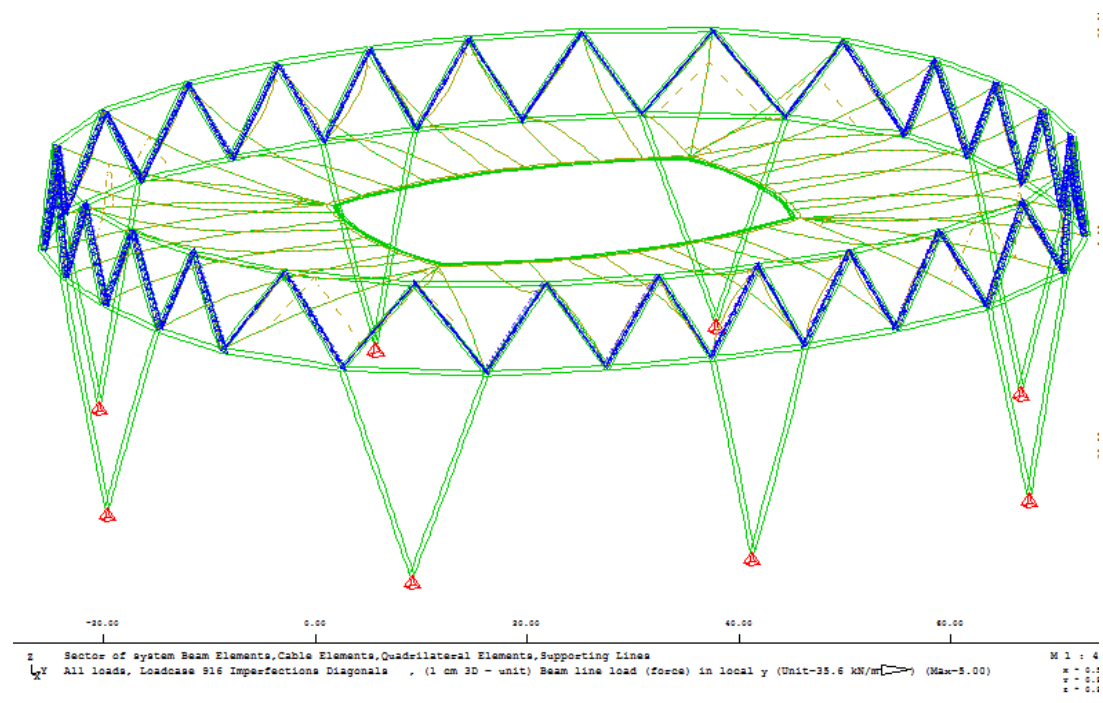


Load Case 915 – 'Imperfections Compression Rings' - Global





Load Case 916 – 'Imperfections Diagonals' - Global



4.6 Load Combination

a) Characteristic Combination – Service Limit State

		Dead Load	Prestress	Wind Down	Wind Up	Wind Steel Columns	Wind Truss	Temp S	Temp W	Snow	Local Wind Down	Local Wind Up	Local Wind Down	Local Wind Up	Local Wind Down	Local Wind Up	Imperfe.	Imperfe.	Ponding
	<b>SLS</b>	-	-	LC 901	LC 902	LC 903	LC 904	LC 905	LC 906	LC 907	LC 908	LC 909	LC 910	LC 911	LC 912	LC 913	LC 914	LC 915	-
Load Case	151	1,00	1,00	-	-	-	-	-	-	-	-	-	-	-	-	-	1,00	1,00	-
Load Case	152	1,00	1,00	-	1,00	1,00	1,00	-	-	-	-	-	-	-	-	-	1,00	1,00	-
Load Case	153	1,00	1,00	1,00	-	1,00	1,00	-	-	-	-	-	-	-	-	-	1,00	1,00	-
Load Case	154	1,00	1,00	-	1,00	1,00	1,00	0,6	-	-	-	-	-	-	-	-	1,00	1,00	-
Load Case	155	1,00	1,00	1,00	-	1,00	1,00	-	0,6	-	-	-	-	-	-	-	1,00	1,00	-
Load Case	156	1,00	1,00	-	1,00	1,00	1,00	-	0,6	-	-	-	-	-	-	-	1,00	1,00	-
Load Case	157	1,00	1,00	1,00	-	1,00	1,00	0,6	-	-	-	-	-	-	-	-	1,00	1,00	-
Load Case	158	1,00	1,00	1,00	-	1,00	1,00	-	0,6	0,5	-	-	-	-	-	-	1,00	1,00	-
Load Case	159	1,00	1,00	-	-	-	-	-	-	-	1,00	-	-	-	-	-	1,00	1,00	-
Load Case	160	1,00	1,00	-	-	-	-	-	-	-	-	1,00	-	-	-	-	1,00	1,00	-
Load Case	161	1,00	1,00	-	-	-	-	-	-	-	-	-	1,00	-	-	-	1,00	1,00	-
Load Case	162	1,00	1,00	-	-	-	-	-	-	-	-	-	-	1,00	-	-	1,00	1,00	-
Load Case	163	1,00	1,00	-	-	-	-	-	-	-	-	-	-	-	1,00	-	1,00	1,00	-
Load Case	164	1,00	1,00	-	-	-	-	-	-	-	-	-	-	-	-	1,00	1,00	1,00	-
Load Case	172	1,00	1,00	-	0,80	0,80	0,80	-	-	-	-	-	-	-	-	-	1,00	1,00	-
Load Case	173	1,00	1,00	0,80	-	0,80	0,80	-	-	-	-	-	-	-	-	-	1,00	1,00	-
Load Case	178	1,00	1,00	0,80	-	0,80	0,80	-	0,6	0,35	-	-	-	-	-	-	1,00	1,00	-
Load Case	179	1,00	1,00	-	-	-	-	-	-	-	-	-	-	-	-	-	1,00	1,00	1,00

The loadcases between 101 and 128 are the same as the loadcases between 151 and 179 but without imperfections. The same for the loadcases 201 to 214 and the loadcases 301 to 314. Ones without and the others with imperfections.

b) Characteristic Combination – Ultimate Limit State

		Dead Load	Prestress	Wind Down	Wind Up	Wind Steel Columns	Wind Truss	Temp S	Temp W	Snow	Local Wind Down	Local Wind Up	Local Wind Down	Local Wind Up	Local Wind Down	Local Wind Up	Imperfe.	Imperfe.	
	<b>ULS</b>	-	-	LC 901	LC 902	LC 903	LC 904	LC 905	LC 906	LC 907	LC 908	LC 909	LC 910	LC 911	LC 912	LC 913	LC 914	LC 915	
Load Case	301	1,35	1,35	-	-	-	-	-	-	-	-	-	-	-	-	-	1,50	1,50	
Load Case	302	1,35	1,35	-	1,50	1,50	1,50	-	-	-	-	-	-	-	-	-	1,50	1,50	
Load Case	303	1,35	1,35	1,50	-	1,50	1,50	-	-	-	-	-	-	-	-	-	1,50	1,50	
Load Case	304	1,35	1,35	-	1,50	1,50	1,50	0,9	-	-	-	-	-	-	-	-	1,50	1,50	
Load Case	305	1,35	1,35	1,50	-	1,50	1,50	-	0,9	-	-	-	-	-	-	-	1,50	1,50	
Load Case	306	1,35	1,35	-	1,50	1,50	1,50	-	0,9	-	-	-	-	-	-	-	1,50	1,50	
Load Case	307	1,35	1,35	1,50	-	1,50	1,50	0,9	-	-	-	-	-	-	-	-	1,50	1,50	
Load Case	308	1,35	1,35	1,50	-	1,50	1,50	-	0,9	0,75	-	-	-	-	-	-	1,50	1,50	
Load Case	309	1,35	1,35	-	-	-	-	-	-	-	1,50	-	-	-	-	-	1,50	1,50	
Load Case	310	1,35	1,35	-	-	-	-	-	-	-	-	1,50	-	-	-	-	1,50	1,50	
Load Case	311	1,35	1,35	-	-	-	-	-	-	-	-	-	1,50	-	-	-	1,50	1,50	
Load Case	312	1,35	1,35	-	-	-	-	-	-	-	-	-	-	1,50	-	-	1,50	1,50	
Load Case	313	1,35	1,35	-	-	-	-	-	-	-	-	-	-	-	1,50	-	1,50	1,50	
Load Case	314	1,35	1,35	-	-	-	-	-	-	-	-	-	-	-	-	1,50	1,50	1,50	



## 5 Dimensioning and Detailed Design

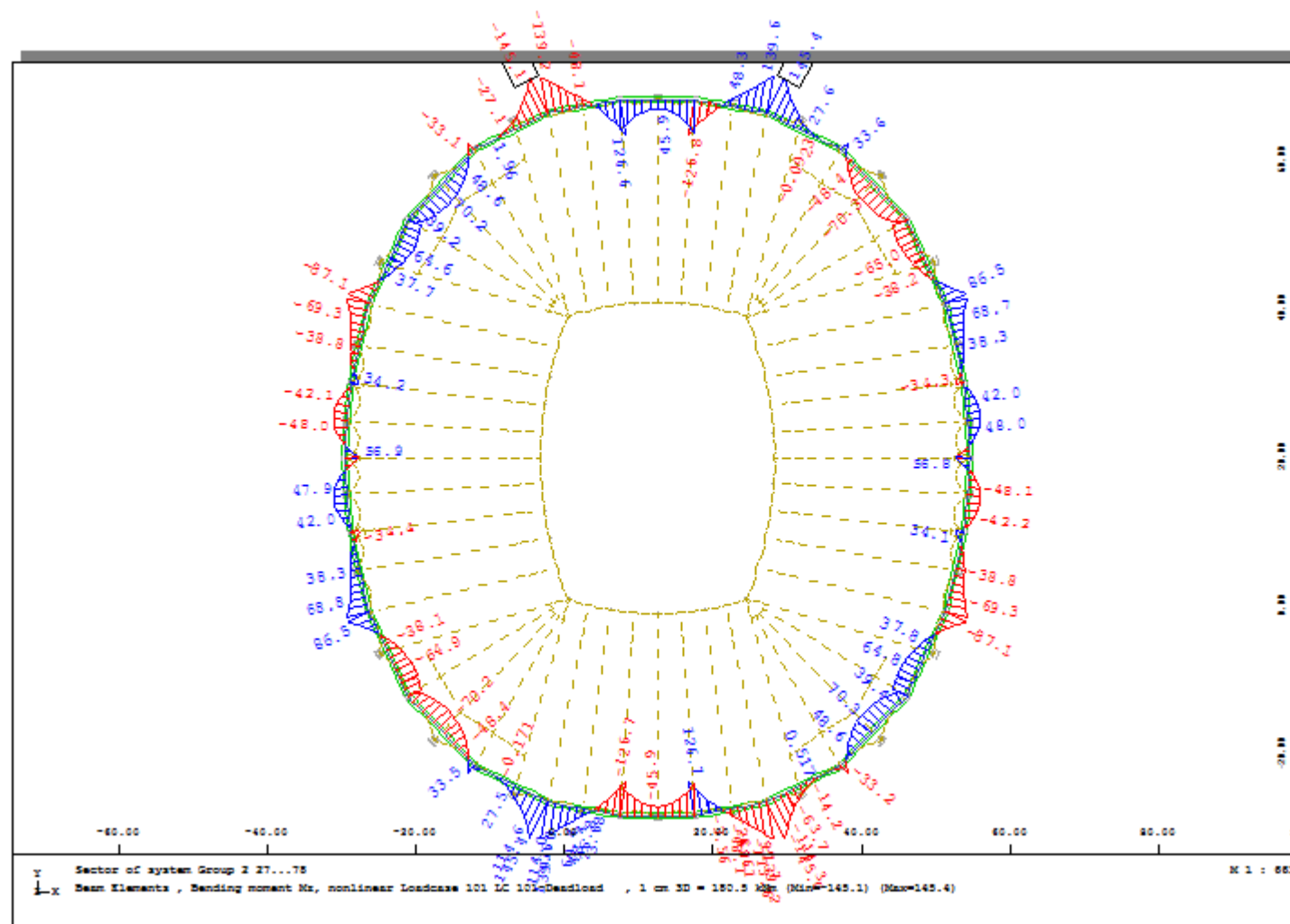
## 5. Dimensioning and Detailed Design

According to the EN 1993-1-1: 2005, chapter 5.2 Global Analysis, the internal forces and moments may generally be determined using second-order analysis, taking into account the influence of the deformation of the structure.

For Uniform members in bending and axial compression in 6.3.3, EN 1993-1-1: 2005, the stability of uniform members with double symmetric cross sections for sections not susceptible to distortional deformations can be carried out using second order analysis with imperfections as given in 5.3.2, EN 1993-1-1: 2005.

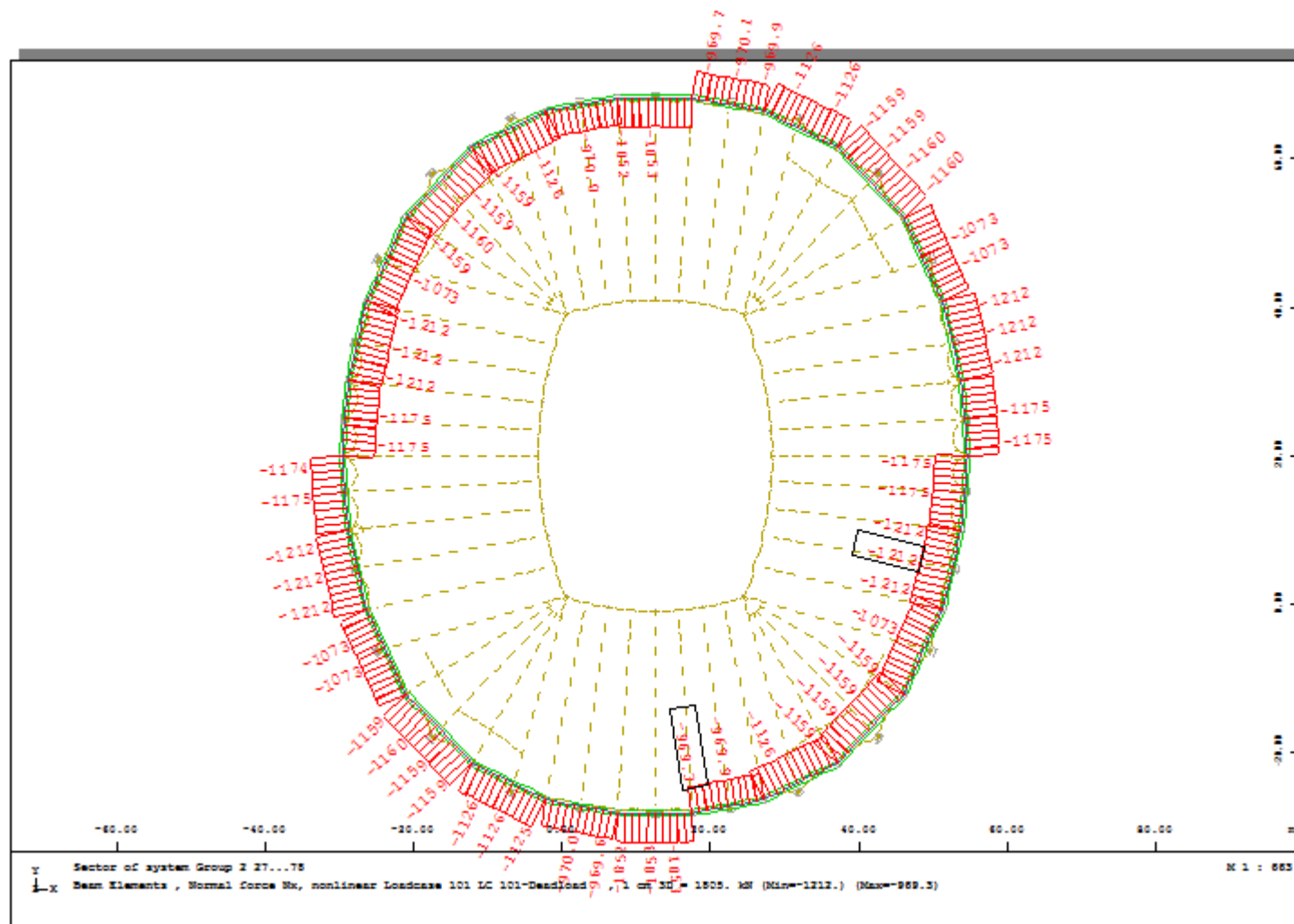
### 5.1 Steel Structure – Upper Compression Ring

Service Limit State: Loadcase Deadload + Prestress – Bending Moments

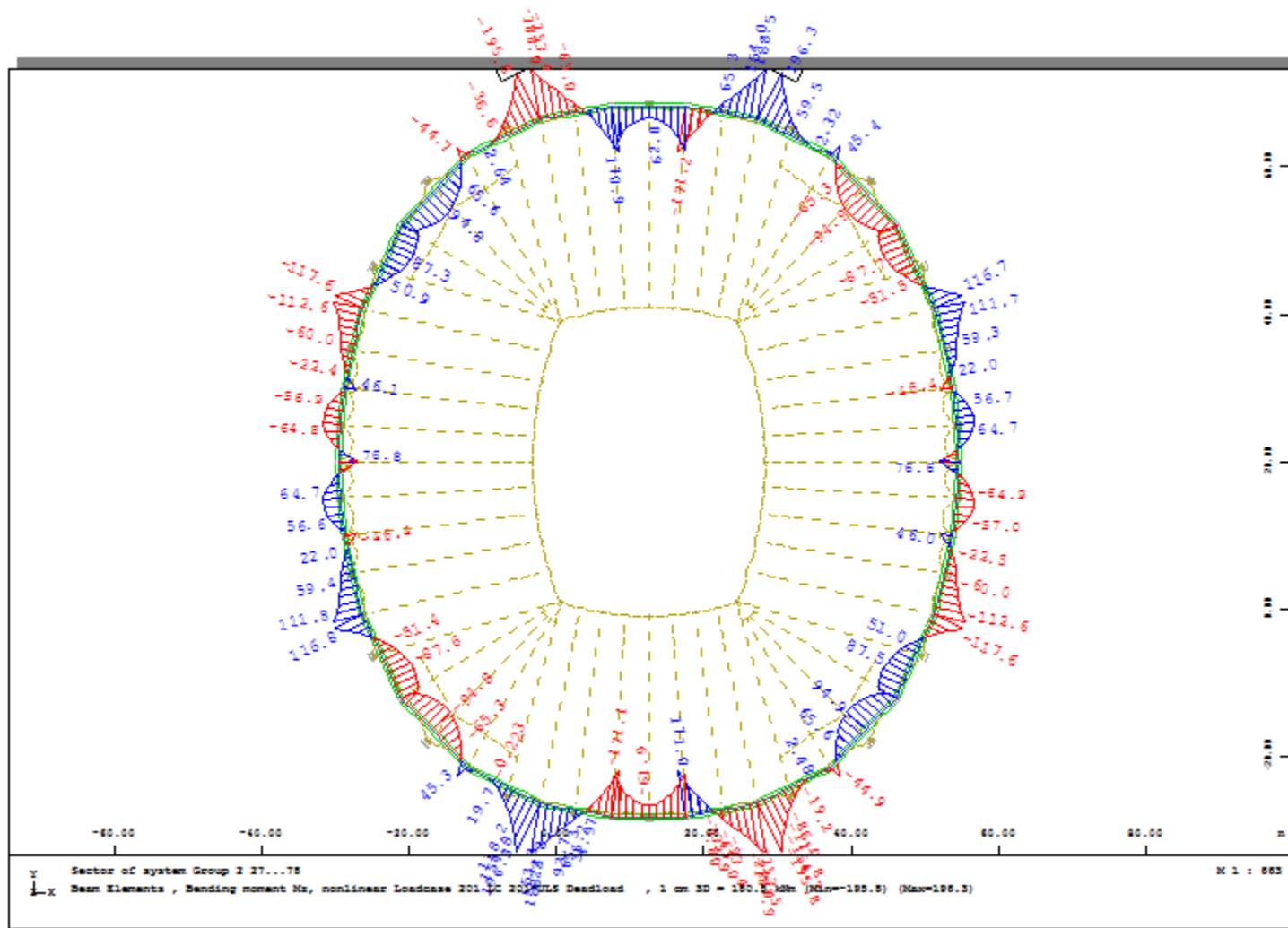




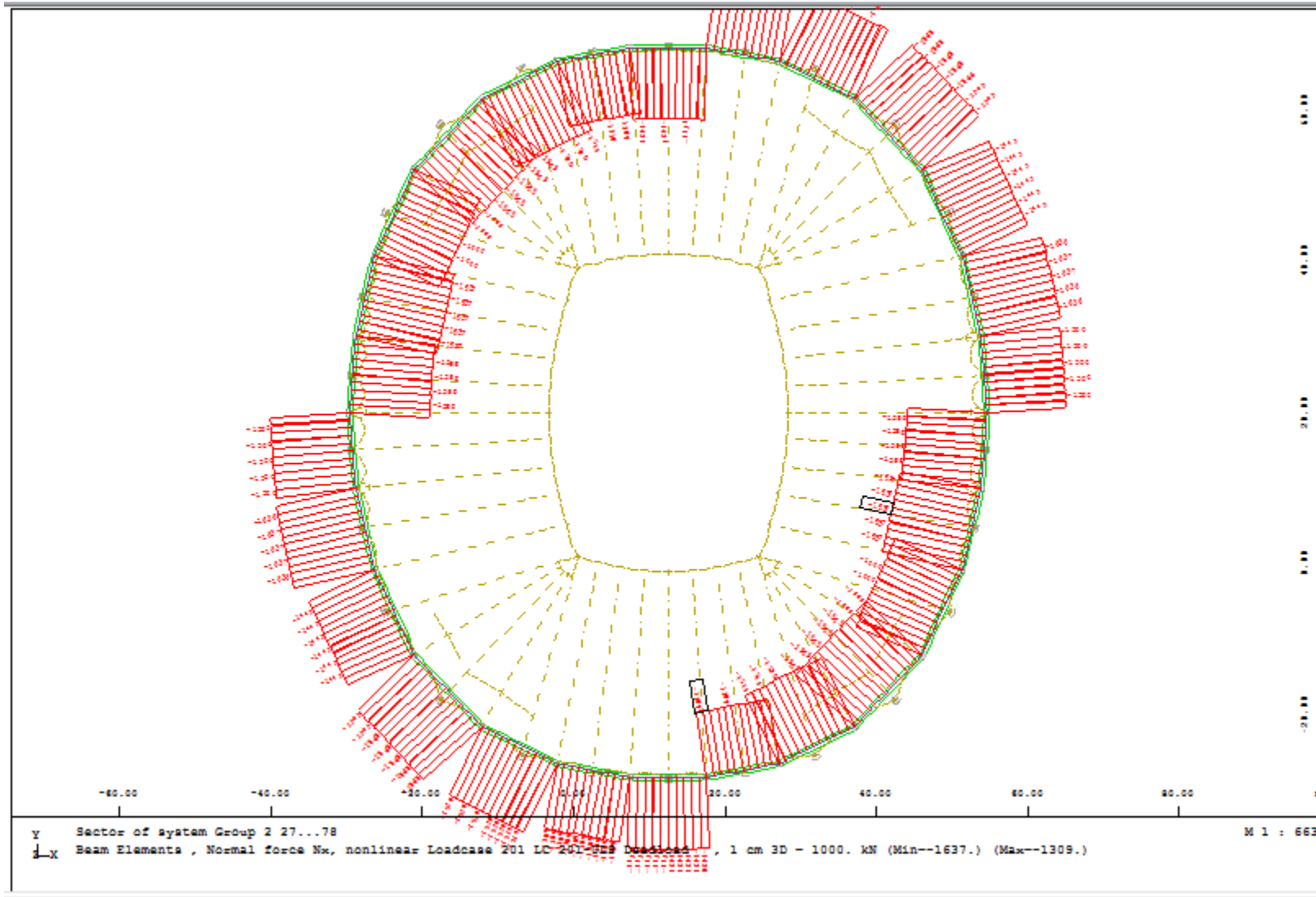
Service Limit State: Loadcase Deadload + Prestress – Axial/Normal Force



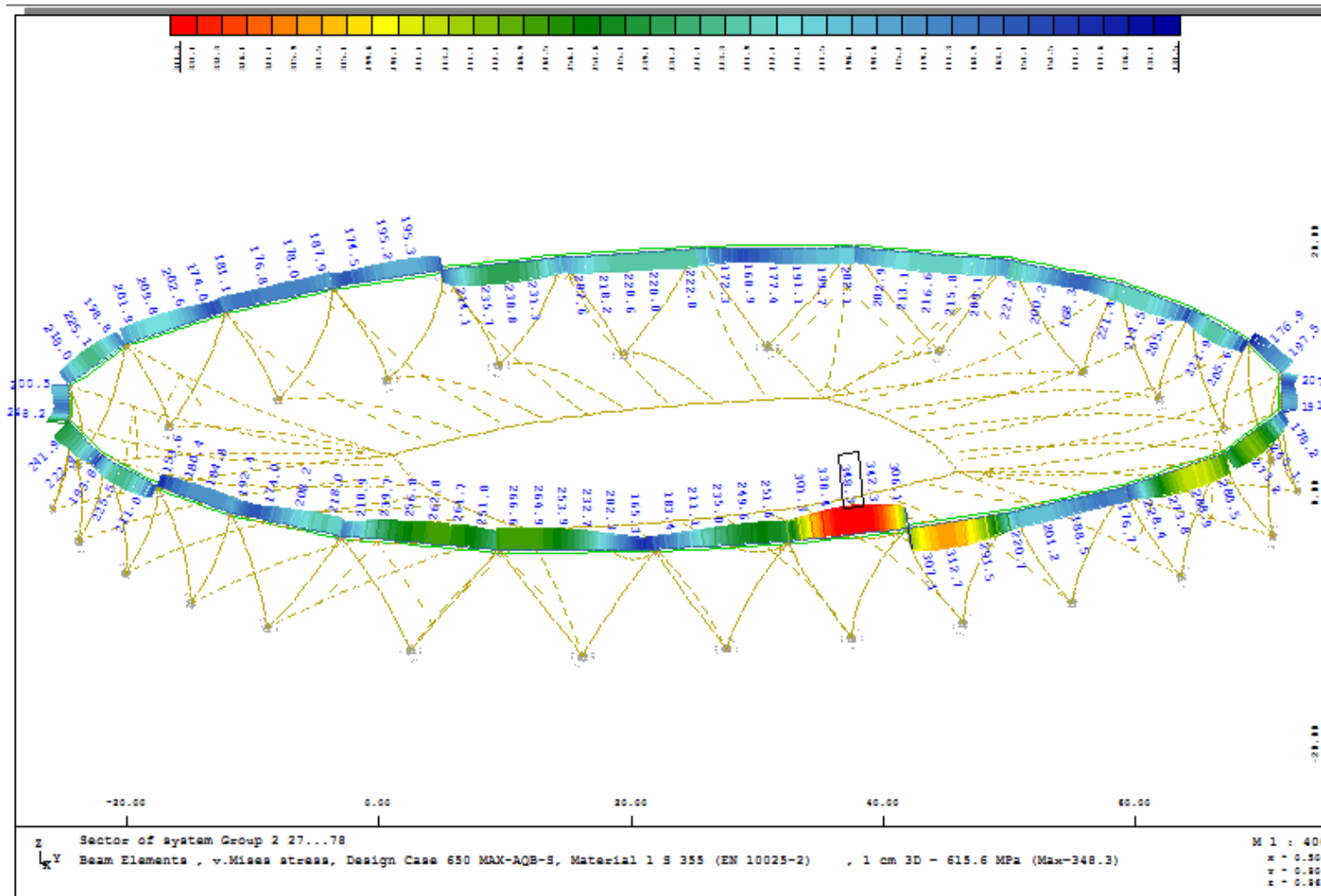
Ultimate Limit State: Loadcase Deadload + Prestress – Bending Moments



Ultimate Limit State: Loadcase Deadload + Prestress – Axial/Normal Force



Ultimate Limit State: Von Mises Stresses : All Load Cases



In the areas where the steel stresses are higher than the admissible value of 323 MPa, the cross section will be locally reinforced.

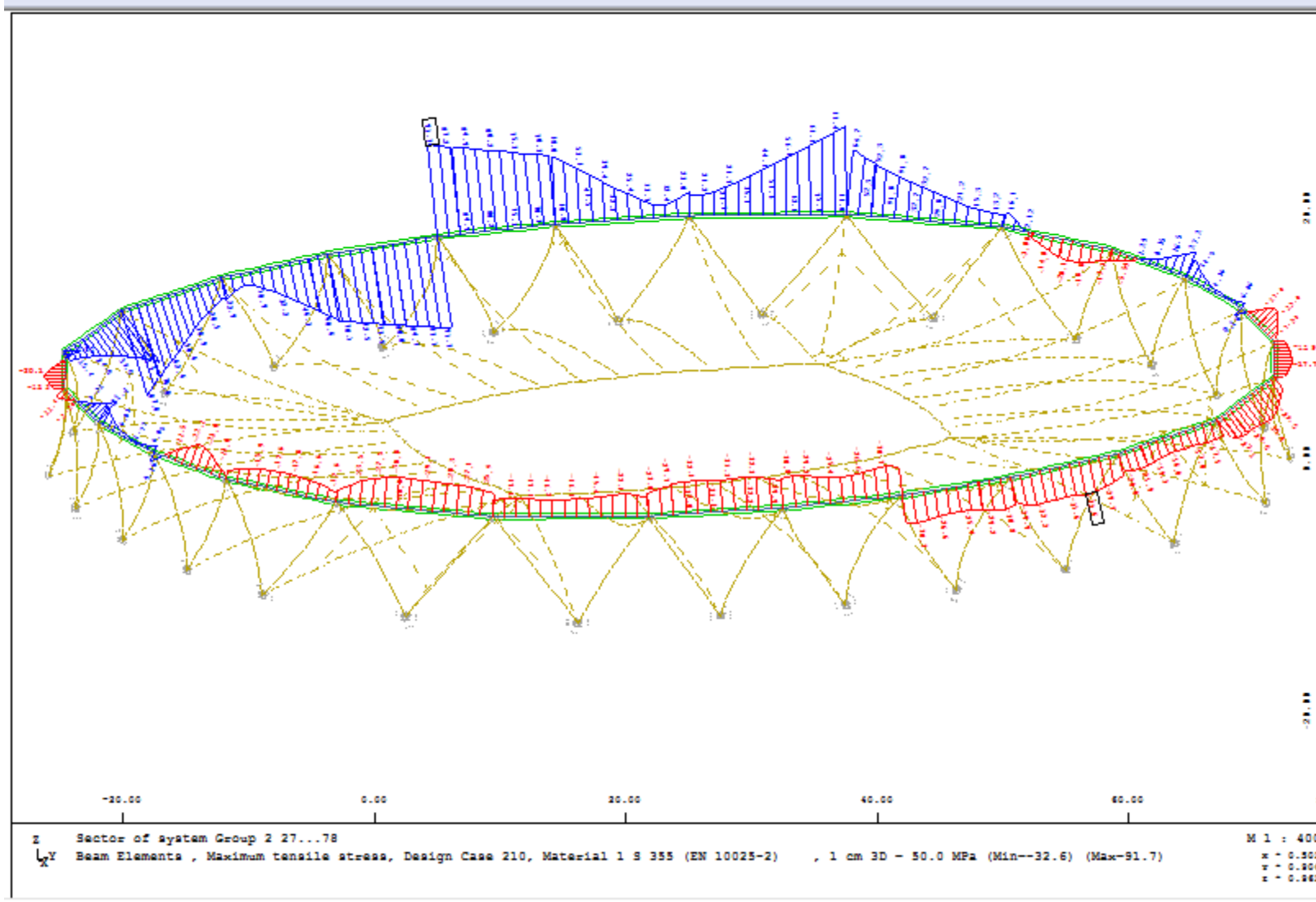
Design cases : 301-314  
 Groups : 2  
 Elements : All  
 Sections : All

Beam Elements

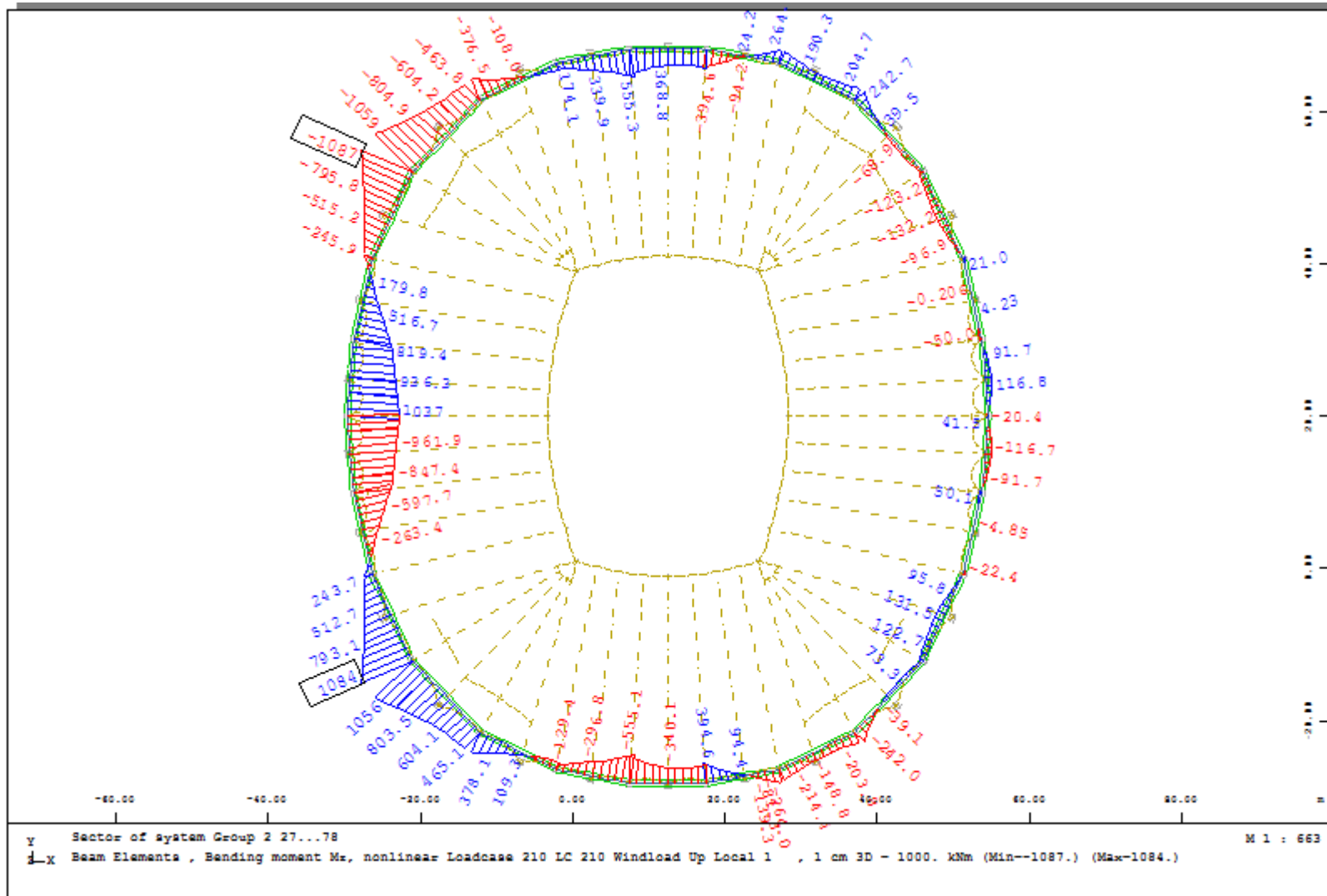
Elem. Nr	X [m]	Mt	DC Name	SIG- [MPa]	SIG+ [MPa]	TAU [MPa]	SIGV [MPa]
132	1,007	1	307 MINZ-SIG-	-348,35	46,95	2,48	348,35
66	0,000	1	302 MAXZ-SIG-	7,97	14,99	3,33	15,82
116	0,000	1	307 MINZ-SIG+	-153,72	-151,33	10,97	153,74
204	1,007	1	310 MAXZ-SIG+	-65,16	84,30	1,78	84,30
267	1,007	1	301 MINZ-TAU	-36,76	-3,25	0,09	36,76
47	0,957	1	308 MAXZ-TAU	-152,11	-131,81	22,36	154,52
213	0,000	1	306 MINZ-SIGV	-2,83	5,92	2,90	5,92
132	1,007	1	307 MAXZ-SIGV	-348,35	46,95	2,48	348,35



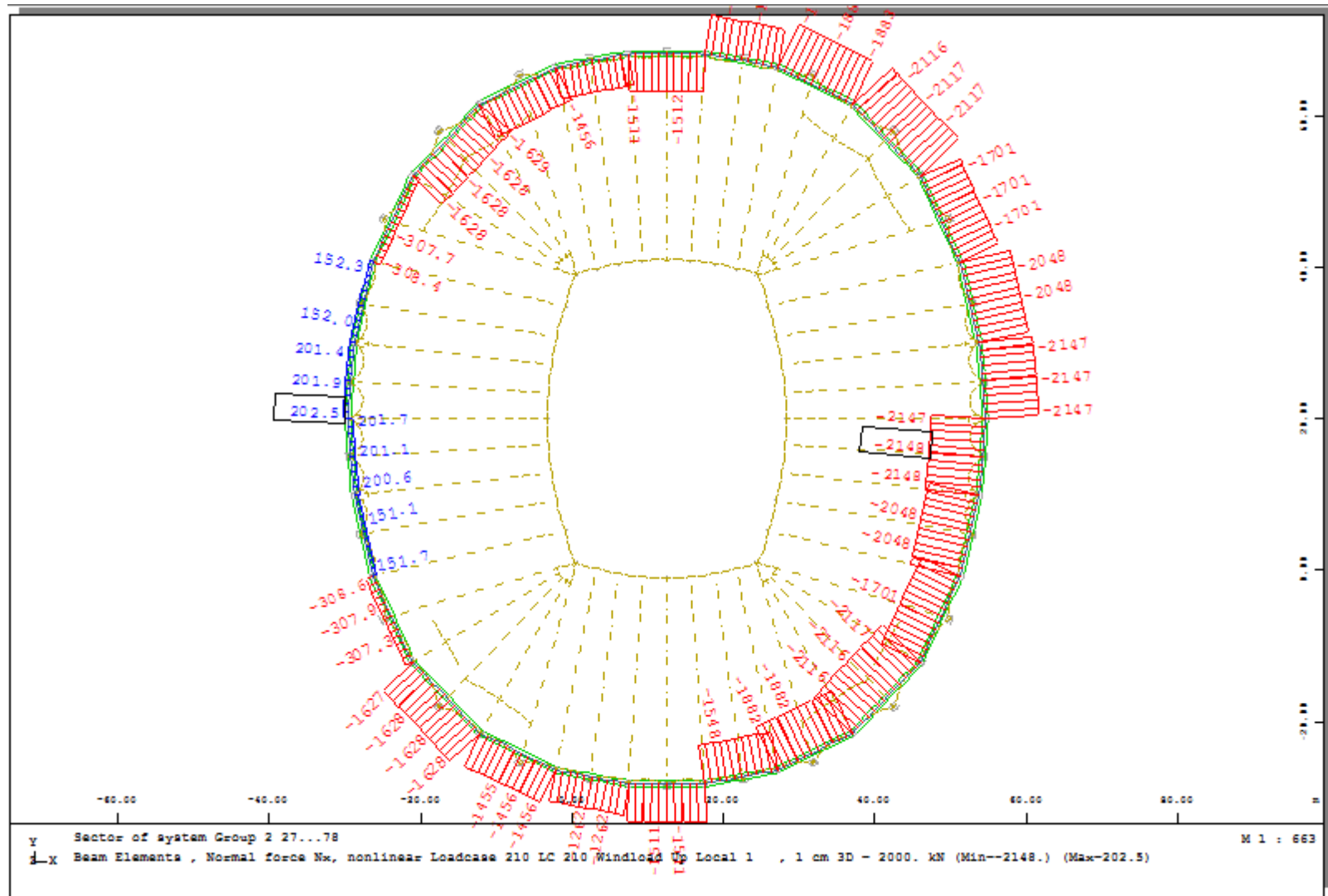
Ultimate Limit State: Loadcase 210 Local Wind Up – Maximum Tensile Stresses



Ultimate Limit State: Loadcase 210 Local Wind Up – Bending Moments

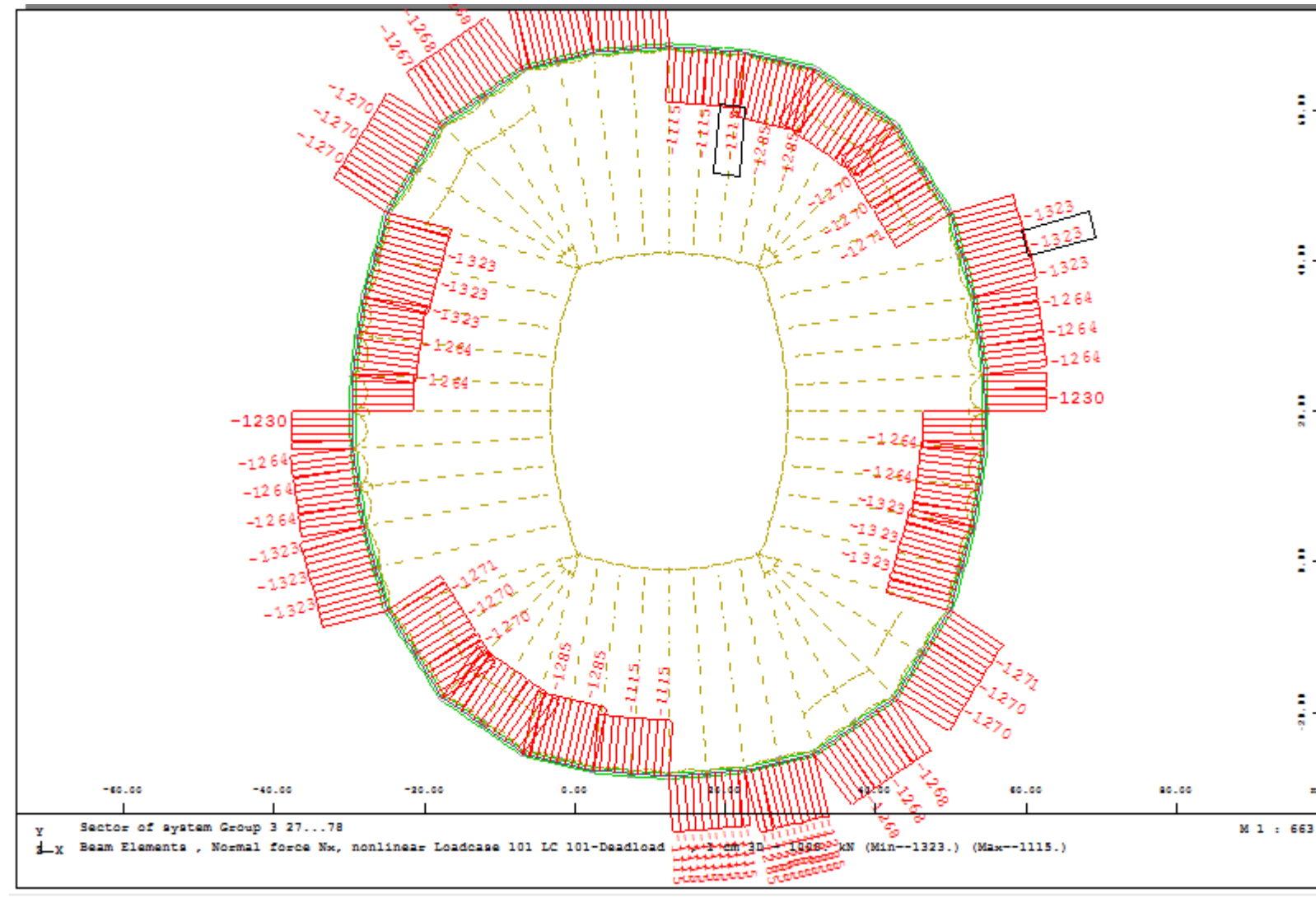


Ultimate Limit State: Loadcase 210 Local Wind Up – Axial/Normal Forces



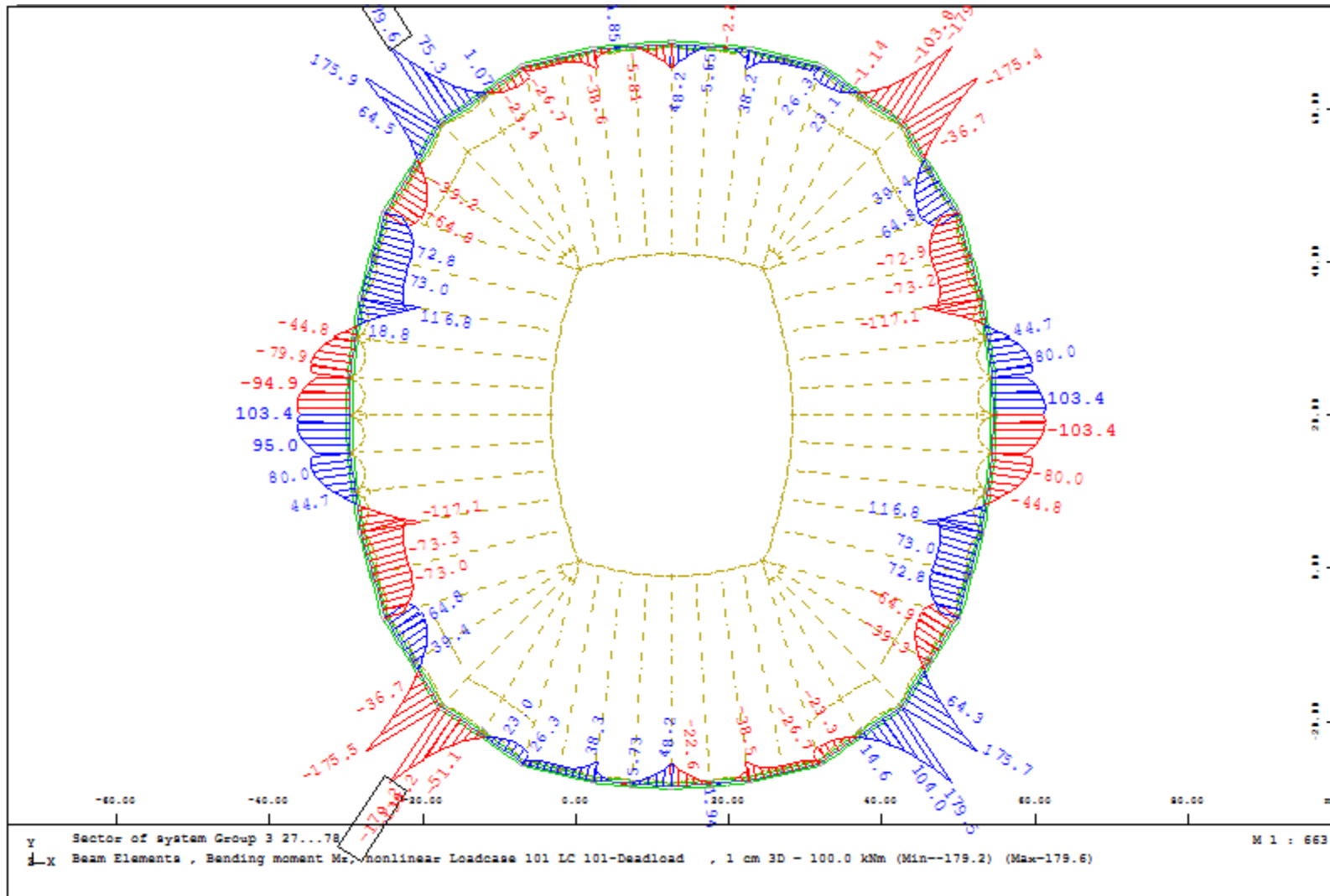
5.2 Steel Structure – Lower Compression Ring

Service Limit State: Loadcase Deadload + Prestress – Axial/Normal Force

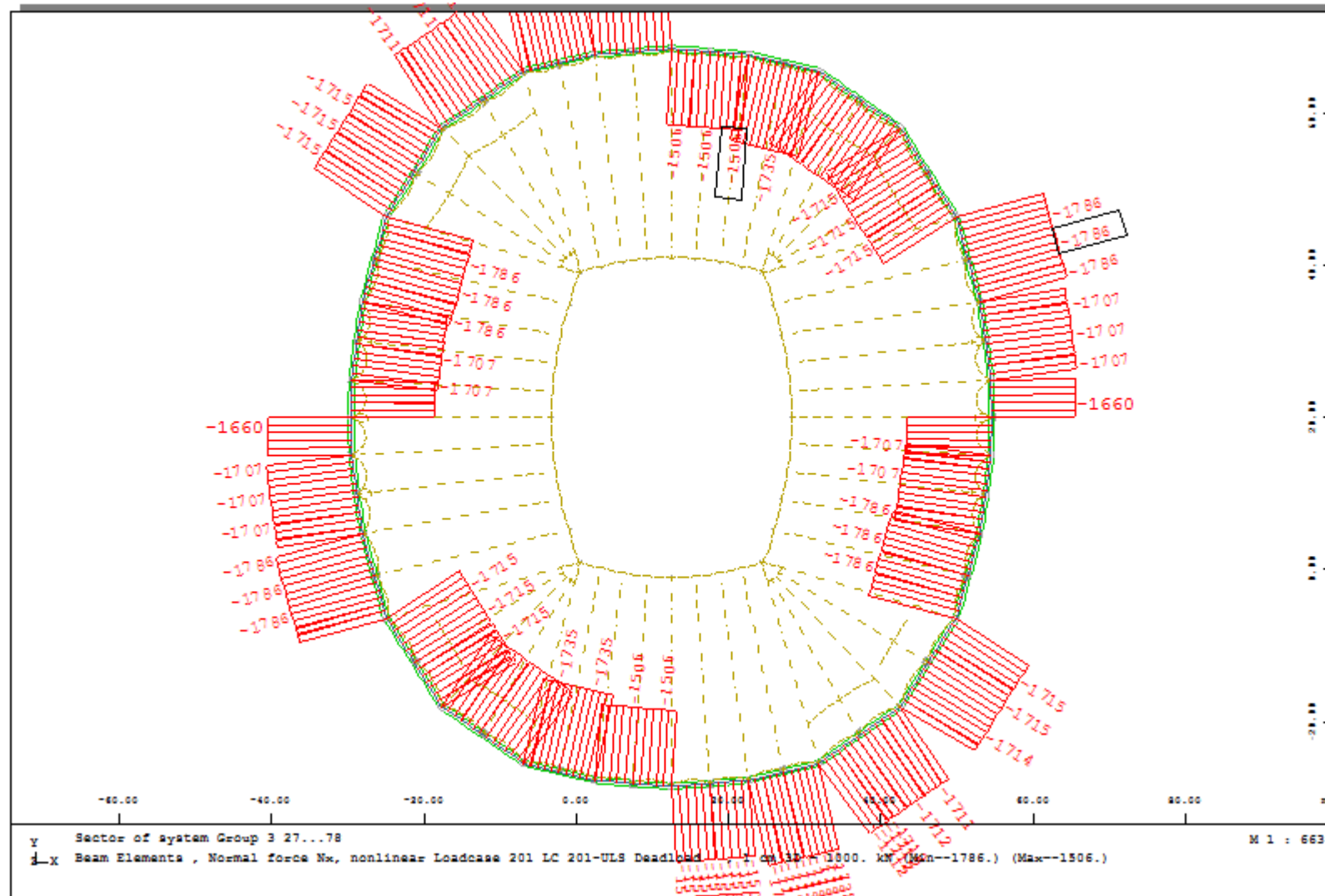




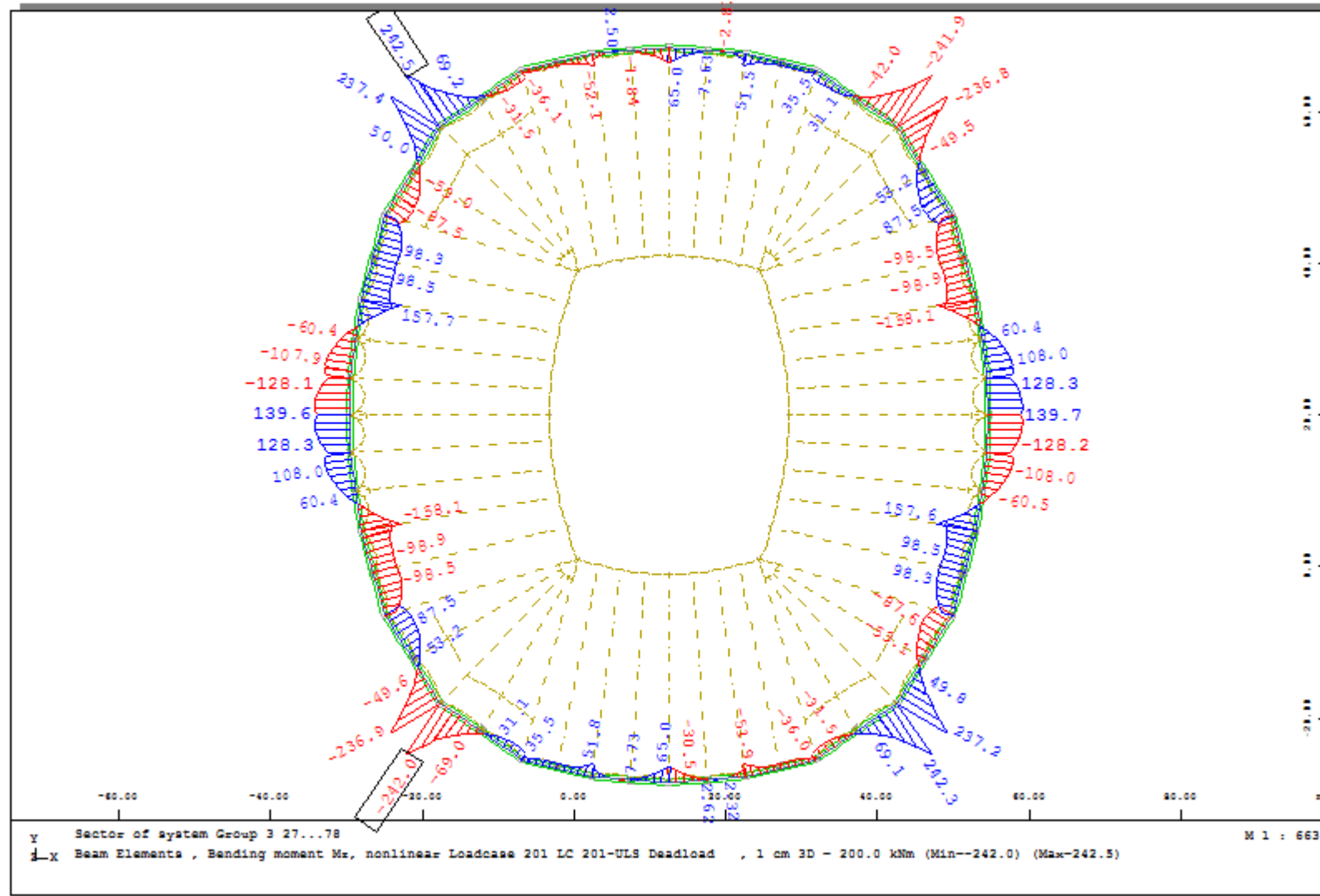
Service Limit State: Loadcase Deadload + Prestress – Bending Moments



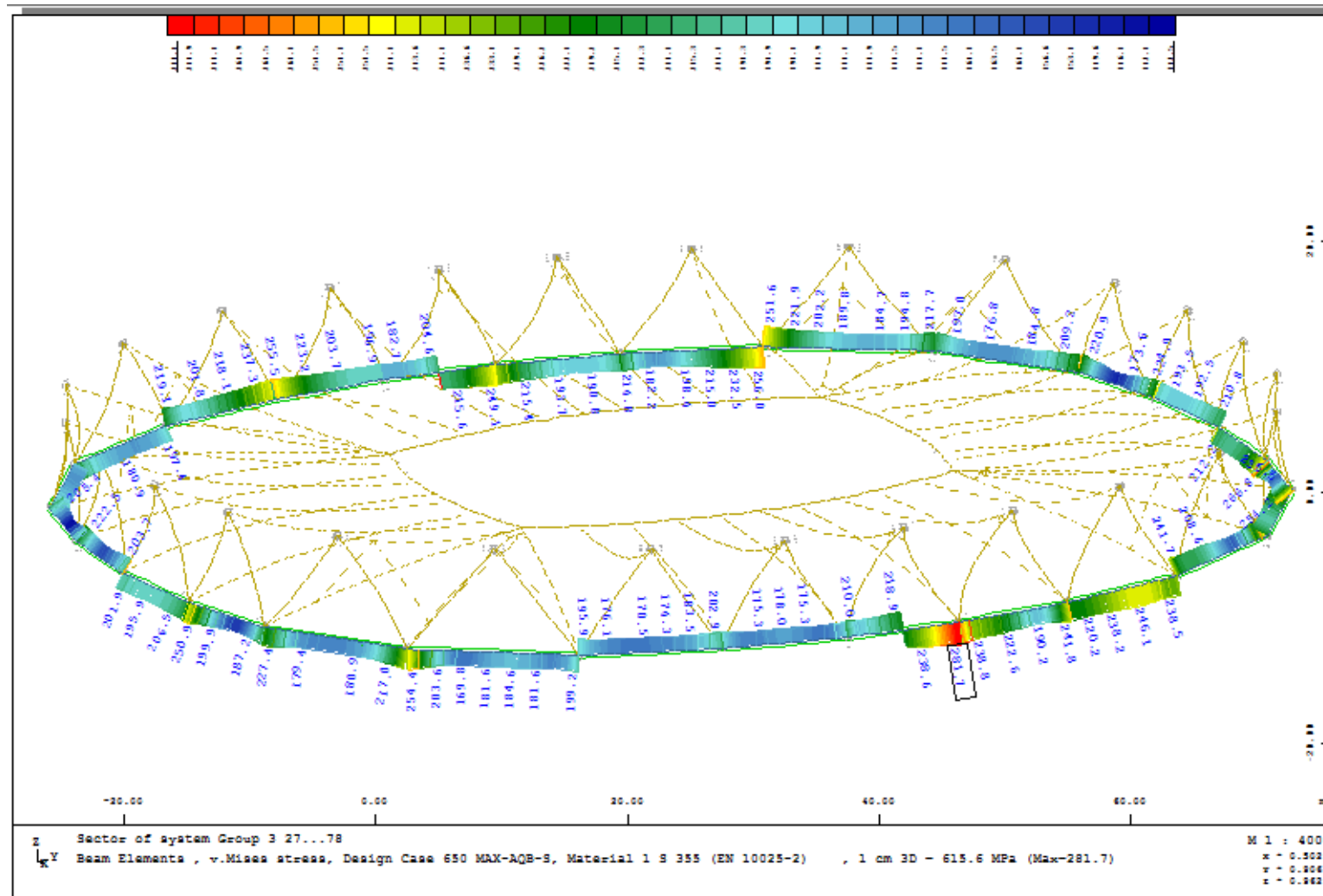
Ultimate Limit State: Loadcase Deadload + Prestress – Axial/Normal Forces



Ultimate Limit State: Loadcase Deadload + Prestress – Bending Moments



Ultimate Limit State: Von Mises Stresses : All Load Cases



Design cases : 301-314  
 Groups : 3  
 Elements : All  
 Sections : All

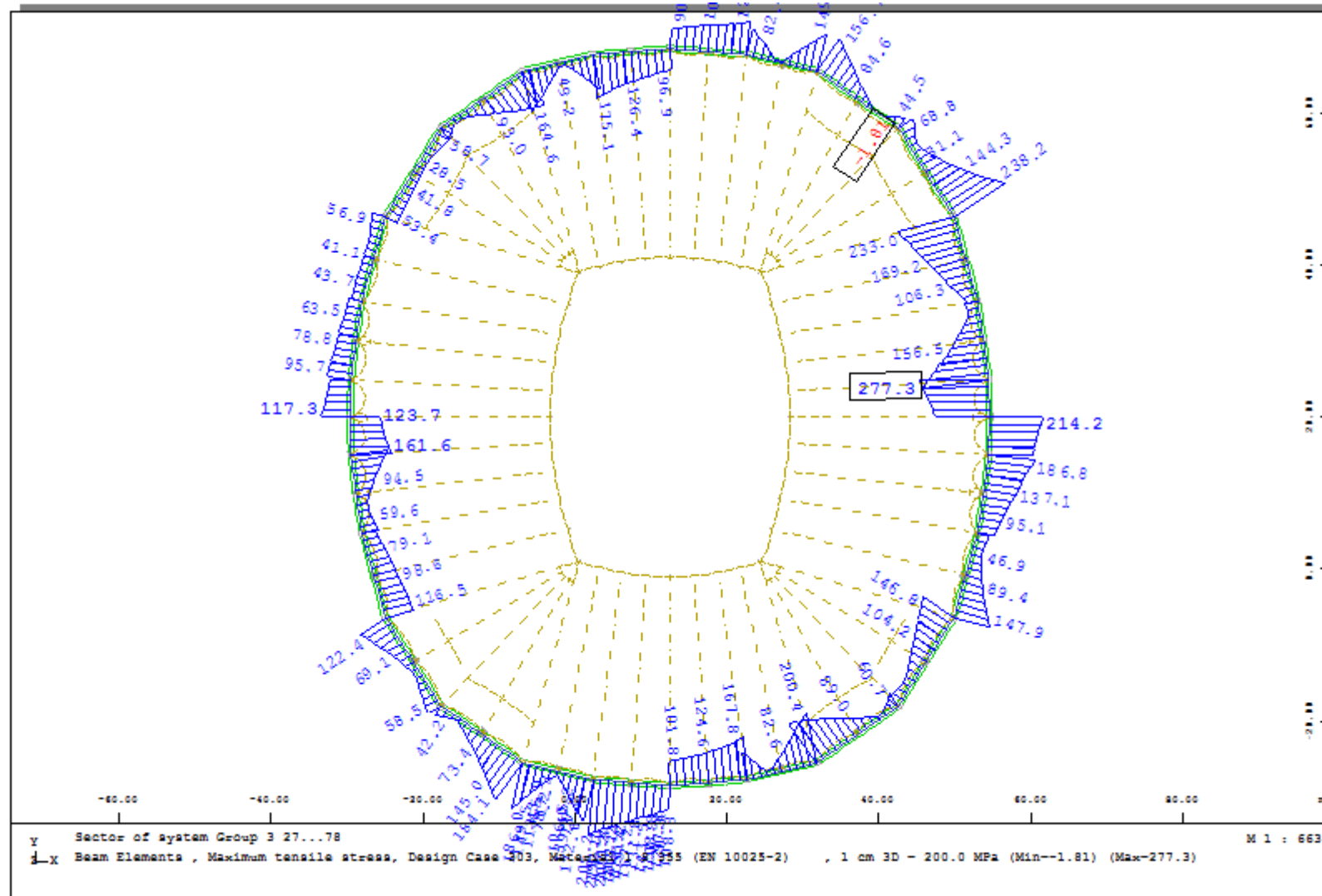
Beam Elements

Stresses

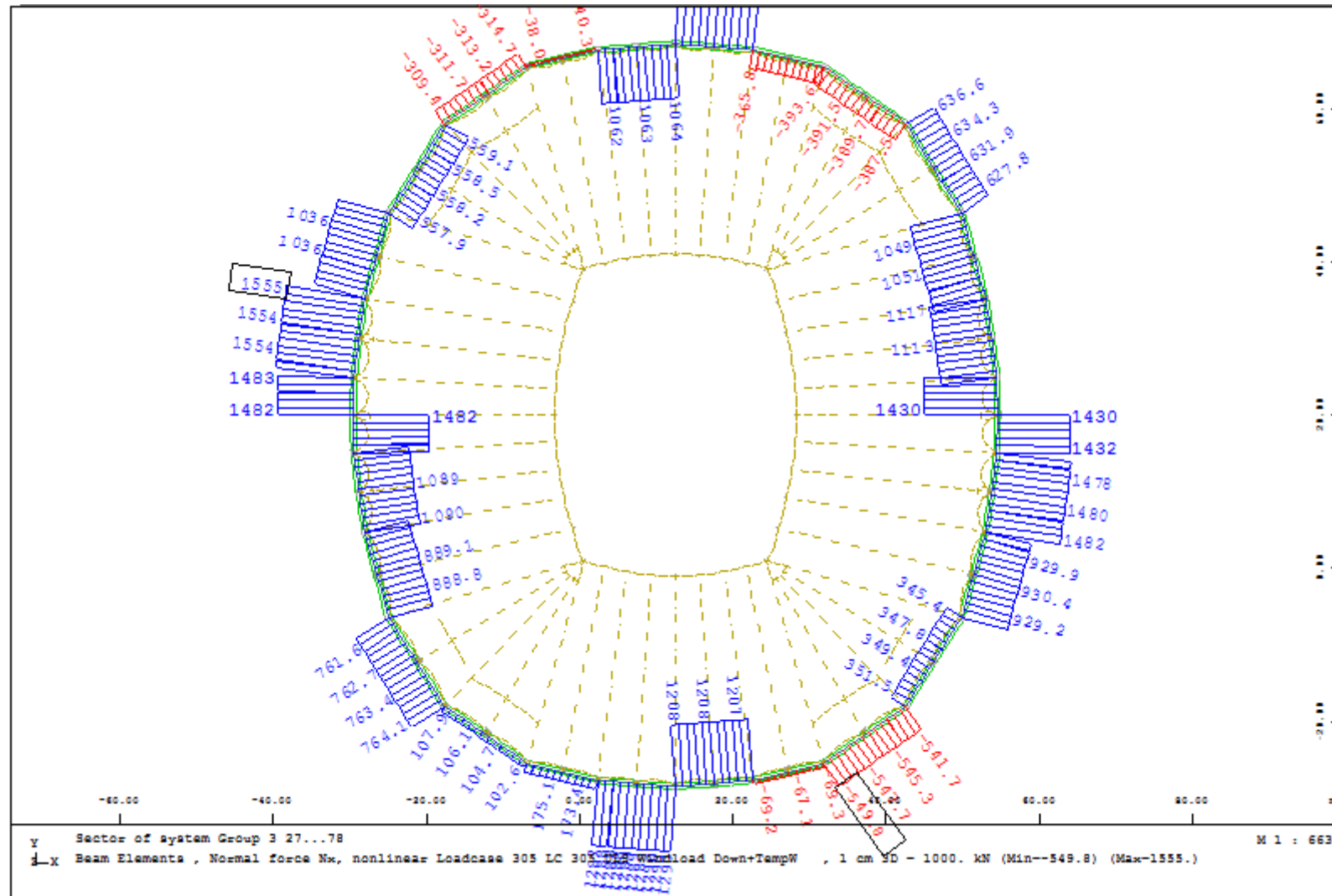
Elem. Nr	X [m]	Mt	DC Name	SIG- [MPa]	SIG+ [MPa]	TAU [MPa]	SIGV [MPa]
1070	0,946	1	304 MINZ-SIG-	-266,14	-23,05	26,35	266,75
1081	0,000	1	308 MAXZ-SIG-	27,24	52,65	5,80	53,25
1203	0,960	1	304 MINZ-SIG+	-168,42	-158,07	12,77	169,85
1146	0,000	1	308 MAXZ-SIG+	-206,55	279,85	24,77	281,67
1177	0,978	1	304 MINZ-TAU	-184,58	-136,09	0,27	184,58
1281	0,000	1	307 MAXZ-TAU	-183,34	184,16	33,27	185,39
1068	0,000	1	313 MINZ-SIGV	-6,57	-1,16	2,74	6,58
1146	0,000	1	308 MAXZ-SIGV	-206,55	279,85	24,77	281,67



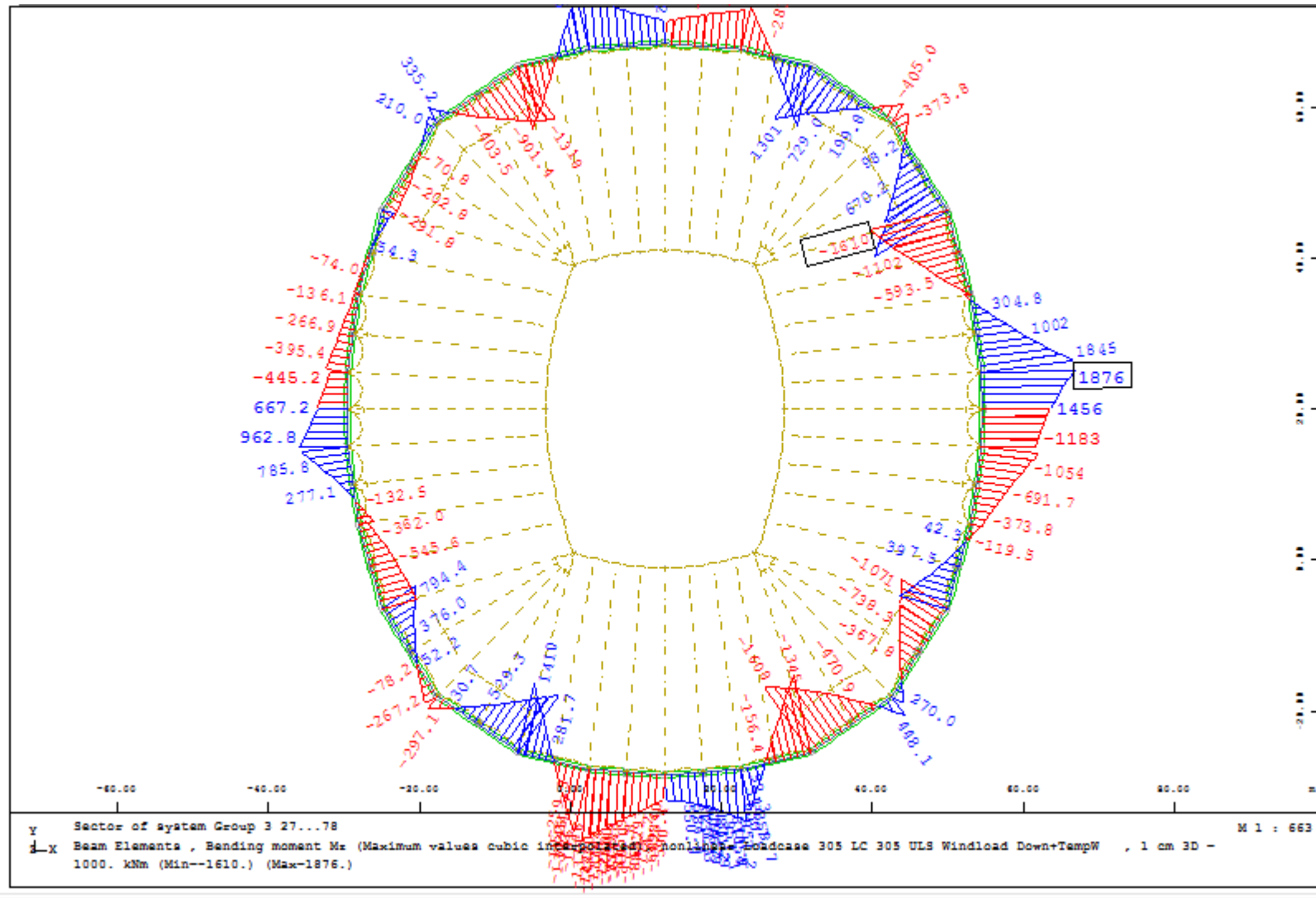
Ultimate Limit State: Loadcase 303 Local Wind Up – Maximum Tensile Stresses



Ultimate Limit State: Loadcase 305 Wind Down + TempW – Axial/Normal Force

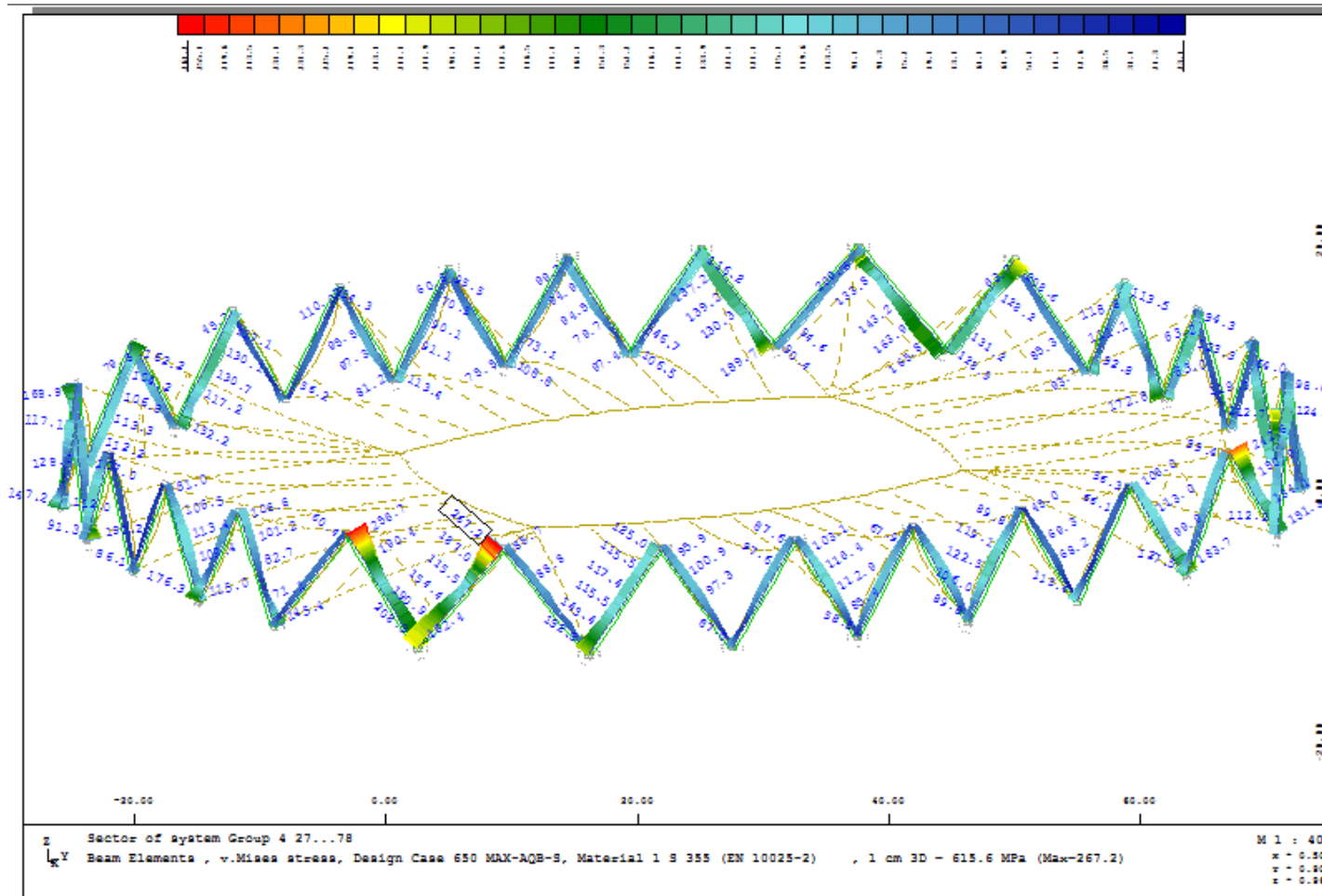


Ultimate Limit State: Loadcase 305 Wind Down + TempW – Maximum Tensile Stresses



5.3 Steel Structure – Diagonals

Ultimate Limit State: Von Mises Stresses : All Load Cases



Design cases : 301-314  
 Groups : 4  
 Elements : All  
 Sections : All

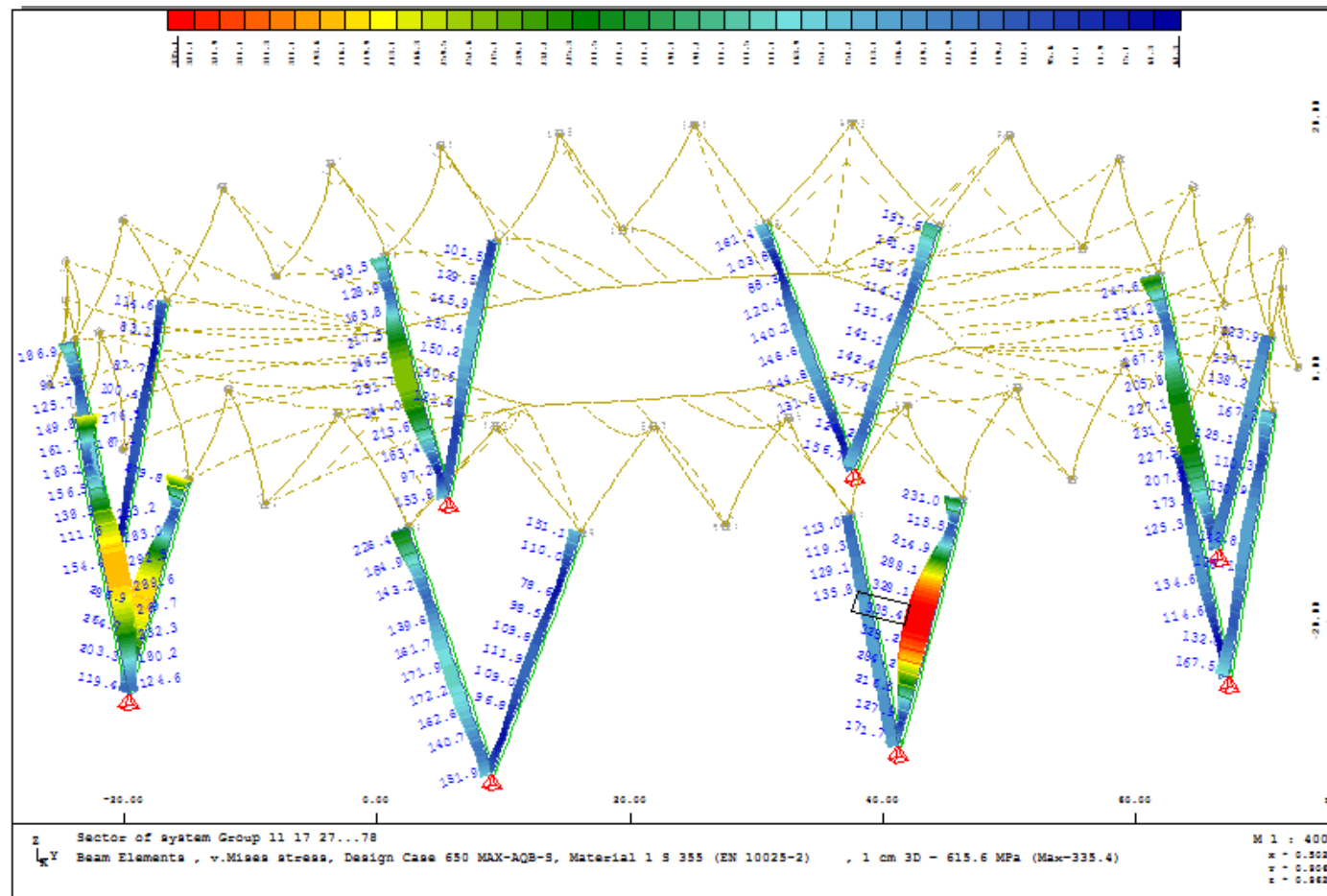
Beam Elements

Stresses						
Elem.	X Mt	DC Name	SIG-	SIG+	TAU	SIGV
Nr	[m]	Nr	[MPa]	[MPa]	[MPa]	[MPa]
2073	0,992	1 308 MINZ-SIG-	-265,52	93,36	26,24	267,24
2471	0,992	1 309 MAXZ-SIG-	32,32	38,32	8,49	38,40
2057	0,000	1 307 MINZ-SIG+	-99,73	-93,55	26,94	110,04
2505	0,000	1 308 MAXZ-SIG+	-146,88	128,45	13,97	146,88
2151	0,996	1 312 MINZ-TAU	-40,85	23,23	0,15	40,85
2188	0,933	1 308 MAXZ-TAU	-178,79	33,51	33,02	183,70
2417	0,980	1 312 MINZ-SIGV	-2,42	2,31	3,61	6,65
2073	0,992	1 308 MAXZ-SIGV	-265,52	93,36	26,24	267,24



5.4 Steel Structure – Columns

Ultimate Limit State: Von Mises Stresses : All Load Cases



Design cases : 301-314  
 Groups : 11-17  
 Elements : All  
 Sections : All

Beam Elements

Stresses						
Elem.	X Mt	DC Name	SIG-	SIG+	TAU	SIGV
Nr	[m]	Nr	[MPa]	[MPa]	[MPa]	[MPa]
8053	0,980	1 308 MINZ-SIG-	-334,76	199,66	12,83	335,38
5119	1,007	1 304 MAXZ-SIG-	50,01	58,78	15,07	63,62
5162	1,007	1 308 MINZ-SIG+	-107,81	-100,29	16,90	111,44
8053	0,980	1 308 MAXZ-SIG+	-334,76	199,66	12,83	335,38
8140	0,000	1 313 MINZ-TAU	-85,84	55,99	0,73	85,84
8063	0,980	1 308 MAXZ-TAU	-230,57	98,38	31,09	231,00
8079	0,000	1 309 MINZ-SIGV	-3,77	0,93	4,66	8,43
8053	0,980	1 308 MAXZ-SIGV	-334,76	199,66	12,83	335,38

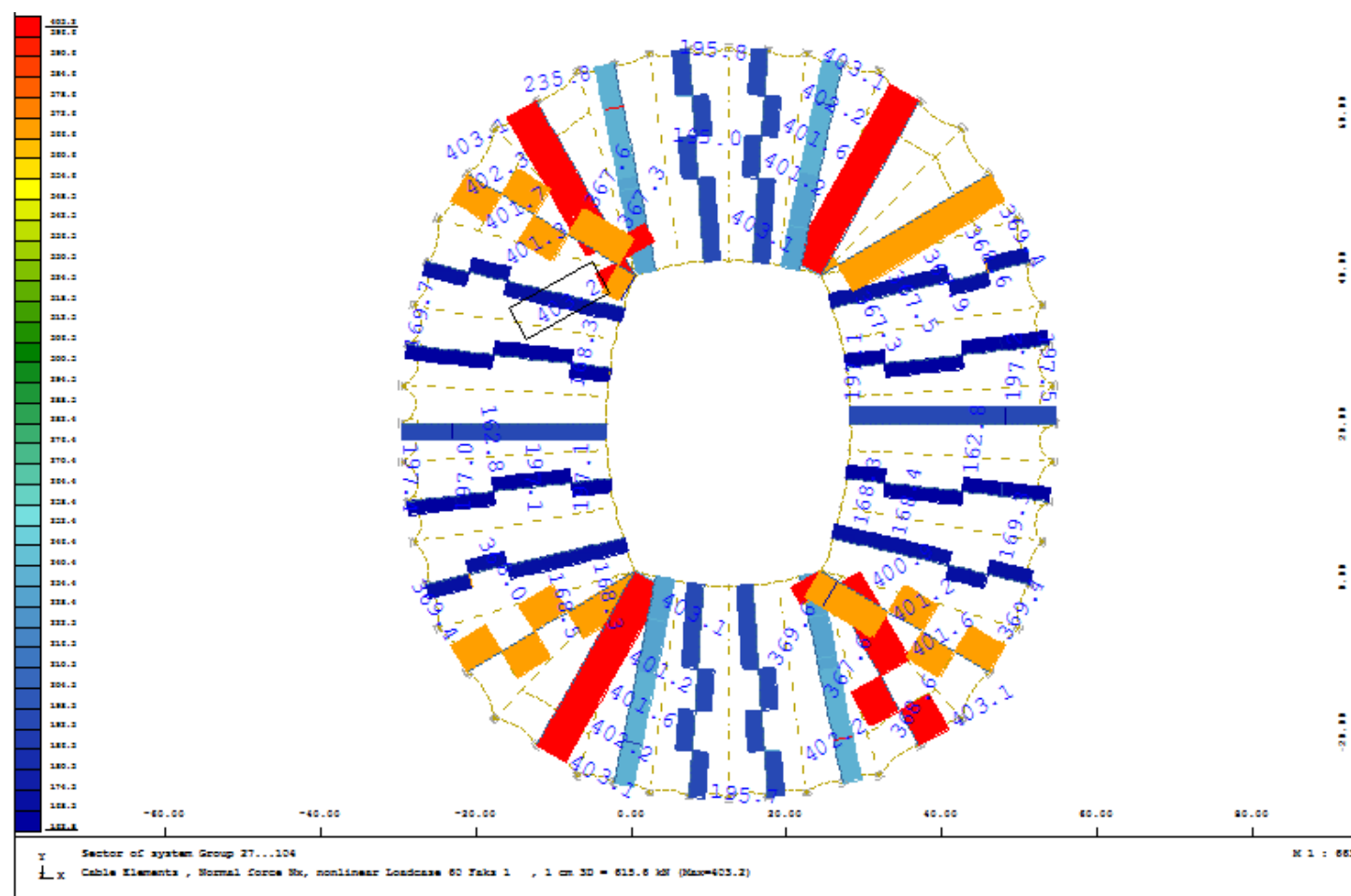
In the areas where the steel stresses are higher than the admissible value of 323 MPa, the cross section will be locally reinforced.

5.5 Cables – Overview

	SLS - Prestress - kN	% Prestress/Beaking Load	ULS - Maximum Force - kN	% ULS Force/Beaking Load	Limit Tension - kN	Breaking load kN	Diameter mm
	Maximum				Pfeifer - Cable Structures		Maximum
Upper Radial Cables	403	6,3	3329	52,10	3873	6390	80
Lower Radial Cables	506	10,3	2375	48,57	2964	4890	70
Tension Ring Cables	612	10,9	2748	48,90	3406	5620	75
Front Edge Cables	32	6,0	189	35,20	326	537	24.4
Back Edge Cables	65	12,1	311	57,91	326	537	24.4

5.6 Cable Structure – Radial Cables

Upper Radial Cables - Prestress



Upper Radial Cables – Maximum Forces

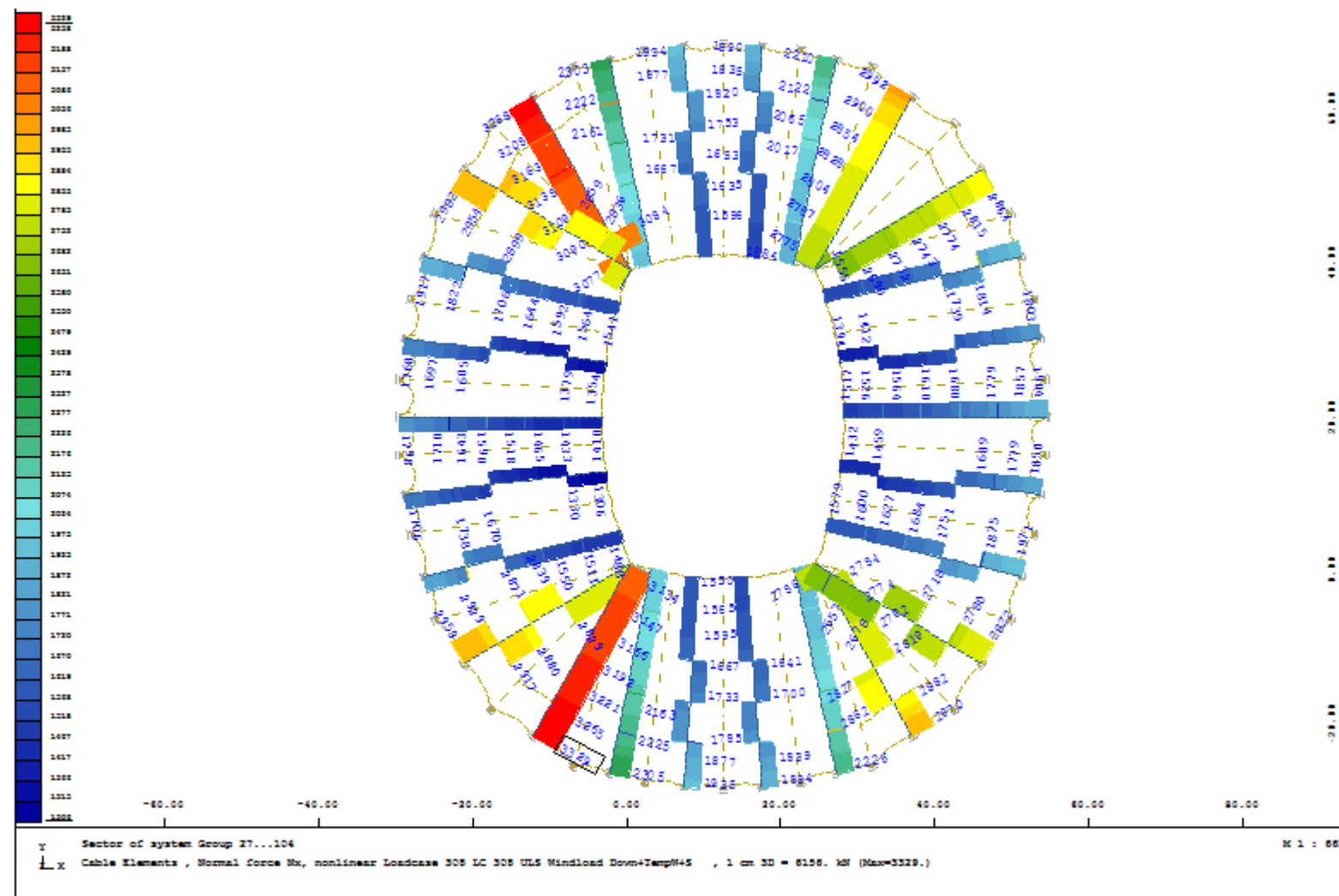
Loadcases : 301-314  
 Groups : 79-104  
 Elements : All

Cable Elements

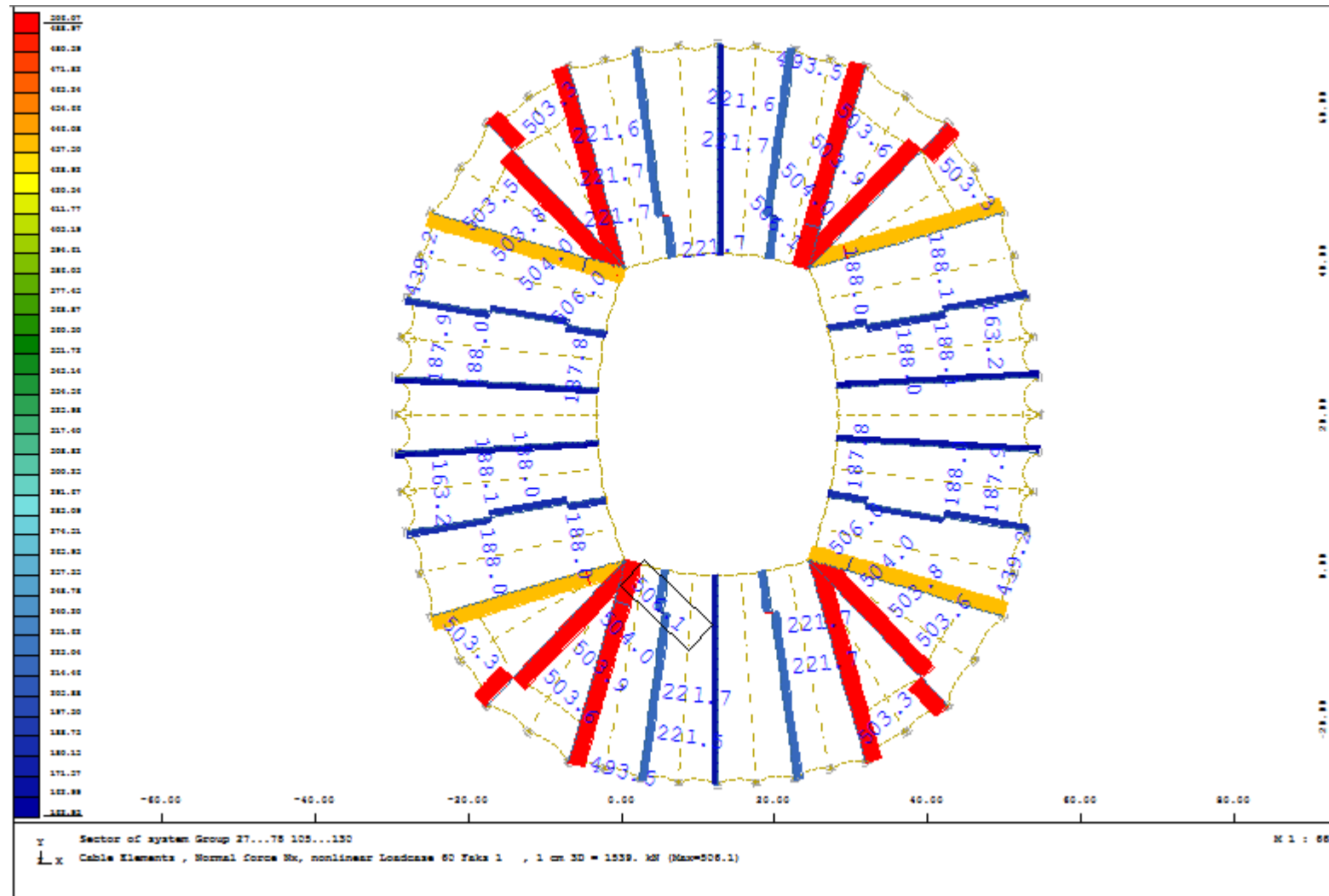
Forces in Cable-Elements

Elem.	LC Name	N	v	vg
Nr	Nr	[kN]	[mm]	[mm]
61015	302 MINZ-N	0,0	-199,992	0,000
65001	308 MAXZ-N	3329,4	36,824	0,000

Upper Radial Cables – Maximum Forces



Lower Radial Cables - Prestress



Lower Radial Cables – Maximum Forces

Loadcases : 301-314  
 Groups : 105-130  
 Elements : All

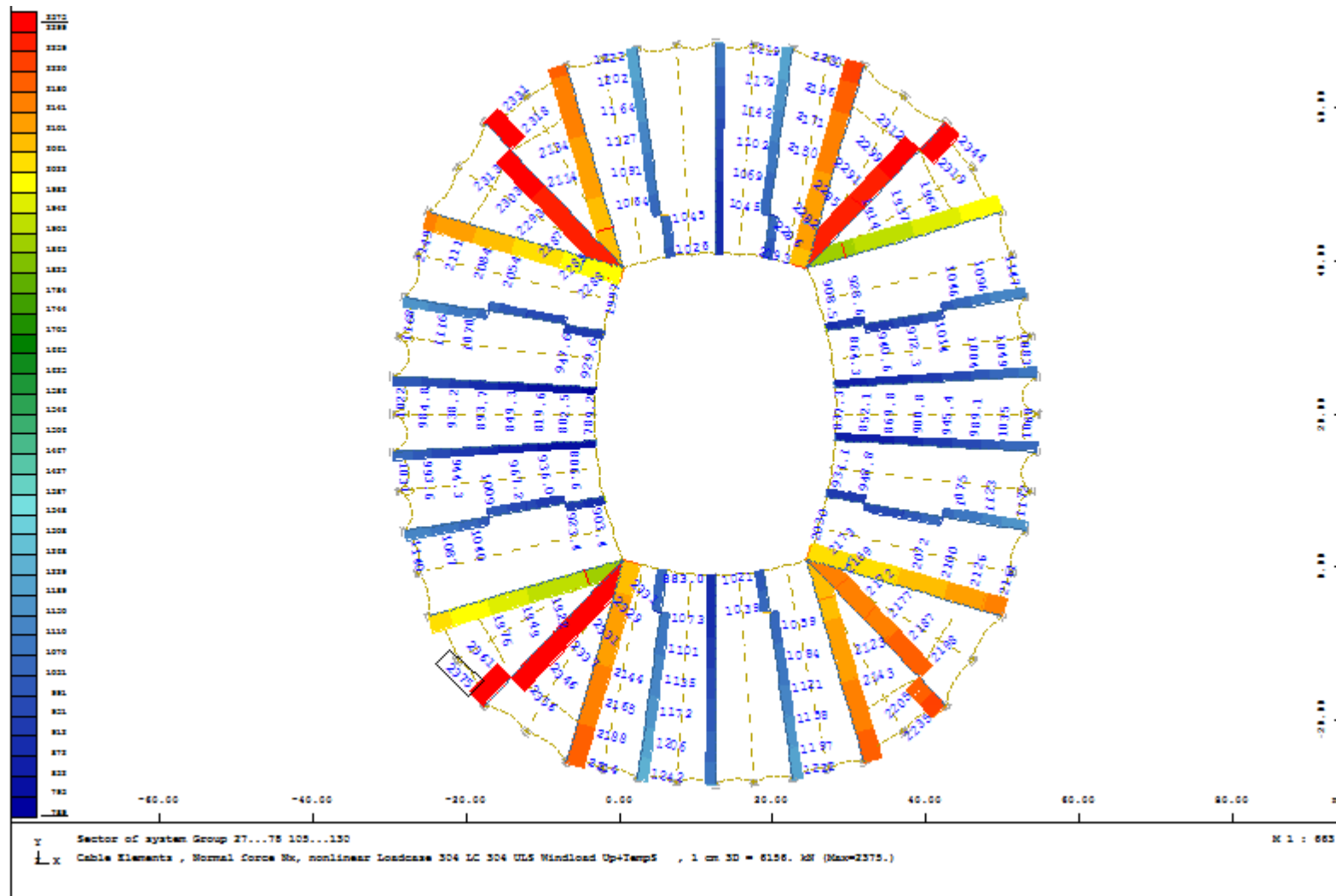
Cable Elements

Forces in Cable-Elements

Elem.	Nr	LC Name	N [kN]	v [mm]	vq [mm]	vqx [mm]	vqy [mm]	vqz [mm]
87001	303	MINZ-N	0,0	-161,484	0,000	0,000	0,000	0,000
90018	304	MAX2-N	2374,8	65,980	0,000	0,000	0,000	0,000

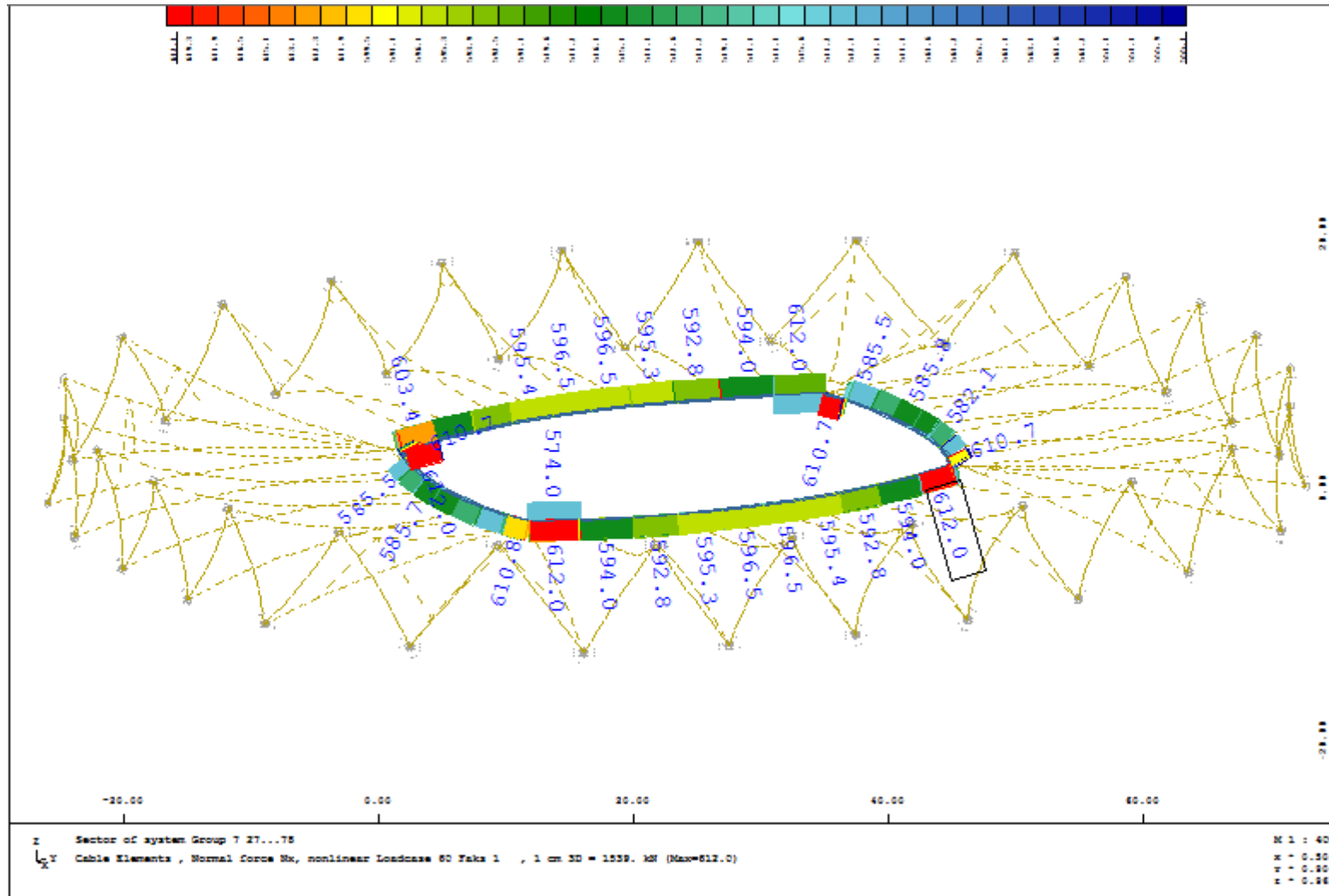


Lower Radial Cables – Maximum Forces



5.7 Cable Structure – Tension Ring

Tension Ring Cables - Prestress



Tension Ring Cables – Maximum Forces

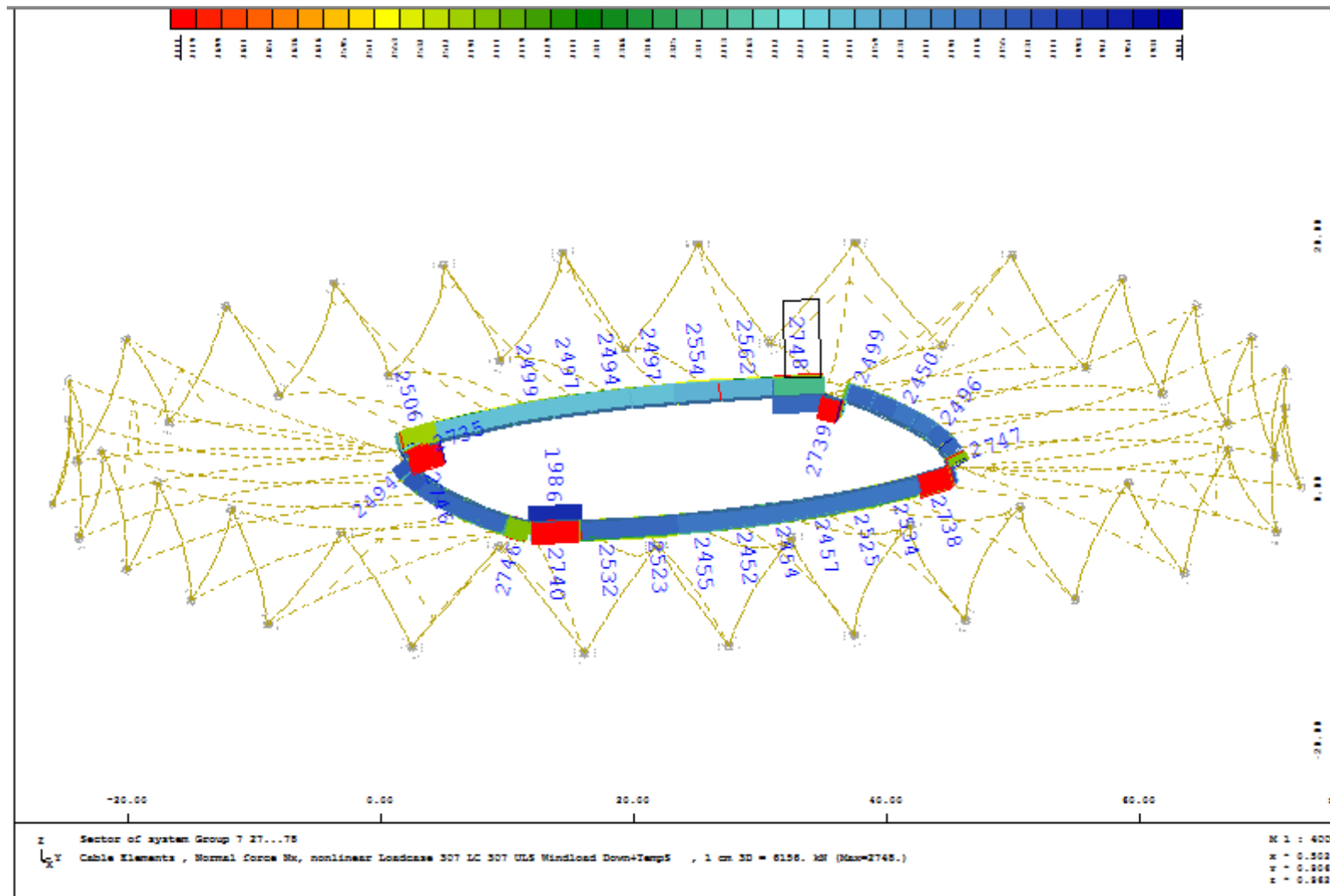
Loadcases : 301-314  
 Groups : 7  
 Elements : All

Cable Elements

Forces in Cable-Elements

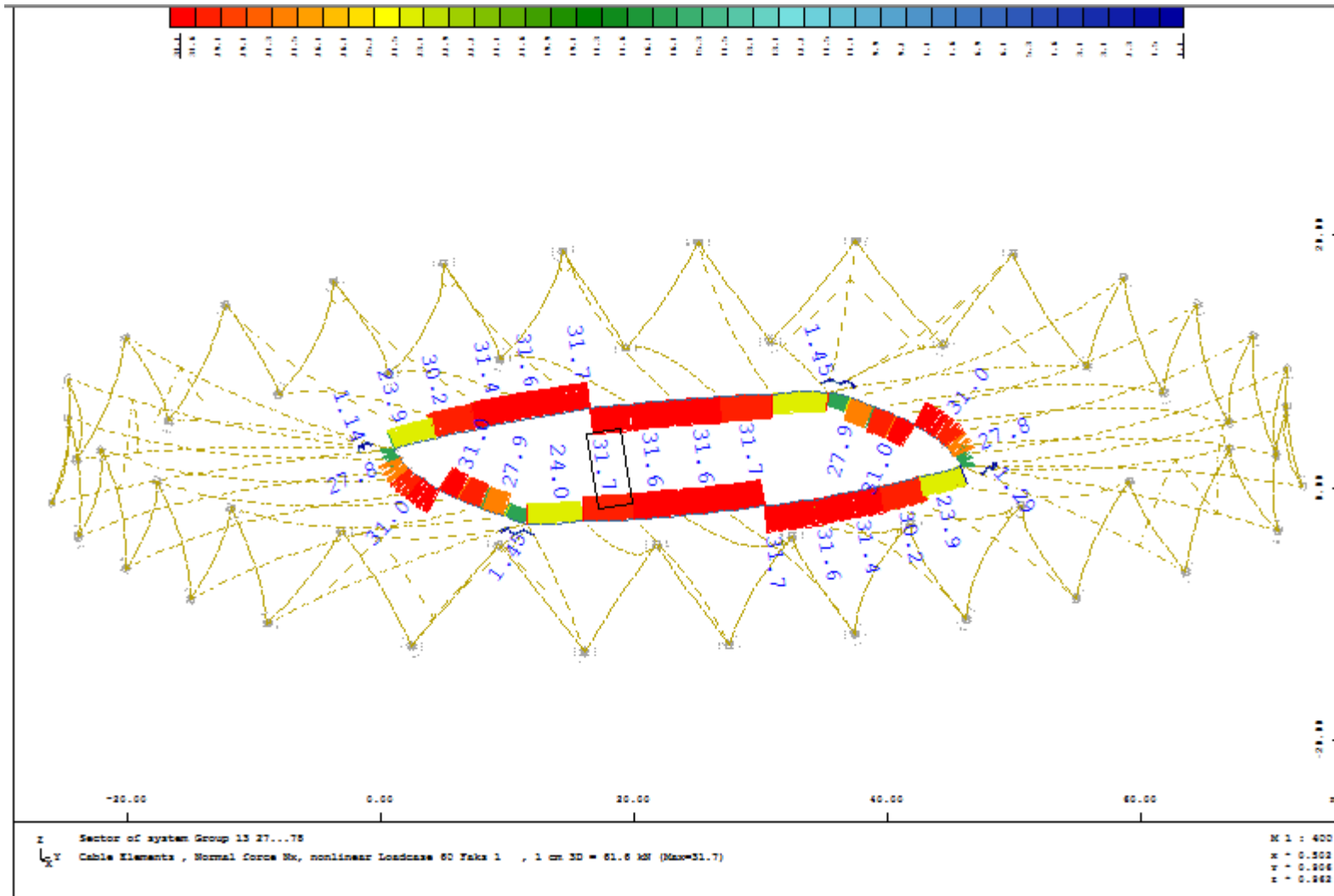
Elem.	LC Name	N	v	vg
Nr	Nr	[kN]	[mm]	[mm]
3141	301 MINZ-N	718,0	-80,376	0,000
3129	307 MAXZ-N	2747,9	-72,885	0,000

Tension Ring Cables – Maximum Forces



5.8 Cable Structure – Front Edge Cables

Front Edge Cables – Prestress



Front Edge Cables – Maximum Forces

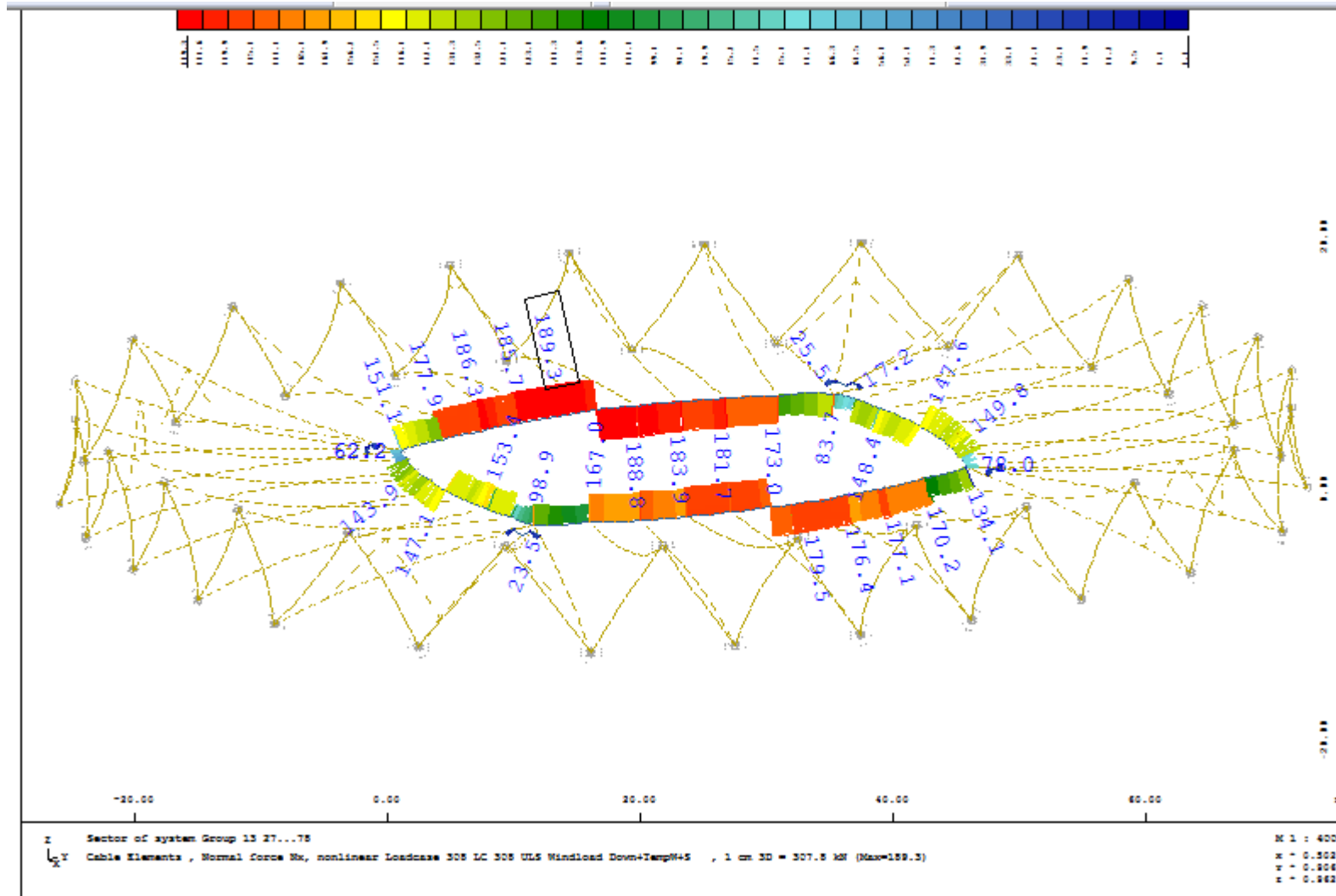
Loadcases : 301-314  
 Groups : 13  
 Elements : All

Cable Elements

Forces in Cable-Elements

Elem.	LC Name	N	v	vq
Nr	Nr	[kN]	[mm]	[mm]
6002	302 MINZ-N	0,0	-54,609	0,000
6072	308 MAXZ-N	189,3	-11,012	0,000

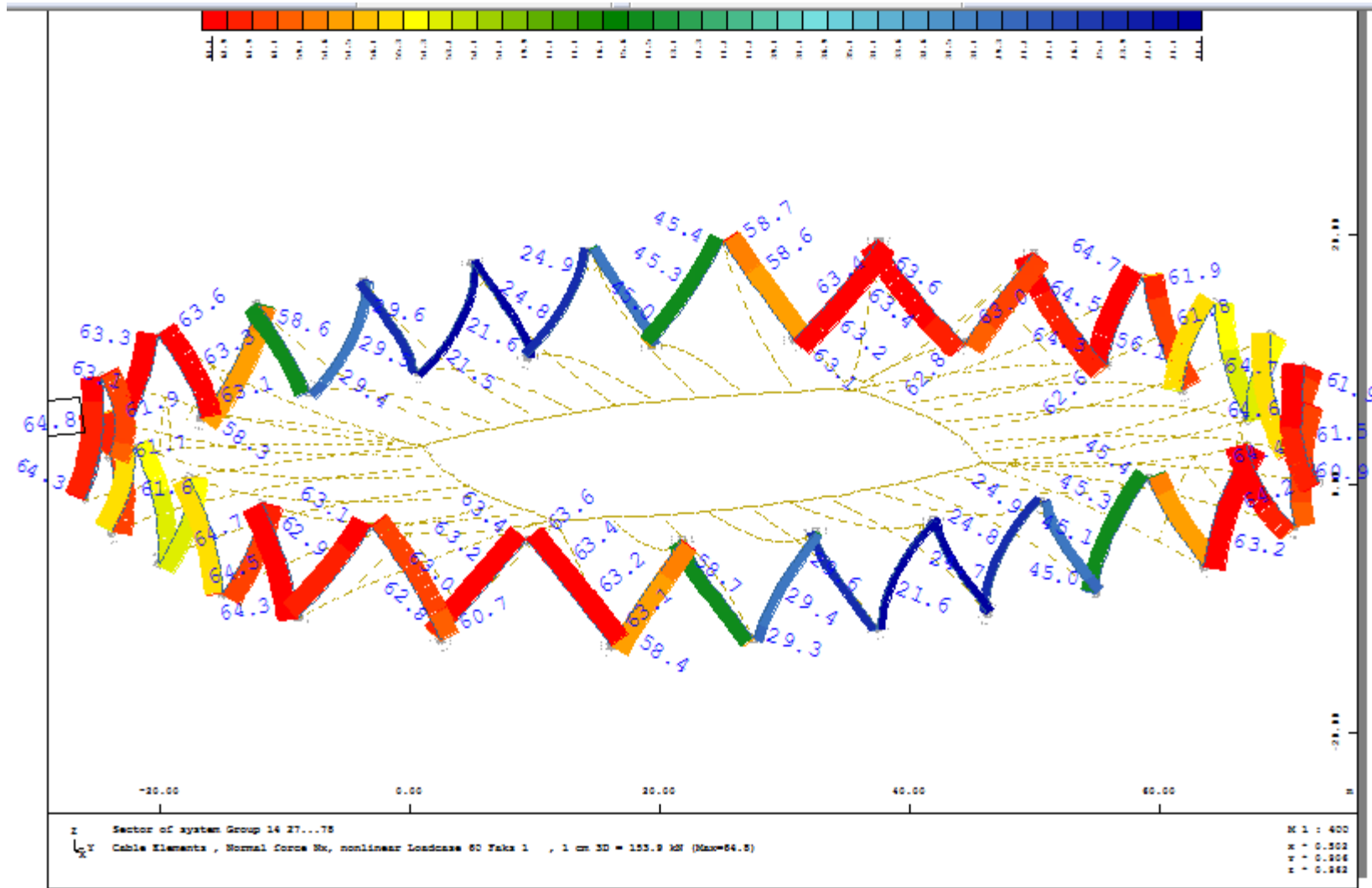
Front Edge Cables – Maximum Forces





5.9 Cable Structure – Back Edge Cables

Back Edge Cables – Prestress



Back Edge Cables – Maximum Forces

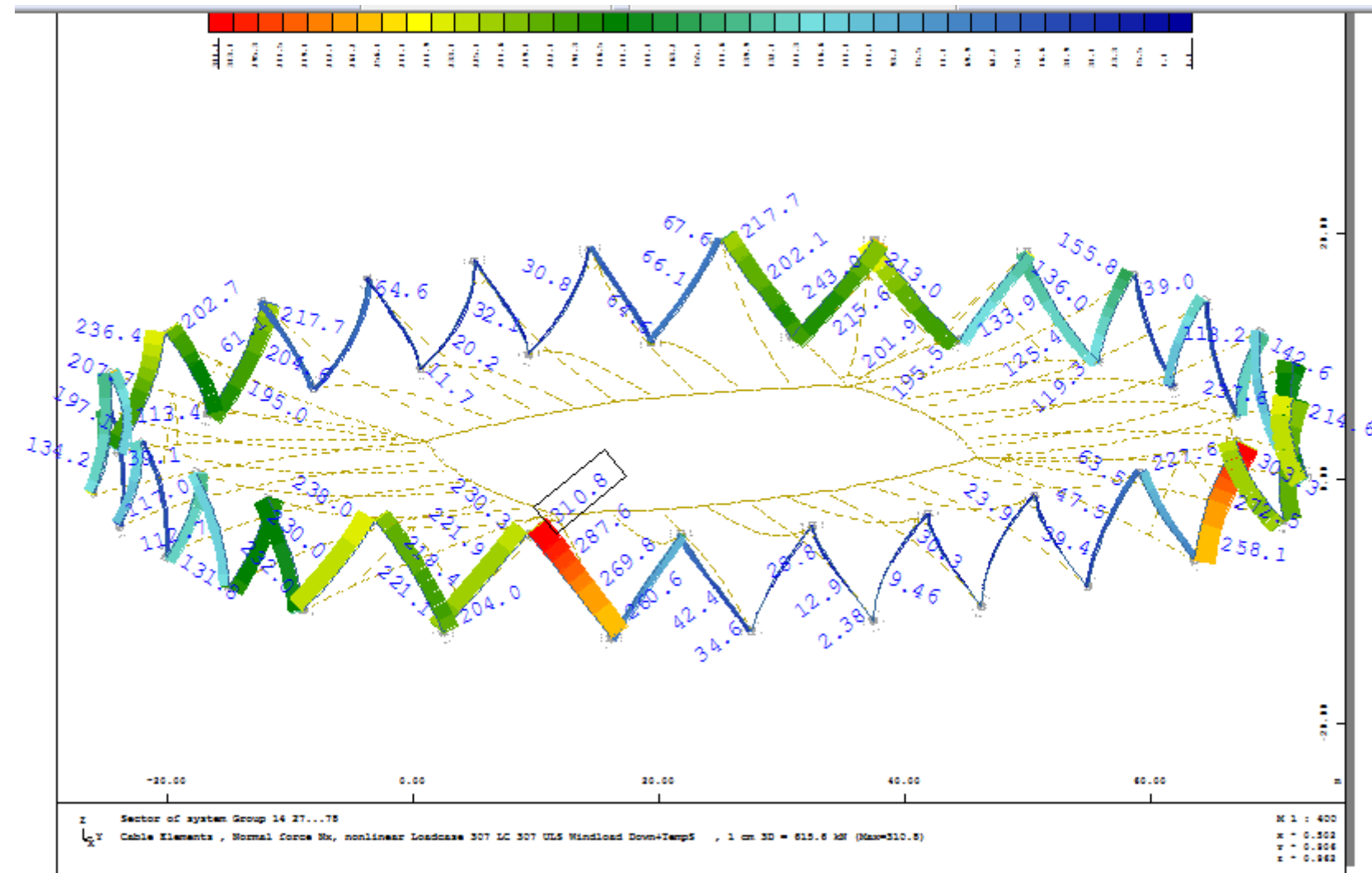
Loadcases : 301-314  
 Groups : 14  
 Elements : All

Cable Elements

Forces in Cable-Elements

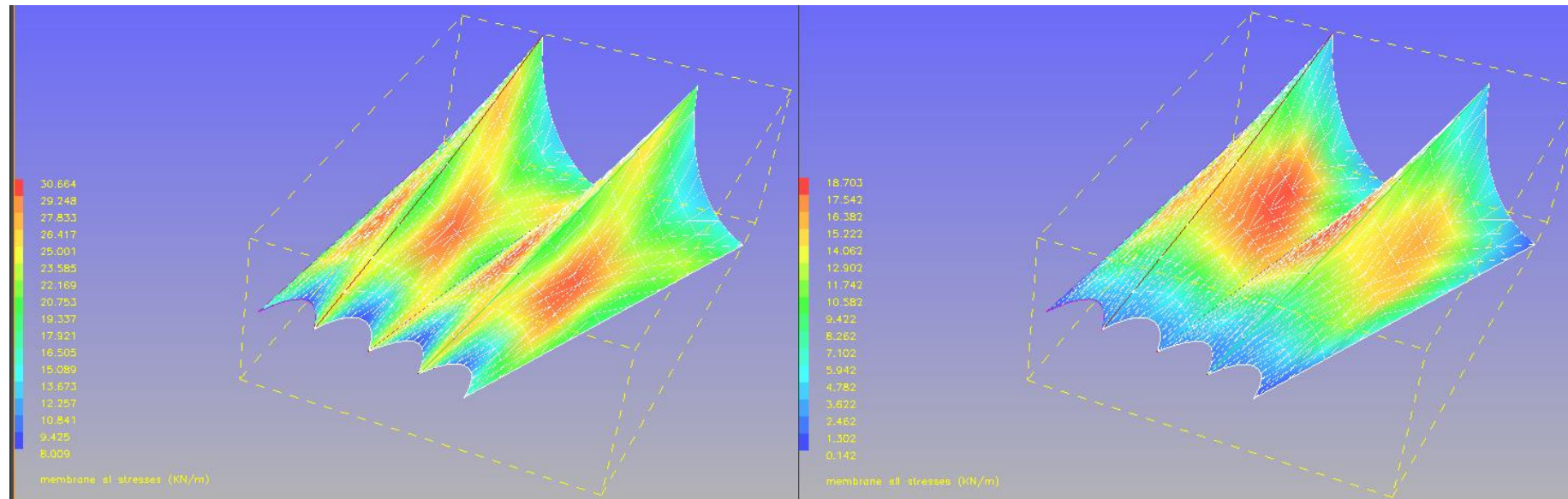
Elem.	LC Name	N	v	vq
Nr	Nr	[kN]	[mm]	[mm]
7010	302 MINZ-N	0,0	-27,960	0,000
7470	307 MAXZ-N	310,8	10,947	0,000

Back Edge Cables – Maximum Forces

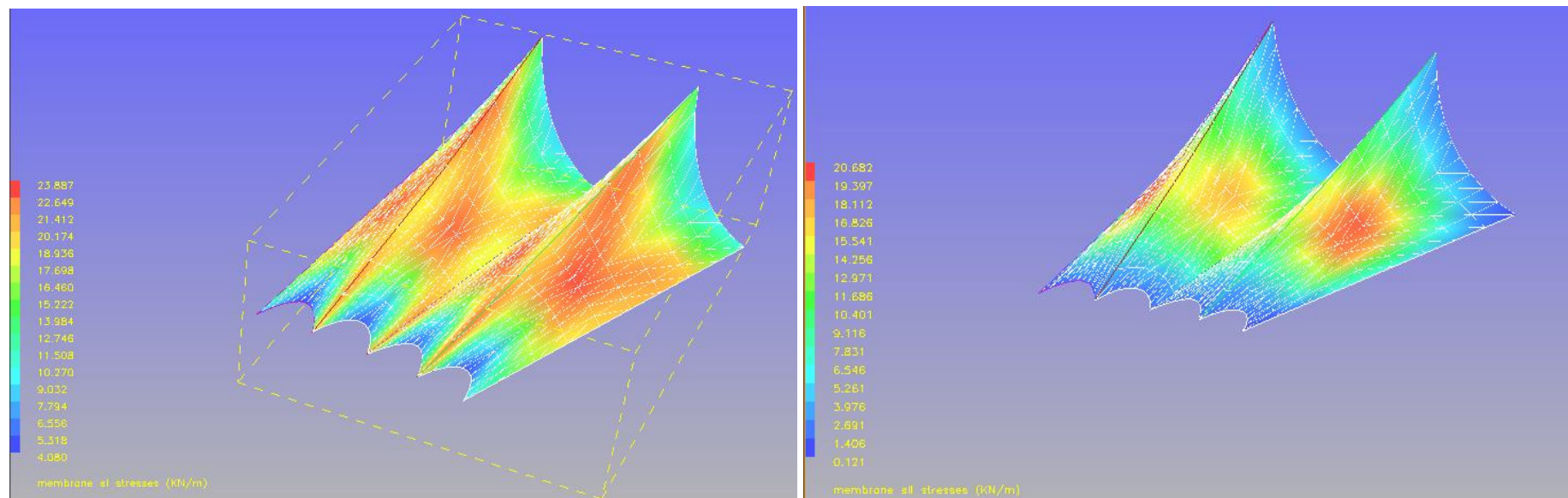


5.10 Membrane Dimensioning

Membrane Wind Local Analysis Down considering Cp Values – Principal Stresses



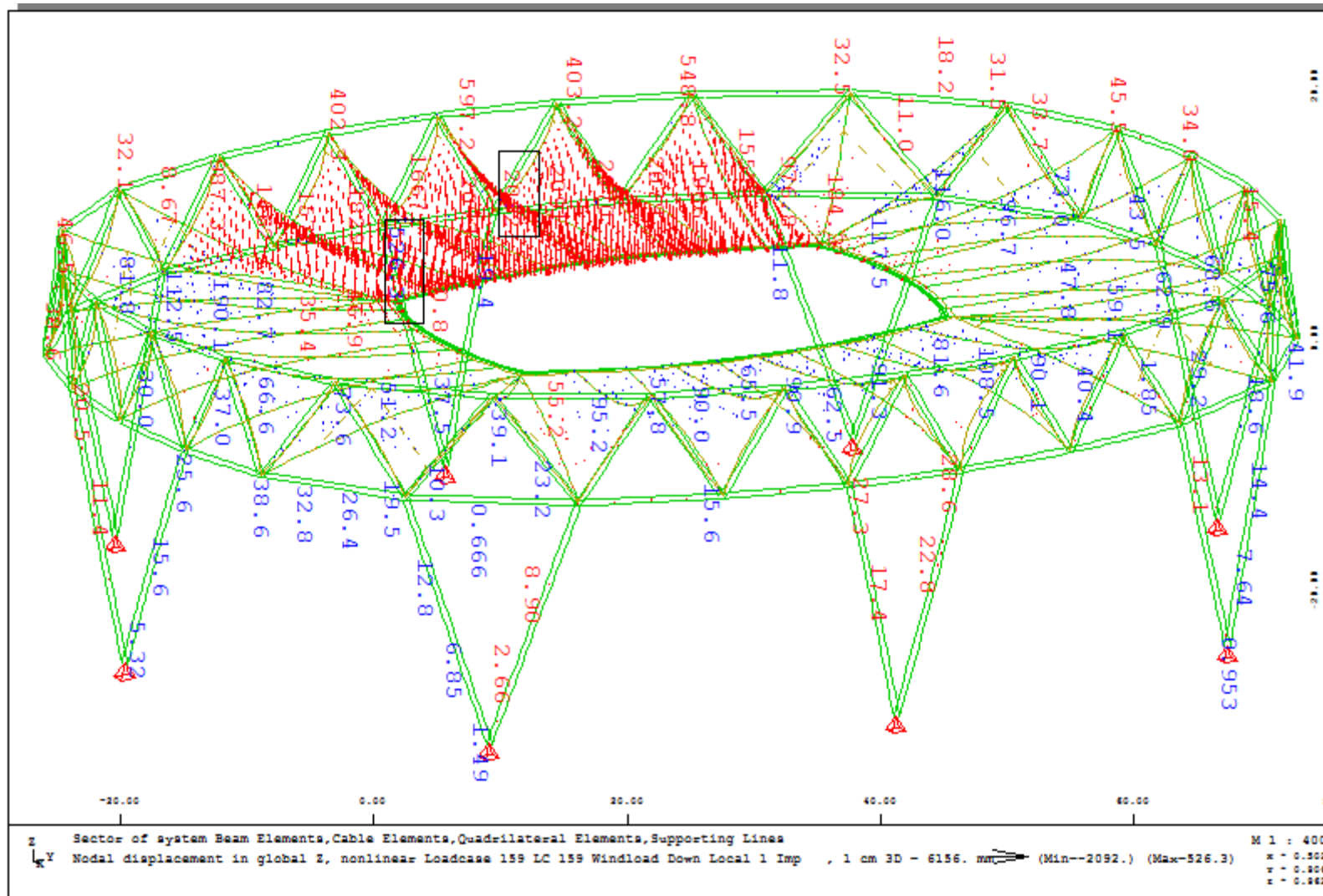
Membrane Wind Local Analysis Up considering Cp Values – Principal Stresses



Values for the actual membrane stresses taken from the global analysis from Sofistik, similar to Forten.

Membrane stress check					
		Fabric		Connection	
	: influence of biaxial stresses	1,2		1,2	
	: long-term loads	1,6		1,5	
	: environmental influences	1,1		1,2	
	: influence of high temperature	1,2		1,5	
	: inaccuracy in the fabrication process	1		1	
<b>Fu,k (ULS),Fabric</b>	: material safety factor (resistant side)	1,4		1,5	
<b>Fu,k (ULS),Fabric</b>	: Load factor	1,5		1,5	
		1,6		1,6	
$\gamma_f \cdot \gamma_m \cdot A_0 \cdot A_1 \cdot A_2 \cdot \gamma_f$	: for permanent load	5,32		7,29	
$\gamma_f \cdot \gamma_m \cdot A_0 \cdot A_2$	: for load combinations with wind load as leading action	2,96		3,46	
$\gamma_f \cdot \gamma_m \cdot A_0 \cdot A_1 \cdot A_2$	: for load combinations with snow as leading action	4,44		4,86	
		Warp	% Warp	Weft	% Weft
<b>Membrane</b>	<b>Ferrari 1202</b>	112		112 kN/m	0,2
$f_{u,k} / A_{res,v}$	: Allowable stress for prestress	21,04	19%	21,04	19%
$f_{u,k} / A_{res,w}$	: Allowable stress for wind load	37,88	34%	37,88	34%
$f_{u,k} / A_{res,s}$	: Allowable stress for Snow load	25,25	23%	25,25	23%
		Warp	% Warp	Weft	% Weft
<b>Connection</b>	<b>Ferrari 1202</b>	112		112 kN/m	0,2
$f_{u,k} / A_{res,v}$	: Allowable stress for prestress	15,36	14%	15,36	14%
$f_{u,k} / A_{res,w}$	: Allowable stress for wind load	32,41	29%	32,41	29%
$f_{u,k} / A_{res,s}$	: Allowable stress for Snow load	23,05	21%	23,05	21%
		<b>S11</b>			
$\gamma_f \cdot \max. f_k$	Max. actual membrane stress for Dead Load Case	15,300		100%	OK
	Max. actual membrane stress for Wind Load Cases	30,660		95%	OK
		<b>S22</b>			
	Max. actual membrane stress for Dead Load Case	14,000		91%	OK
	Max. actual membrane stress for Wind Load Cases	18,700		58%	OK

5.11 Service – Displacements

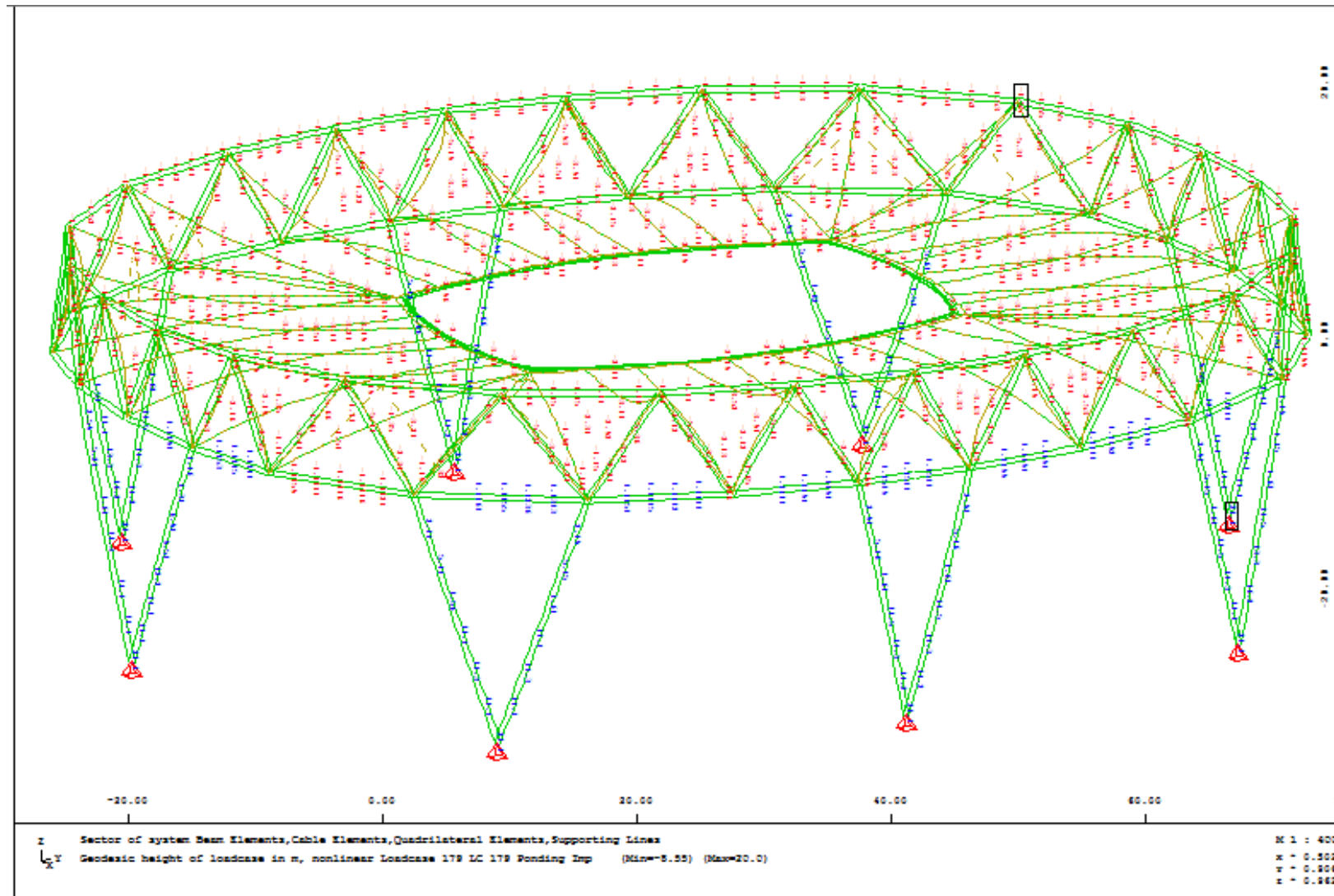


The maximum displacement for the membrane roof is two meters downwards. The roof depth is about thirty meters. With some wind tunnel analysis the result would be more accurate.



5.12 Ponding

According to the French Code, a load of 0.60 kN/m<sup>2</sup> should be considered for Ponding Analysis. In this case, a 1.0 kN/m<sup>2</sup> was analyzed and no ponding areas were found.



## 5.13 Detail – Column Foot

```

Printvolume : Max. or/and min. values
for all selected columns of results with
corresponding values of selected load cases
and elements.
Loadcases   : 301-801
Elements    : All

Nodes

Supporting Forces in Nodes
Node.      LC Name      PX      PY      PZ      MX      MY      MZ
Nr         Nr          [kN]    [kN]    [kN]    [kNm]   [kNm]   [kNm]
1013      304 MINZ-PX    -292,1   461,9  -1457,3   0,00    0,00    0,00
1005      308 MAXZ-PX     335,1   249,1   3052,5   0,00    0,00    0,00
1011      304 MINZ-PY     260,2  -358,1  -1555,7   0,00    0,00    0,00
1013      304 MAXZ-PY    -292,1   461,9  -1457,3   0,00    0,00    0,00
1011      302 MINZ-PZ     238,0  -317,0  -1562,0   0,00    0,00    0,00
1015      307 MAXZ-PZ    -201,7  -256,1   4819,1   0,00    0,00    0,00

```

1 Column –  $P_z = 4819 / 2 = 2410 \text{ kN}$  ;  $P_x = 101 \text{ kN}$  ;  $P_y = 128 \text{ kN}$

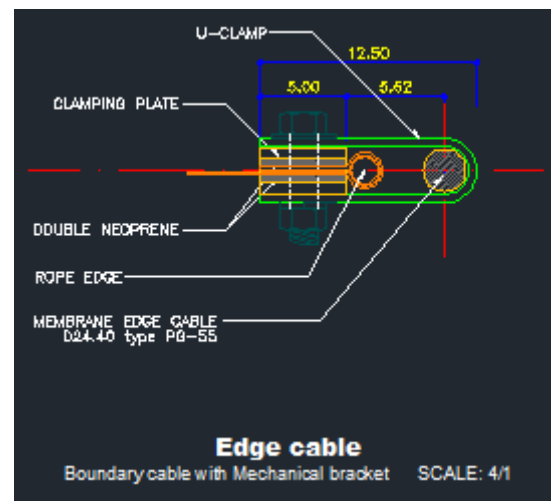
Total Force:

$$\sqrt{2410^2 + 101^2 + 128^2} = 2415.5 \text{ kN}$$

<b>Design of the Eye Plate according to DIN 18800</b>								
<b>Force</b>	Nd	2415,5	kN					
<b>Geometry</b>	t end	45	mm					
	t boss	20	mm					
	r boss	0	mm					
	d bolt	140	mm					
	t side	30	mm					
	aw	0	mm					
	clearance s	5	mm					
	e	0	mm					
	hole clearance	2	mm					
<b>Material</b>	fy,plates,k	355	N/mm2					
	fy,bolt,k	355	N/mm2					
	fu,bolt,k	-	N/mm2					
	gamma	1,1						
	alpha,a	0,8						
<b>Eye Plate</b>								
<b>Middle Plate</b>								
	limit a	139	mm	<	actual a	140	mm	OK
	limit c	91	mm	<	actual c	95	mm	OK
<b>Side Plates</b>								
	limit a	157	mm	<	actual a	160	mm	OK
	limit c	110	mm	<	actual c	115	mm	OK
<b>Design of the Bolt</b>								
<b>Max Forces within Bolt</b>								
	Max Mbolt,d	49,8	kNm	<	Mbolt,Rd	69,6	kNm	OK
	Max Vbolt,d	1207,75	kN	<	Vbolt,Rd	2033	kN	OK
	$(M_d/M_{Rd})^2 + (V_d/V_{Rd})^2 =$		0,87	<	1			OK
<b>Bearing Capacity</b>								
<b>Middle Plate</b>								
	Max VPlate,d	2415,5	kN	<	VPlate,Rd	5761	kN	OK
<b>Side Plates</b>								
	Max VPlate,d	1207,75	kN	<	VPlate,Rd	2033	kN	OK

5.14 Detail – Membrane with flexible Edge

<b>Flexible Membrane Edge</b>	
Membrane Stress - kN/m	29
Spacing between Clamps - m	0,4
Force per Clamp - KN	11,6
Number of Clamps	2
Width of Steel Clamp - m	0,035
Grade of Steel for the Clamp	275
Stresses of Steel - Mpa	55,2
Chosen Clamp Thickness - m	0,003
Bolt - Shear Strength M12 8.8 - kN	32,4



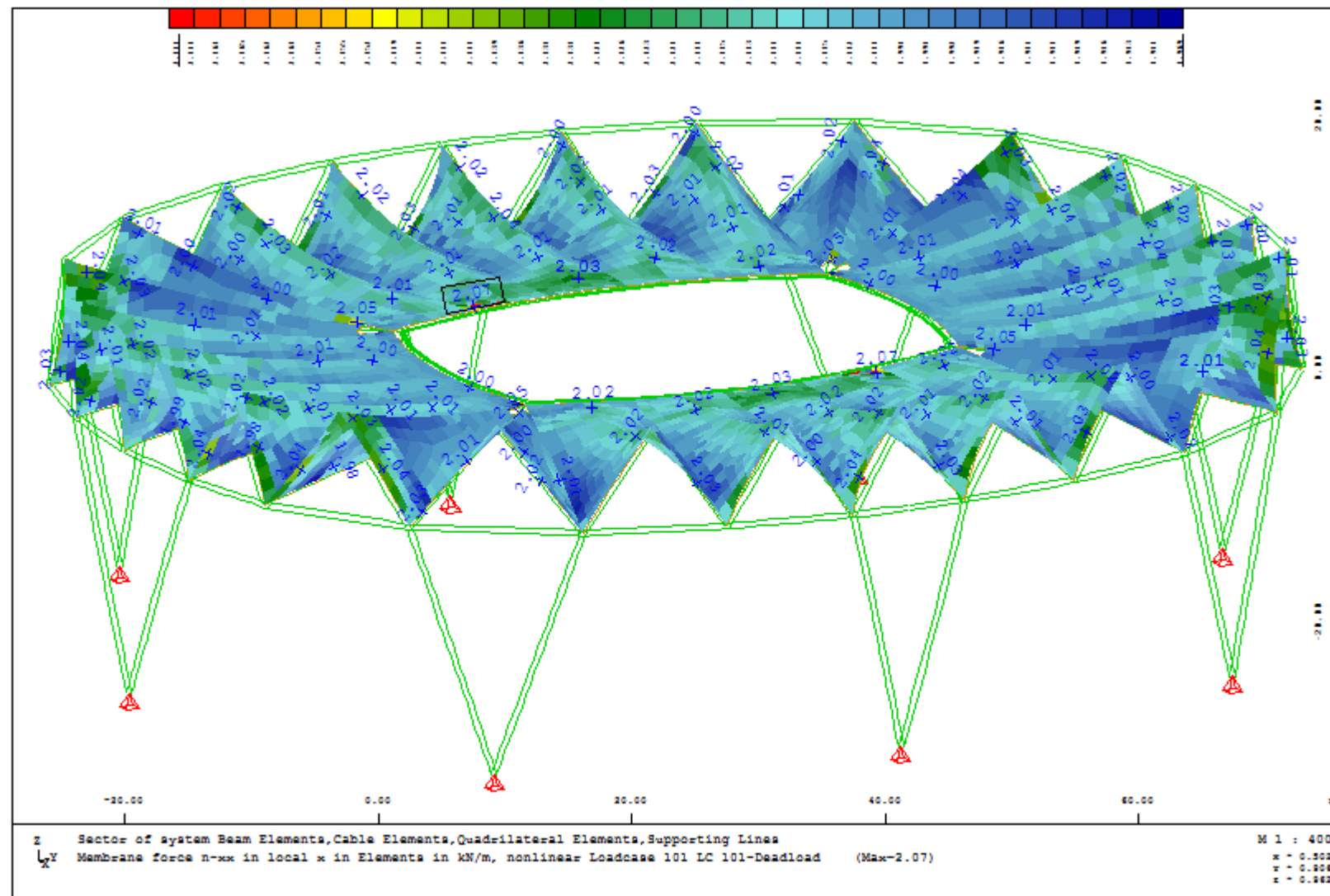


## 6 Membrane Patterning

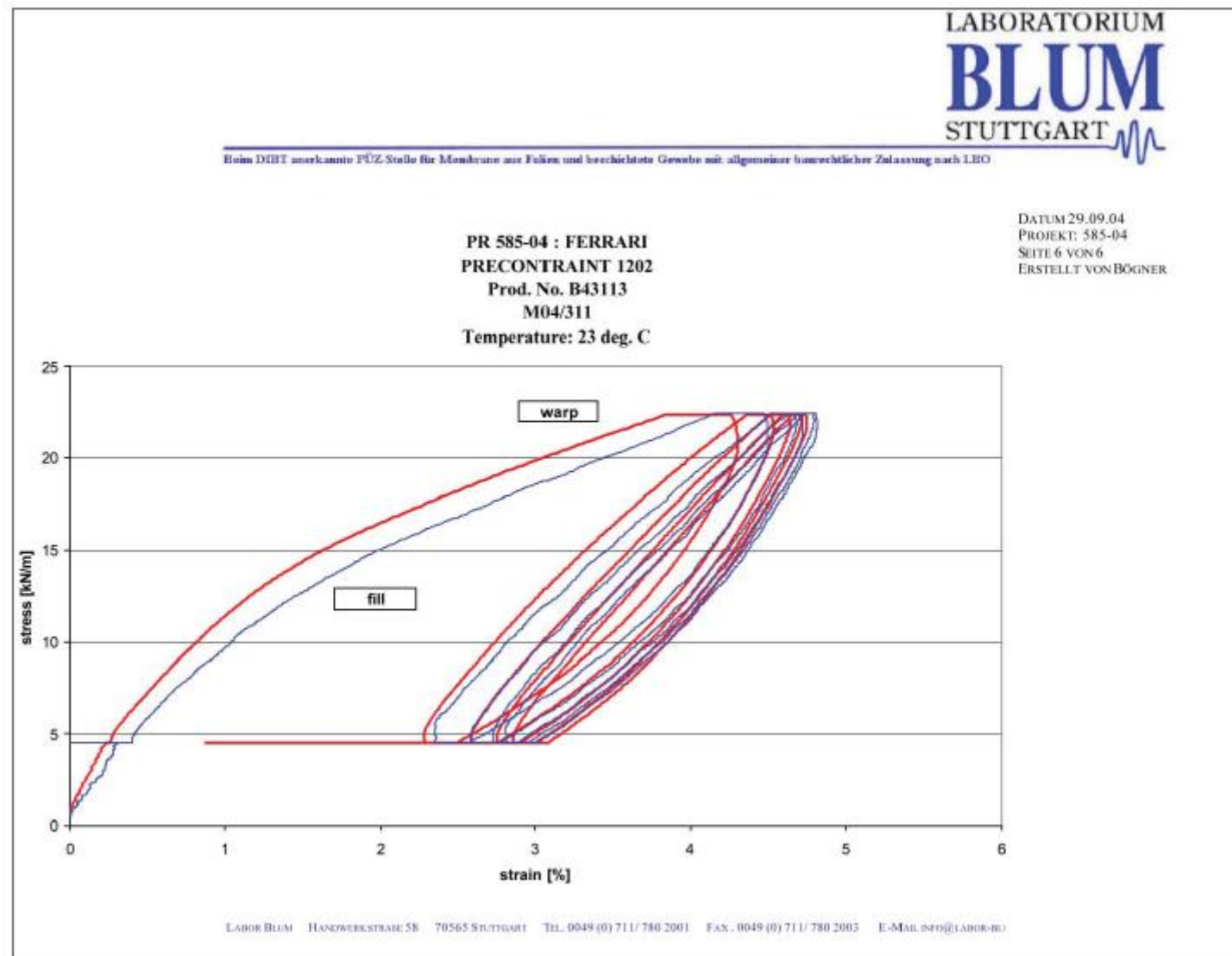


## 6. Membrane Patterning

Membrane Prestress Level – 2 kN/m



Material chosen for the Membrane: Ferrari Preconstraint 1202, Type 3

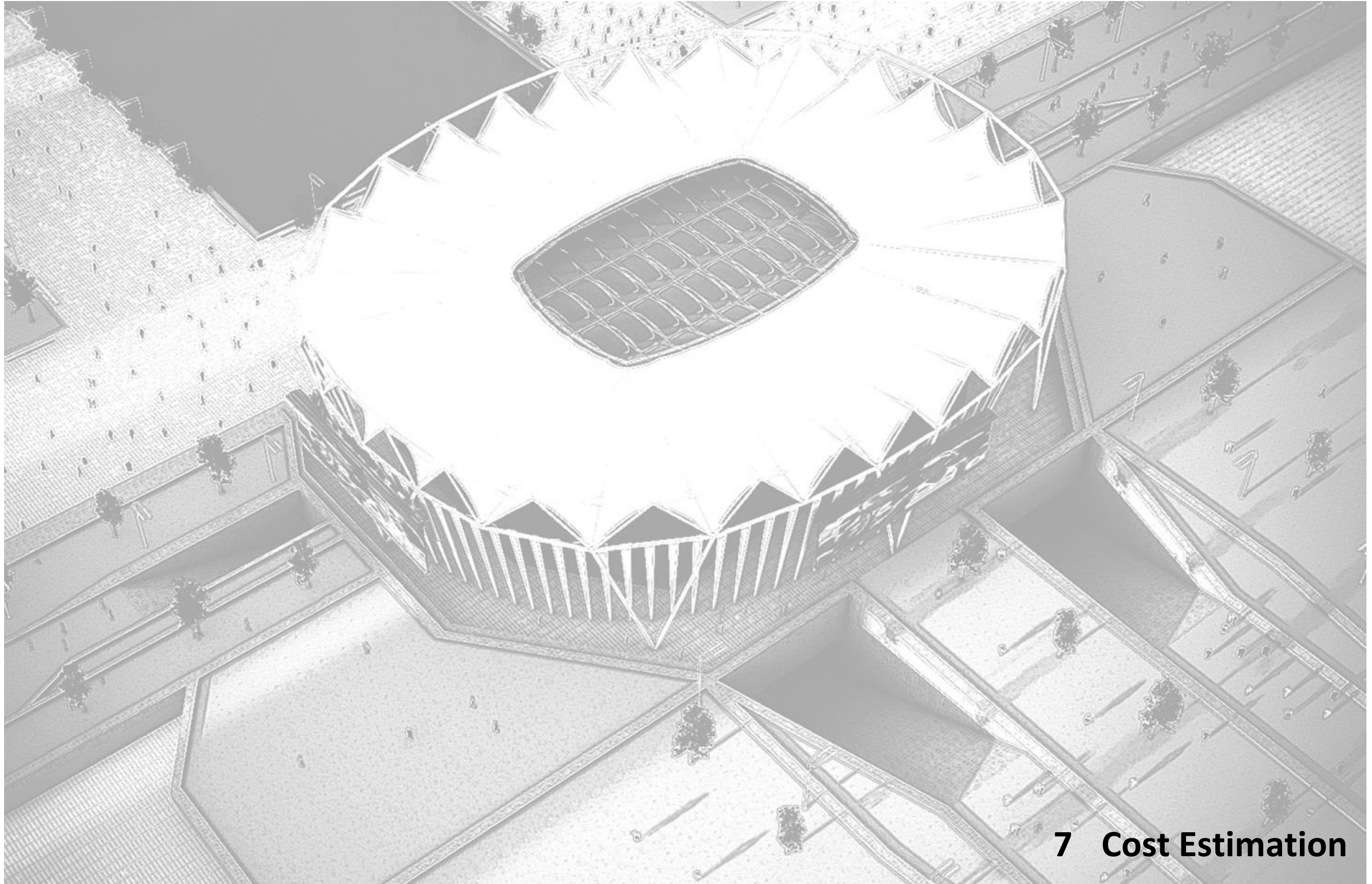


Compensation Value chosen for Patterning for both directions: 0.35 % for a prestress level of 2 kN/m

Width of the Welding for the Seams: 60 mm

Roll width 2.67m and length 50m.



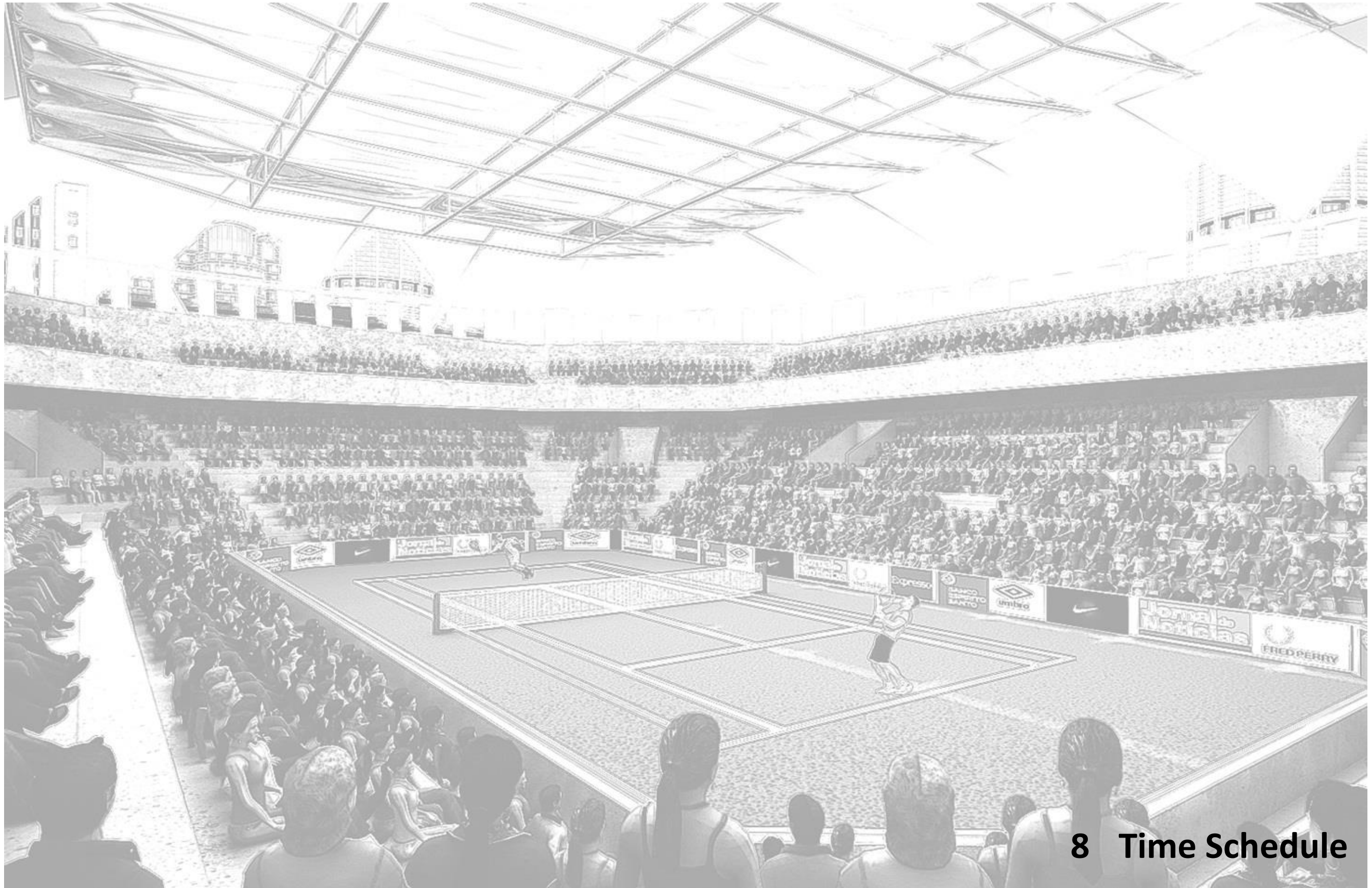


## 7 Cost Estimation

7. Cost Estimation

Design								
Static Calculations and Detailed Design (Erection Calculations incl.)				Costs All Inclusive			100000	
				Subtotal Design Works			100000	
Construction Material								
Steel Elements								
V-Columns			342 m		82500	2,20	Euros/Kg	181500
Upper Compression Ring			290 m		140500	2,20	Euros/Kg	309100
Lower Compression Ring			292 m		92000	2,20	Euros/Kg	202400
Diagonals			531 m		92500	2,20	Euros/Kg	203500
							Sub-Total	896500
Cables								
Ring Cables		dia. 75mm	503			45	Euros/m	22635
Upper Radial Cables		dia. 80mm	716,2			48	Euros/m	34377,6
Lower Radial Cables		dia. 70mm	698,3			42,0	Euros/m	29328,6
Edge Cables - Front		dia. 24.4mm	145,5			14,6	Euros/m	2124,30
Edge Cables - Back		dia. 24.4mm	531			14,6	Euros/m	7752,6
							Sub-Total	96218
Accessories and Detailing								
Details - Upper Radial Cables/C. Ring			26 Pieces			300	Euros/Piece	7800
Details - Lower Radial Cables /C. Ring			26 Pieces			300	Euros/Piece	7800
Cable Clamps - Radial/Ring Cables			52 Pieces			400	Euros/Piece	20800
Foot Detail - V Columns			8 Pieces			400	Euros/Piece	3200
Ring Cable Thread Fitting			4 Pieces			514,5	Euros/Piece	2058
Upper Radial Cable Sockets			52 Pieces			1820	Euros/Piece	94640
Lower Radial Cable Sockets			52 Pieces			1600	Euros/Piece	83200
Edge Cables Sockets			144 Pieces			631	Euros/Piece	90864
Water Drainage			26 Pieces			50	Euros/Piece	1300
							Sub-Total	311662
Membrane								
Material: Preconstraint 1202 S Back PVDF, Type 3 (one layer)			7794 m2					
Waste Factor (30%)			2338 m2					
Doublings and Edges (18%)			1559 m2					
			Sub-Total		11691 m2	15	Euros/m2	175365
Fabrication			9353			50	Euros/m2	467650
Testing Membrane								20000
							Sub-Total	663015
Foundation								
Mast Foot - V-Columns		8 Pieces	9,6 m3			250	Euros/m3	19200
							Sub-Total	19200
Erection								
Man-Days (days of 10 hours work)				7 men	180 days	250	Euros/day	315000
Travel				7 men		300	Euros/flight	2100
Accommodation				7 men	180 days	30	Euros/night	37800
Scaffolding					180 days	1000	Euros/day	180000
Truck crane with telescopic boom					60 days	2000	Euros/day	12000
							Sub-Total	546900
Transport Supply to Site								
Steelwork					407500 kg	0,1	Euros/kg	40750
Cable					53000 kg	0,1	Euros/kg	5300
Membrane					7949 kg	0,15	Euros/kg	1192
							Sub-Total	47242
Approval								
Fees								50000
							Total Euros	2730737

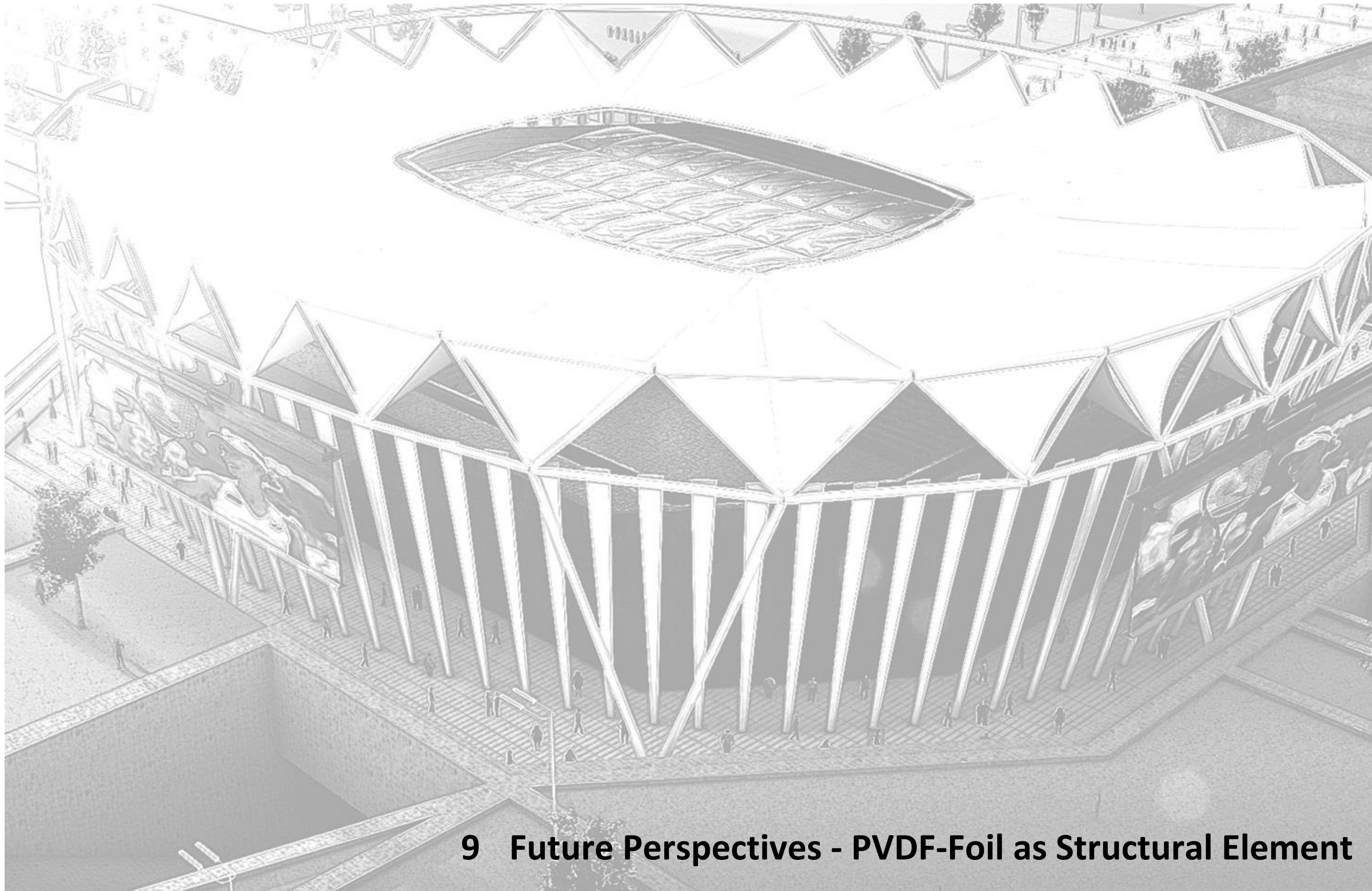




## 8 Time Schedule







## 9 Future Perspectives - PVDF-Foil as Structural Element

## 9. Future Perspectives - PVDF-Foil as Structural Element

While the piezoelectric effect has been around for some years, it has only recently caught interest as a potential sustainable energy harvesting solution.

Among the polymeric material, PVDF exhibits higher piezo and pyroelectric properties. The combination of the mechanical properties of a plastic material with those of a piezoelectric material led to new sensors and transducers. Currently PVDF is used in a variety of applications in the electronic field. Its success in these applications is due to some advantages, such as: flexibility, low density, resistance to chemical attack, possibility of manufacturing the form of thin films and areas greater than 1m<sup>2</sup> with a reduced production cost. These features are not presented by piezoelectric ceramics materials which are hard and brittle. Piezoelectric polymer materials can generate higher voltage/power than ceramic based piezoelectric materials and it was proved that producing energy from renewable sources such as rain drops and wind is possible by using piezoelectric polymer materials.

Piezoelectric effect is defined as the electric charge generated in certain materials by mechanical stresses. Piezoelectricity has gained significant importance in research and development for extracting energy from the environment.

Pyroelectric effect is defined as the electric charge generated in certain materials as response to temperature variations.

PVDF can crystallize in at least four distinct forms, called phases  $\alpha$ ,  $\beta$ ,  $\gamma$  and  $\delta$ . The  $\beta$  phase (polar) is of greater interest for the present, which has piezo and pyroelectric properties. However phase  $\alpha$  (nonpolar) is more easily obtained by the industry. There are several mechanisms that transform  $\alpha$  phase in  $\beta$  phase, the most common is by mechanical deformation of the  $\alpha$  phase in temperatures below 80 degrees, resulting in polar material with the total dipole moment of the order of  $6.9 \times 10^{-30} \text{C.m}$ . To obtain high levels of piezoelectric activity, the beta phase polymer is exposed to very high electric fields to align the crystallites relative to the poling field.

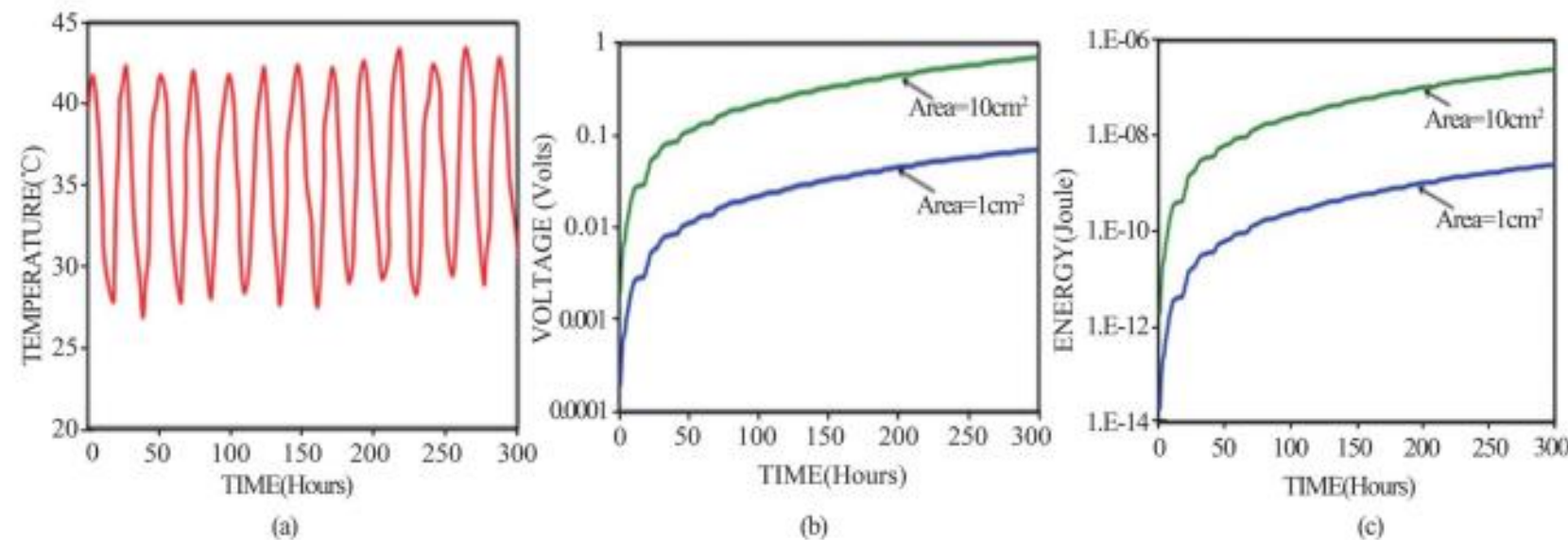
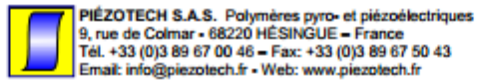


Figure 15 - PVDF-based Pyroelectric Energy Harvester - Plot of (a) Environment Temperature at Saudi Arabia and Respective (b) Generated Voltage and (c) Energy (Source: <http://www.cscanada.net/>)

The potential for energy harvesting through Pyroelectric effect was studied by using piezoelectric materials such as PVDF. Peak power density was experimentally determined to be  $0.12 \mu\text{W}/\text{cm}^2$  for PVDF. It can be estimated that thin films with larger area and higher pyroelectric coefficient can generate nearly three orders of magnitude improved peak power density for PVDF samples. (Source: [http://www.kam.k.leang.com/academics/pubs/XieJ\\_2010.pdf](http://www.kam.k.leang.com/academics/pubs/XieJ_2010.pdf))





### 5. Piézotech's PVDF piezoelectric films properties <sup>(1)</sup>

Characteristics	Bioriented Films
Nominal thickness (µm)	9 to 50
Thickness regularity (%)	± 10
Poled width of roll (cm)	25
Length of roll (m)	Variable: 5 to > 200
Piezoelectric properties (non metallized films)	Bioriented Films
$d_T = d_{33}^*$ , ( $10^{-12}$ C/N)	13 to 22
$d_{31}^*$ ( $10^{-12}$ C/N)	6 to 10
$d_{32}^*$ ( $10^{-12}$ C/N)	6 to 10
Regularity of piezoelectric coefficients, (%)	± 10
Variation of the coefficients at metallization, (%)	0 to 15 <sup>(2)</sup>
Relative dielectric constant $\epsilon/\epsilon_0$ ( $\epsilon_0 = 8.85 \cdot 10^{-12}$ F/m), between 50 Hz and 100kHz, $T^\circ = 25^\circ\text{C}$ to $90^\circ\text{C}$	10 to 12
$g_{33}^*$ (V.m/N)	0.14 to 0.22
Pyroelectric coefficient, $\rho$ ( $10^{-6}$ C/m <sup>2</sup> .K)	24 to 26
Transverse resistivity ( $\Omega$ .cm)	$5 \cdot 10^{14}$
Electromechanic coupling factor $K_T$ (%)	10 to 15
Mechanical properties	Bioriented Films
Tensile strength (MPa):	
- Machine direction:	60 – 160
- Transverse:	60 – 160
Elongation at break (%):	
- Machine direction:	40 – 140
- Transverse:	40 – 140
Modulus of elasticity (MPa):	
- Machine direction:	1600 – 2200
- Transverse:	1600 – 2200
Shrinkage after 1 hour, Oven at $160^\circ\text{C}$ (%):	
- Machine direction:	2 – 15
- Transverse:	1 – 13
Shrinkage after 100 hour, Oven at $80^\circ\text{C}$ (%):	
- Machine direction:	2 – 3
- Transverse:	N.A.

<sup>(1)</sup>: This range is experimental and susceptible to changes.

<sup>(2)</sup>: Excessive heating may destroy piezoelectricity. It is advised not to heat above  $90^\circ\text{C}$  for more than 1 h.

Figure 16 – PVDF Piezoelectric Film Properties (source: <http://www.piezotech.fr/>)

#### Advantages of PVDF Film:

- Excellent chemical resistance
- Stable to UV & effects of weather
- Low NBS smoke generation & superior LOI
- Excellent Transmittance of Solar Energy & Excellent Dielectric Strength
- Excellent Physical & Mechanical Properties
- PVDF is FDA & FM 4910 compliant
- Thicknesses are displayed in inches. (see metric conversion): 001" = 25.3 micron, .003 = 76.2 micron, .005" = 127 micron, .010" = 254 micron, .020" = 508 micron

## Ajedium™ Films -- Solef® PVDF 9009

polyvinylidene fluoride

Solef® 9009 PVDF homopolymer is a semi-crystalline fluoropolymer. Solef® film is chemically inert to most acids, aliphatic and aromatic organic compounds, chlorinated solvents and alcohols.

Solef® PVDF film has a very high purity, abrasion resistance comparable to that of polyamides and relatively low coefficient of friction. These films can be used in a wide range of temperatures and have excellent intrinsic fire resistance.

Solef® PVDF films have demonstrated excellent weathering properties and are extremely resistant to UV radiation and common industrial and environmental pollutants.

Solef® PVDF films can be used in a wide range of applications, including: release films, filters, chemical resistance lining, outdoor UV resistant needs as well as electric and electronic applications.

### Standard Thicknesses and Widths

- Widths are available from 22" (559 mm) to 56" (1422 mm).

- Products with widths <22 inches or >56 inches are available upon request.
- Tolerances for widths are +/- 4mm.
- For PVDF film, the standard thicknesses are 25 microns (1 mil) to 1016 microns (40 mil), with a tolerance of +/- 10%.

### Surface Finishes

- Standard surface finish is P/M (polished / matte).
- Custom finishes of P/P (polished / polished) and M/M (matte / matte) are available.

### Packaging

- Film is supplied in a roll form of high quality, cardboard core of 3" (76mm) or 6" (152mm).
- PVC cores are available upon request in 3" and 6" sizes.

### Labeling

- Products are labeled to comply with national and international standards.
- Labels include product grade, unique batch number, roll length, roll width, product thickness, and net weight.

### General

Material Status	• Commercial: Active	
Availability	• Asia Pacific	• Latin America
	• Europe	• North America
Features	• Homopolymer	

Physical	Typical Value	Unit	Test method
Specific Gravity	1.75 to 1.80		ASTM D792
Water Absorption (23°C, 24 hr)	< 0.040	%	ASTM D570

Mechanical	Typical Value	Unit	Test method
Coefficient of Friction			ASTM D1894
vs. Itself - Dynamic	0.15 to 0.35		
vs. Itself - Static	0.20 to 0.40		
Taber Abrasion Resistance			ASTM D4060
1000 Cycles, 1000 g, CS-10 Wheel	5.00 to 10.0	mg	

Films	Typical Value	Unit	Test method
Film Thickness - Tested	25	µm	
Secant Modulus			ASTM D882
MD	2000	MPa	
TD	2100	MPa	

Revised: 7/4/2014

Solvay Specialty Polymers

Page: 1 of 2

## Ajedium™ Films -- Solef® PVDF 9009

polyvinylidene fluoride

Films	Typical Value	Unit	Test method
Tensile Strength			ASTM D882
MD : Yield	55.0	MPa	
TD : Yield	56.0	MPa	
MD : Break	57.0	MPa	
TD : Break	54.0	MPa	
Tensile Elongation			ASTM D882
MD : Yield	6.0	%	
TD : Yield	6.2	%	
MD : Break	200	%	
TD : Break	250	%	
Free Shrinkage (130°C)	0.70	%	ASTM D2732
Area Factor	108	ft <sup>2</sup> /lb/mil	

Thermal	Typical Value	Unit	Test method
Glass Transition Temperature	-40.0	°C	ASTM D4065
Melting Temperature	162 to 168	°C	ASTM D3418
Peak Crystallization Temperature (DSC)	133 to 140	°C	ASTM D3418
CLTE - Flow	0.00014	cm/cm/°C	ASTM D696
Specific Heat (100°C)	1600	J/kg°C	ASTM C351
Thermal Conductivity	0.20	W/mK	ASTM C177

Electrical	Typical Value	Unit	Test method
Surface Resistivity	> 1.0E+14	ohm	ASTM D257
Volume Resistivity	> 1.0E+14	ohm-cm	ASTM D257
Dielectric Strength (23°C, 1.00 mm)	20 to 25	kV/mm	ASTM D149
Dielectric Constant	7.50		ASTM D150

Flammability	Typical Value	Unit	Test method
Oxygen Index (3.00 mm)	44	%	ASTM D2863

### Notes

Typical properties: these are not to be construed as specifications.

Figure 17 – PVDF Film Properties – Copyright Solef



The possible applications for PVDF-Foil as Structural Element in the Building Industry are the following:

a) Active Acoustic Control

Passive noise control aims to suppress the sound by absorbing the sound waves. “Modifying and canceling sound field by electro-acoustical approaches is called active noise control” (source: <http://en.wikibooks.org/>). The actuators, as an acoustic source, produce completely out of phase signals to eliminate the disturbances.

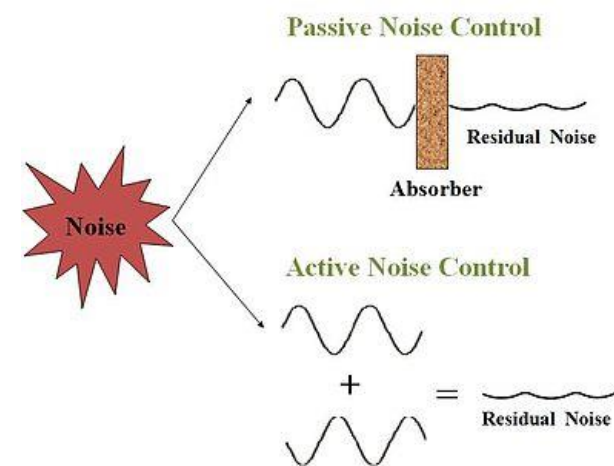


Figure 16 – Passive and Active Noise Control (source: <http://en.wikibooks.org/>)

It is known that Ete cushions offer poor acoustic insulation. One solution to improve this situation could be to introduce pvdf film as a middle layer in a cushion and use it as an active acoustic control panel to reduce residual noise.

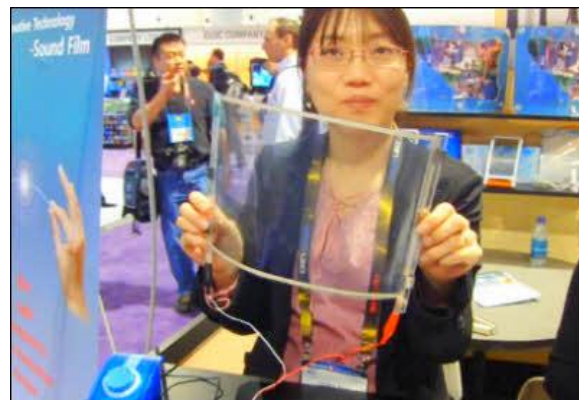


Figure 17 – Film speaker is made from piezoelectric film called PVDF (source: <http://www.telovation.com/articles/stereo-film-speakers.html>)

“Developed by Korean electronics manufacturer FILS, this innovative and transparent material is actually a stereo speaker system. It is thin and flexible and has a wide frequency and dynamic band, low impedance, high induced electricity and mechanism, low density and high sensitivity.” (Source: <http://www.telovation.com/articles/stereo-film-speakers.html>)

b) Piezoelectric PVDF Cushions for Façades and Roofs.

Etfе Cushions have been constructed around the world in buildings in the last years. An alternative to ETFE could be the use of PVDF. The mechanical characteristics are identical for both materials.

	Thickness	Tensile Strength Yield	Tensile Strength Break	Tensile Elongation Yield	Tensile Elongation Break	Secant Modulus	Flexural Modulus	Flammability Rating	Melt Point
ETFE Film (Dupont)	0.050 mm	-	41 MPa	-	300%	-	830 MPa	V-0	260-280 C
PVDF Film (Solef)	0.025 mm	54 MPa	54 MPa	6.2%	250%	2100 MPa	-	V-0	160 C

Temperature variation and wind loads could generate energy through piezoelectric effect on the PVDF Cushion.

PVDF has an excellent chemical resistance and is stable to UV and weather effects. The only thing that is discussable is the low Melting Point of PVDF.

Further research to the use of PVDF film in the building industry should be done.

c) Renewable Energy – Solar Updraft Tower roof collector

PVDF single layers could be used for the Solar Updraft tower roof collector. The collector is used to warm up air (greenhouse effect), which is then “sucked” by the tower (chimney effect) generating energy from wind turbines. Instead of using a “passive” material just with the function of creating a greenhouse, there is the possibility of using a material like piezoelectric PVDF film that produces also energy with temperature variations and wind loads.



Figure 18 –Solar Updraft Tower (left) and ETFE film for solar updraft tower in Manzanares, Spain (right) (Copyright: Schlaich Bergermann und Partner)

The Peak Power density was experimentally determined to be  $0.12 \mu\text{W}/\text{cm}^2$  for PVDF. The collector area for a 100 MW Solar Updraft Tower is around  $14505151 \text{ m}^2$ . Thus, the peak power generated by the collector is 17.4 MW!

There is the chance of building a 100 MW solar updraft tower by phases. First a part of the roof collector, which can start generating energy by the piezoelectric effect due to temperature and wind. Then, on a second phase the whole roof and the energy generated can start subsidizing the chimney/tower project. On the last phase, the tower can be built.

Pvdf film has a higher light transmittance than ETFE film. Thus, the greenhouse effect is guaranteed under the roof collector.

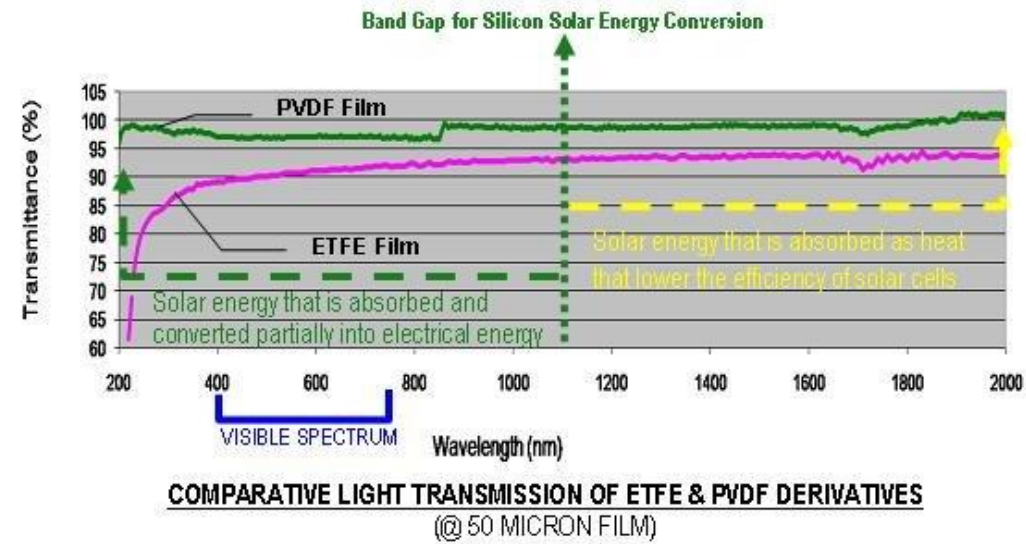
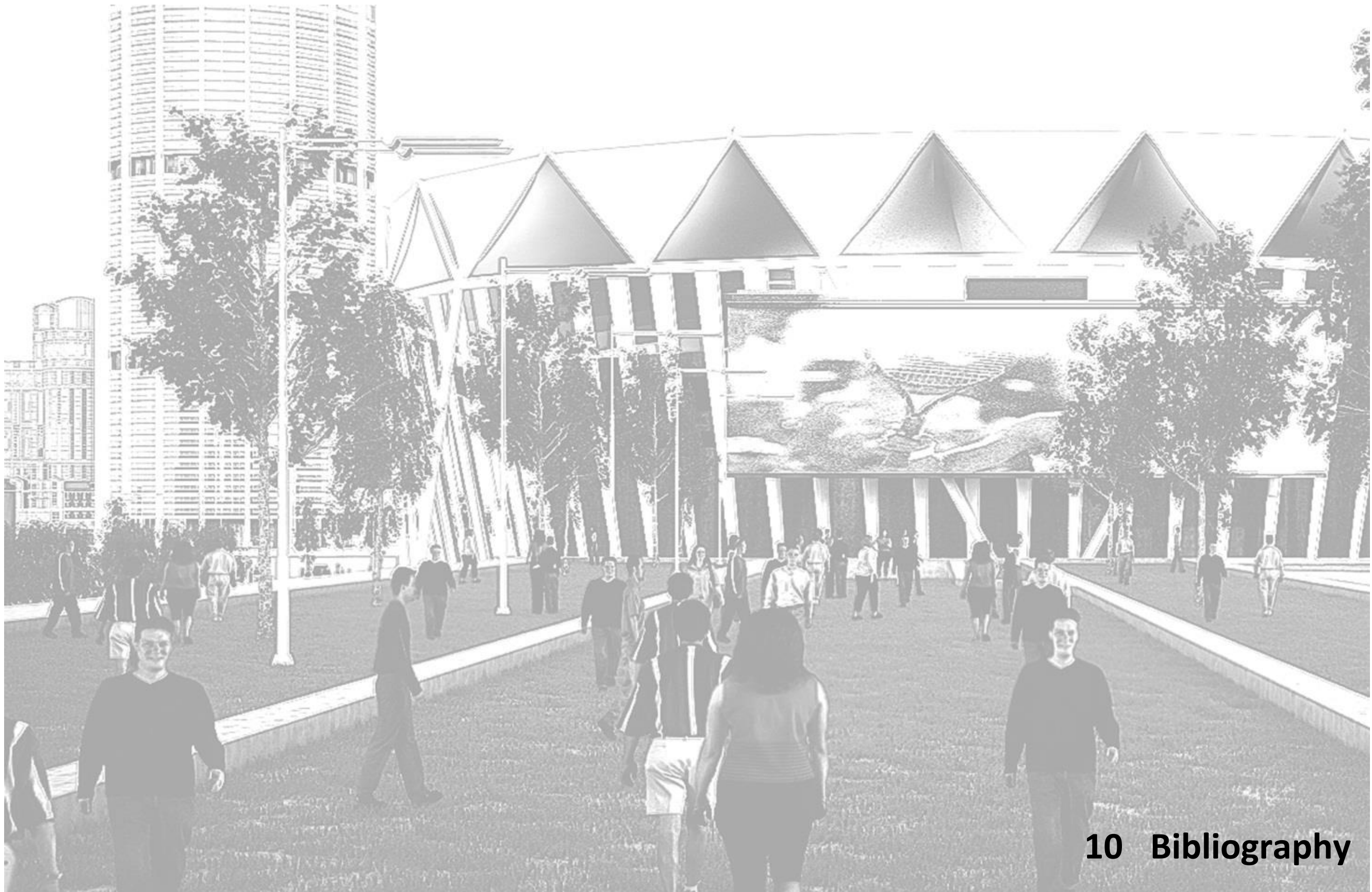


Figure 19 –Transmittance of PVDF and ETFE film (Source: <http://www.aitechnology.com/products/solar/transparent-pvdf-encapsulating-front-sheet/>)

The boundaries of lightweight structures and materials can be overcome once more in the near future with the use of PVDF film.





## 10 Bibliography



## 10. Bibliography

EN 1991-1-4\_2005 Eurocode 1: Actions on structures - Part 1-4: General actions - Wind actions

EN 1993-1-1\_2005 Eurocode 3: Design of steel structures - Part 1-1: General rules and rules for buildings

European Design Guide for Tensile Surface Structures (2004) (English) Brian Forster and Marijke Mollaert – TensiNet

Tensile Surface Structures. A Practical Guide to Cable and Membrane Construction (2009) Michael Seidel

Design Recommendations for ETFE Foil Structures – Tensinet ETFE Working Group – European Design Guide for Tensile Structures Appendix A5

Membrane Structures in Japan. Kazuo Ishii

Pfeifer – Seilbau - Cable Structures Catalogue 11/2012

SergeFerrari Data Information from 2012 Catalogue

Drawing List:

- 01 General Plans: Second Level
- 02 General Plans: Top View
- 03 General Plans: View and Section
- 04 Detail 1: Upper Compression Ring
- 05 Detail 2: Lower Compression Ring
- 06 Detail 3: Radial Cables
- 07 Detailing - Radial cable - Ridge cable
- 08 Detailing - Radial cable - Valley cable
- 09 Detail 4: Tension Ring / Detail 5: Node Point
- 10 Detailing - Cable Fittings
- 11 Detail 5: Front Edge Cable
- 12 Detail 6: V Column Foot
- 13 Detail 7: V Column Head
- 14 Patterning: Preliminary Cuts
- 15 Patterning: T1, T2, T3, T4
- 16 Patterning: T5, T6, T7, T8
- 17 Patterning: T9, T10
- 18 Patterning: PT11, T12, T13